

2010

The use of thermal mass and phase change material to reduce a building's thermal load

Robert B. Gilbert
University of Dayton

Follow this and additional works at: https://ecommons.udayton.edu/graduate_theses

Recommended Citation

Gilbert, Robert B., "The use of thermal mass and phase change material to reduce a building's thermal load" (2010). *Graduate Theses and Dissertations*. 2901.
https://ecommons.udayton.edu/graduate_theses/2901

This Dissertation is brought to you for free and open access by the Theses and Dissertations at eCommons. It has been accepted for inclusion in Graduate Theses and Dissertations by an authorized administrator of eCommons. For more information, please contact mschlange1@udayton.edu, ecommons@udayton.edu.

THE USE OF THERMAL MASS AND PHASE CHANGE MATERIAL TO
REDUCE A BUILDING'S THERMAL LOAD

Dissertation

Submitted to

The School of Engineering of the

UNIVERSITY OF DAYTON

Dayton, Ohio

in Partial Fulfillment of the Requirements for

The Degree

Doctor of Philosophy in Mechanical Engineering

By

Robert B. Gilbert

UNIVERSITY OF DAYTON

Dayton, Ohio

May 2010

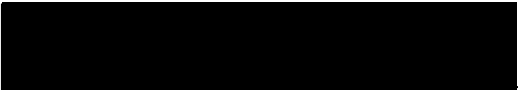
THE USE OF THERMAL MASS AND PHASE CHANGE MATERIAL TO

REDUCE A BUILDING'S THERMAL LOAD HFG.


*Please Do Not
Remove This Note!*

Original

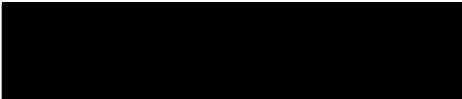
APPROVED BY:



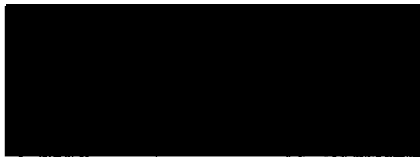
Kelly Kissock, Ph.D.
Advisory Committee Chairman
Professor
Mechanical and
Aerospace Engineering



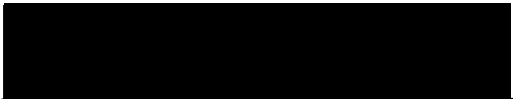
John Schauer, Ph.D.
Committee Member
Professor
Mechanical and
Aerospace Engineering



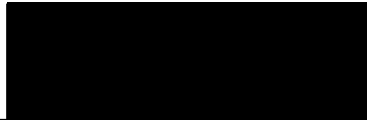
Robert Brecha, Ph.D.
Committee Member
Professor Mann Chair in the Sciences
Physics



Kevin Hallinan, Ph.D.
Committee Member
Professor and Chairperson
Mechanical and
Aerospace Engineering



Malcolm W. Daniels, Ph.D.
Associate Dean
School of Engineering



Tony E. Saliba, Ph.D.
Dean
School of Engineering

ABSTRACT

THE USE OF THERMAL MASS AND PHASE CHANGE MATERIAL TO REDUCE A BUILDING'S THERMAL LOAD

Name: Gilbert, Robert B.
University of Dayton

Advisor: Kissock, Kelly

A finite-difference model is used to simulate the effects of thermal mass and phase change material on thermal transmission through a building's envelope wall. The exterior temperature is simulated by a sinusoidal function. The inside temperature is held constant. A comparison is given between the effects of thermal mass and phase change material. The required climate conditions for thermal mass and phase change material to reduce thermal transmission are given. The maximum reduction in net thermal transmission is given for both thermal mass and phase change material. Equations are given to calculate the minimum thermal load resulting from thermal mass and therefore the maximum thermal load reduction with thermal mass. Equations and methods are given to calculate the minimum thermal load resulting from thermal mass from weather data files, TMY or TMY2 files.

The IECC, International Energy Conservation Code, allows for a reduction in R-value and/or an increase in U-factor of the exterior wall of a building with the incorporation of what it defines as a MASS WALL within the wall. A study is conducted to determine the required U-factor of the MASS WALL for it to perform with equal net thermal transmission and net thermal load, under transient ambient sol-air temperature conditions, as the required U-factor of the no-mass wall. The IECC defines eight CLIMATE ZONES with different requirements for each. The required U-factors are given for four of the zones. A finite-difference model was developed specifically to simulate the BESTEST qualification cases. This model is used to verify the results obtained when applied within the entire building envelope.

A test cell is constructed with a heater and a thermostat within the cell to maintain the interior air temperature at a predetermined set point. The test cell is placed in the ambient cyclic weather conditions. Data is logged of the temperature of the interior cell air, mass wall surfaces, and the ambient air. The amount of energy required to maintain the cell at the set point is also logged. The test cell is placed in different cyclic weather temperature conditions with respect to the interior cell set point temperature. The logged data verifies the conclusions offered resulting from the finite-difference study.

ACKNOWLEDGEMENTS

I wish to express my appreciation to Dr. Kelly Kissock for being my advisor and for serving as an inspiration to me to change directions, at this point in my life, and enter into a whole new field of energy efficiency and renewable energy. It has truly been a very rewarding venture and has opened up totally new opportunities to me.

I wish to express my appreciation to Dr. Kevin Hallinan for serving on my committee and helping guide me through this endeavor and helping me keep on the path to completion. I also greatly appreciate his forming collaborations with the University of Dayton, Wright State University, and Sinclair Community College.

A special "Thank you" to Dr. John Schauer for serving on my committee and for being an excellent and dedicated teacher. Of the many teachers I have had, Dr. Schauer stands out as the best. He has a unique ability to develop complicated concepts from the very basics.

I wish to express my appreciation to Dr. Robert Brecha for serving on my committee and bringing another perspective. Dr. Brecha is dedicated to sustainability and energy efficiency and serves as an inspiration with his community involvements.

TABLE OF CONTENTS

Abstract.....	iii
Acknowledgements.....	v
Table of Contents.....	vi
List of Figures.....	x
List of Tables.....	xvi
 Chapter 1: Introduction	 1
1.1 Energy Use in Buildings	2
1.2 IECC The International Energy Conservation Code	3
1.3 BESTEST and Thermal Mass “Mass Wall”	4
1.4 Phase Change Material (PCM)	5
1.5 Purpose of Research	6
 Chapter 2: The Effects of Thermal Mass on Thermal Transmission	 7
2.1 Finite-Difference Model	9
2.2 Simulation Results	11
2.3 Maximum Thermal Load Reduction with Thermal Mass	23

2.4 Using Weather Files to Determine Maximum Thermal Load Reduction with Thermal Mass	25
2.5 Summary	27
Chapter 3: The Effects of PCM on Thermal Transmission	29
3.1 Finite-Difference Model for PCM	30
3.2 Simulation Results of PCM	32
3.3 Summary of Effect of PCM on Thermal Load	37
Chapter 4: Finite-Difference Model	38
4.1 Finite Difference Model for Concrete	38
4.2 Finite-Difference Equations	39
4.3 Simulation of Exterior Ambient Temperature with Sinusoidal	41
4.4 Determination of Required Number of Nodes with Concrete as Thermal Mass	43
4.5 Determination of Required Time Step with Concrete as Thermal Mass	48
Chapter 5: Thermal Mass and the IECC	50
5.1: IECC R-Values and U-Factors	51
5.2: Finite-Difference Model for Concrete	56
5.3: Values and Constants used in IECC "Mass Wall"	60
5.4: Detailed Investigation of "Mass Wall" in Dayton	62
5.5: Analysis of Other Locations in Climate Zone 5 and Marine 4	69
5.5.1: Boulder, Colorado	69

5.5.2 Portland, Oregon	75
5.5.3 Summary of Climate Zone 5 and Marine 4	79
5.6: Analysis of Locations in Climate Zone 2	79
5.6.1: Tampa, Florida	80
5.6.2: San Antonio, Texas	84
5.6.3: Summary of Climate Zone 2	85
5.7: Analysis of Locations in Climate Zone 3	86
5.7.1: Tulsa, Oklahoma	86
5.7.2: Topeka, Kansas	90
5.7.3: Summary of Climate Zone 3	92
5.8: Summary	92
5.9: PCM on Exterior as "Mass Wall"	93
 CHAPTER 6: Effect of Thermal Mass on Thermal Transmission using TMY2 Weather File for Dayton, Ohio	 94
6.1: TMY2 Weather File for Dayton, Ohio	94
6.2: Comparison of Heat Transfer of "Mass Wall" to No Mass Wall for Hours 0 to 1500 and Hours 2500 to 4000	95
 CHAPTER 7: Experiment of Effect of Thermal Mass on Thermal Transmission	 101
7.1: Experimental Apparatus	101
7.2: Test Procedure	107
7.3: Results	108

7.3.1: Determination of Test Cell UA	108
7.3.2: Data Analysis of Average and Peak Exterior Air Temperature Below Interior Set Point	110
7.3.3: Data Analysis of Average Exterior Air Temperature At the Interior Set Point Temperature	112
7.4: Conclusion	114
7.5: Recommendations	115
CHAPTER 8: Summary and Conclusions and Future Work	116
BIBLIOGRAPHY	122

LIST OF FIGURES

2.1: Wall configuration used in finite-difference model	10
2.2: Time-temperature profile through thermal mass with interior temperature of 20 °C , exterior sol-air temperature of 20 °C and a temperature amplitude of 10 °C . Thermal mass density-specific heat product set to zero.	13
2.3: Time-temperature profile through thermal mass with interior temperature of 20 °C , exterior mean sol-air temperature of 20 °C and a temperature amplitude of 10 °C . Thermal mass density-specific heat product set to $1.4 \times 10^6 \text{ J/K} \cdot \text{m}^3$	14
2.4: Time-temperature profile of node 8 on inner surface of thermal mass with interior temperature of 20 °C , exterior mean sol-air temperature of 20 °C and a temperature amplitude of 10 °C . Thermal mass density-specific heat product increased from to $5.6 \times 10^6 \text{ J/K} \cdot \text{m}^3$.	17
2.5: Heating thermal load with interior temperature of 20 °C , exterior mean sol-air temperature of 20 °C and a temperature amplitude of 10 °C . Thermal mass density-specific heat product increased from to $5.6 \times 10^6 \text{ J/K} \cdot \text{m}^3$.	17
2.6: Amplitude temperature of node 8 with interior temperature of 20 °C , exterior mean sol-air temperature of 20 °C and a temperature amplitude of 10 °C . Thermal mass density-specific heat product increased from to $5.6 \times 10^6 \text{ J/K} \cdot \text{m}^3$.	18
2.7: Temperature time delay of node 8 with respect to the sol-air temperature with interior temperature of 20 °C , exterior mean sol-air temperature of 20 °C and a temperature amplitude of 10 °C . Thermal mass density-specific heat product increased from to $5.6 \times 10^6 \text{ J/K} \cdot \text{m}^3$.	18

2.8: Time-temperature profile of node 8 on the inner surface of the thermal mass with interior temperature of 20 °C , exterior mean sol-air temperature of 15 °C and a temperature amplitude of 10 °C . Thermal mass density-specific heat product is varied from 0 to $2.8 \times 10^6 J/K \cdot m^3$	19
2.9: Amplitude temperature of node 8 on the inner surface of the thermal mass with interior temperature of 20 °C , exterior mean sol-air temperature of 15 °C and a temperature amplitude of 10 °C . Thermal mass density-specific heat product is varied from 0 to $2.8 \times 10^6 J/K \cdot m^3$	20
2.10: Amplitude temperature of node 8 on the inner surface of the thermal mass with interior temperature of 20 °C , exterior mean sol-air temperature of 15 °C and a temperature amplitude of 10 °C . Thermal mass density-specific heat product is varied from 0 to $2.8 \times 10^6 J/K \cdot m^3$	21
3.1: Configuration of Finite-Difference Model for PCM	31
3.2: Time-temperature profile through PCM with interior temperature of 20 °C , exterior sol-air temperature of 20 °C and a temperature amplitude of 8 °C . Melting temperature of PCM of $28 \pm 1/2^\circ C$. Heating and cooling loads are $3.36 WH/m^2 day$	32
3.3: Time-temperature profile through PCM with interior temperature of 20 °C , exterior sol-air temperature of 20 °C and a temperature amplitude of 8 °C . Melting temperature of PCM of $18 \pm 1/2^\circ C$. Heating and cooling loads are $3.36 WH/m^2 day$.	33
3.4: Time-temperature profile through PCM with interior temperature of 20 °C , exterior sol-air temperature of 20 °C and a temperature amplitude of 8 °C . Latent heat of PCM zero. Heating and cooling loads are $4.35 WH/m^2 day$. PCM exterior to insulation.	35
3.5: Time-temperature profile through PCM with interior temperature of 20 °C , exterior sol-air temperature of 20 °C and a temperature amplitude of 8 °C . Melting temperature of PCM of $18 \pm 1/2^\circ C$. Latent heat of PCM 180 kJ/kg . Heating and cooling loads are $2.47 WH/m^2 day$.	36

3.6: Comparison of average node temperatures with latent heat of PCM of 0 kJ/kg and 180 kJ/kg .	37
4.1: Finite-difference model for concrete simulation	39
4.2: Sinusoidal simulation cyclic ambient temperature	42
4.3: Number of nodes vs. insulation arrangements for 12-inch thick concrete	44
4.4: Fitted curve of WH / Day vs. simulated WH / Day	46
4.5: Lag time of inner concrete wall	47
4.6: Intersection of WH / Day curve with the X axis	47
4.7: Time step, seconds vs. $WH / m^2\text{day}$	49
4.8: Time step vs. lag time in hours	49
5.1: Climate Zones	51
5.2: REScheck TM printout	55
5.3: Model of wall	57
5.4: Cooling vs. Concrete Thickness, Dayton, Ohio	63
5.5: Comparison of U-factor "mass wall" to U-factor no-mass wall, 2-1/2-inch thick concrete	63
5.6: Comparison of U-factor "mass wall" to U-factor no-mass wall, 6-inch thick concrete	64
5.7: Heating vs. concrete thickness, Dayton, Ohio	65
5.8: Comparison of U-factor "mass wall" to U-factor no-mass wall, 2-1/2-inch thick concrete, heating	66
5.9: Comparison of U-factor "mass wall" to U-factor no-mass wall, 6-inch thick concrete, heating	66

5.10: Total heating and cooling vs. concrete thickness, Dayton, Ohio	67
5.11: Comparison of U-factor "mass wal" to U-factor no-mass wall, 6-inch thick concrete, total heating and cooling	68
5.12: Total heating and cooling vs. location of insulation, Dayton, Ohio	68
5.13 Cooling load vs. concrete thickness, Boulder, Colorado	70
5.14 Heating vs. concrete thickness, Boulder, Colorado	71
5.15 Total cooling and heating vs. concrete thickness, Boulder, Colorado	72
5.16 Cooling vs. U-factor of mass wall compared to U-factor of no-mass wall	73
5.17 Heating vs. U-factor of "mass wall" compared to U-factor of no-mass wall	74
5.18 Total cooling and heating vs. U-factor of "mass wall" compared to U-factor of no-mass wall	75
5.19 Cooling vs. concrete thickness, Portland, Oregon	76
5.20 Heating vs. concrete thickness, Portland, Oregon	77
5.21 Total cooling and heating vs. concrete thickness, Portland, Oregon	78
5.22 Total cooling and heating vs. U-factor of "mass wall" compared to U-factor of no-mass wall	78
5.23 Cooling vs. concrete thickness, Tampa, Florida	80
5.24 Heating vs. concrete thickness, Tampa, Florida	81
5.25 Total cooling and heating vs. concrete thickness, Tampa, Florida	82
5.26 Total cooling and heating vs. U-factor of "mass wall" compared to U-factor of no-mass wall	83
5.27 Total cooling and heating vs. insulation location, Tampa, Florida	83
5.28 Total cooling and heating vs. concrete thickness, San Antonio, Texas	84

5.29 Total cooling and heating vs. U-factor of "mass wall" compared to U-factor of no-mass wall	85
5.30 Cooling vs. concrete thickness, Tulsa, Oklahoma	87
5.31 Heating vs. concrete thickness, Tulsa, Oklahoma	88
5.32 Total cooling and heating vs. concrete thickness	89
5.33 Total cooling and heating vs. U-factor of "mass wall" compared to U-factor of no-mass wall	90
5.34 Total cooling and heating vs. concrete thickness, Topeka, Kansas	91
5.35 Total cooling and heating vs. U-factor of "mass wall" compared to U-factor of no-mass wall	91
6.1 Average sol-air temperature vs. hour of year for Dayton, Ohio, TMY2 weather file	95
6.2 Comparison of heat transfer of no-mass wall and "mass wall" with 6-inches of concrete hours 0 to 1500	96
6.3 Comparison of heat transfer of no-mass wall and "mass wall" with 6-inches of concrete hours 2500 to 4000	97
6.4 Heat transfer through a no-mass wall with a U-factor of 0.082 vs. sol-air temperature $^{\circ}F$	97
6.5 Heat transfer through a "mass wall" with a U-factor of 0.082 vs. sol-air temperature $^{\circ}F$, hours 0 to 1500	98
6.6 Heat transfer through a "mass wall" with a U-factor of 0.082 vs. sol-air temperature $^{\circ}F$, hours 2500 to 4000	99
7.1 1-foot square 5-1/2-inch thick wall section being cast	102
7.2 1-foot square 5-1/2-inch thick wall section on test platform	102
7.3 Test platform with the concrete wall section in place and the thermostat-CFL circuits	103
7.4 Photo of the test platform with the temperature probes mounted, the photo cell in location and the data logger	104

7.5 Photo of the original location of the temperature probe on the outer surface of the concrete wall	105
7.6 Photo of beginning of the construction of the bead board walls	105
7.7 Photo of front of completed test cell	106
7.8 Photo of rear of completed test cell	106
7.9 Interior cell, interior concrete surface, and outside air temperature	110
7.10 Plots of interior cell temperature vs. outside air temperature	111
7.11 Interior cell, inside concrete surface, outside air temperature, and CFL heat on indicator vs. time. Average outside temperature approximately equal to the interior cell set point temperature	112

LIST OF TABLES

4.1: Number of nodes and percentage change in <i>WH / Day</i>	45
4.2: Time lag vs. percentage change between nodes	48
5.1: 2006 IECC Insulation and Fenestration Requirements By Component	52
5.2: 2006 IECC Equivalent U- Factors	53
5.3: 2009 IECC Insulation and Fenestration Requirements by Component	54
5.4: 2009 IECC Equivalent U-Factors	55
5.5: Calculation of U-factor	61
5.6: Climate zones, IECC U-factor of no-mass wall and "mass wall," and the U-factor for the "mass wall" to transmit the same amount of heat as IECC no-mass wall	92

CHAPTER 1

INTRODUCTION

President Barack Obama proposed that the easiest and least expensive way to make the economy stronger and cleaner is to make the economy more energy efficient. He also stated that the focal point of the Recovery Act needs to be investments about energy efficiency and those technologies that will benefit American homes and businesses. These initiatives will not only reduce energy demand, but will also give hard-working Americans more spendable income.

Secretary Chu supported this initiative when he commented that the most prosperous and competitive economies in the 21st century will be those that use energy efficiently. He ended his comments by urging Americans to lead the way.

AIA, US Green Building Council, US Conference of Mayors, State of New Mexico etc. have proposed: The 2010 Imperative:

It is to achieve, by 2010, complete ecological literacy in design education, including: design / studio, history / theory, materials /technology, structures /construction, professional practice / ethics.

Also proposed: The 2030 Challenge:

The goal is for new buildings to be "carbon-neutral" and use no energy from fossil fuels that produce greenhouse gasses by 2030. It calls for a fossil fuel reduction of 60% in 2010, 70% in 2015, 80% in 2020, 90% in 2025, and a 100% Energy Efficient Design by 2030.

1.1 Energy Use in Buildings

Buildings consume approximately 39% of all the energy used in the United States. Of the 39%, residential building use makes up approximately 22% and commercial building use makes up approximately 17%. Approximately 43% of total residential energy use is for space heating and cooling. Approximately 24% of the total commercial energy use is for space heating and cooling. This energy use of buildings for space heating and cooling clearly demonstrates the need to address a building's envelope and its HVAC and mechanical systems to determine means to reduce this energy use.

The International Energy Conservation Code (IECC) 2009 [1] states that buildings will be designed to maintain an interior dry bulb temperature of $72^{\circ}F$ in the winter season and $75^{\circ}F$ in the summer season. To conserve energy and maintain these interior human comfort conditions, it is necessary to design and use efficient heating and air conditioning systems and design and construct the envelope of the building to reduce thermal transmission.

1.2 IECC The International Energy Conservation Code

The IECC specifies eight different climate zones in the United States. Many of the required building envelope U-factors and R-values are climate specific.

There are three paths to demonstrate energy code compliance; prescriptive, (UA) trade-off, and simulation. The prescriptive path states exact R-values and U-factor as respectively code minimums and maximums. As long as the envelope components meet or exceed these values, the building envelope is considered energy code compliant. The UA trade-off allows for the calculation of the entire building envelope's heat loss/gain coefficient. Some components are allowed to be less than the specific required value of that component as long as some other component exceeds the specified requirements in an amount to offset the other component. The simulation path requires an annual energy use simulation of the building and the IECC specifies a maximum allowable annual energy use.

In the prescriptive path, the IECC allows a specific reduction in R-value or increase in U-factor for the use of a "mass wall." A "mass wall" is defined as an envelope wall having a specific heat of $6.0 \text{ Btu/ft}^2 \text{ } ^\circ\text{F}$ and having no more than one-half of the thermal resistance of the required insulation on the interior of the "mass wall." When more than one-half of the thermal resistance of the insulation is on the interior of the "mass wall," there is a reduction in the allowed reduction in R-value and increase in U-factor. The

determination of the exact amount of material required which will constitute a "mass wall" is assigned to local code officials.

1.3 BESTEST and Thermal Mass "Mass Wall"

The Building Energy Simulation Test ("BESTEST") [2] is a project developed by the International Energy Agency for practical implementation procedure and data for an overall IEA, International Energy Agency, validation methodology which has been under development by NREL since 1981 [1]. BESTEST describes fourteen qualification cases. Six are described as lightweight, using materials with a low product of density and specific heat. Six are heavyweight cases using material with a high product of density and specific heat. Two of the qualification cases are Free-Float cases as defined by BESTEST.

Thermal mass is known to reduce a building's thermal loads [3]. For example, the BESTEST protocol describes cases in which the thermal load was reduced by more than 60 % in a heavyweight building compared to a lightweight building. However, the mechanism by which thermal mass affects thermal loads is not widely understood or easily quantified. Moreover, different climate conditions result in different thermal load reductions with increasing thermal mass [4].

There are several mechanisms which can contribute to this reduction in thermal load. Thermal transmission through the envelope of the building can be reduced with increased thermal mass [5, 6]. Internal load dampening

can also be increased with the addition of thermal mass [7, 8, 9]. Thermal mass can also be used to store solar energy, using either passive or active systems [10].

1.4 Phase Change Material (PCM)

Phase change material can be used in place of large space consuming thermal mass materials. Phase change building materials installed on the interior of a building to dampen a building's interior temperature and therefore reduce the space heating and cooling loads have been studied [11, 12, 13, 14]. Phase change materials have the advantage of having a large thermal storage for their size and space requirements. However, for PCM's to be effective, their temperature must go through their melting/freezing point. PCM's stabilize the temperature at their melting/freezing temperature and must be selected to be consistent with the human comfort conditions. Phase change materials have not been well studied as a method of reducing thermal transmission and they have not been well studied when installed on the exterior of the building envelope. With the proper selection of the melting/freezing temperatures or the use of more than one PCM with different melting/freezing temperatures they may offer control of thermal transmission [15].

1.5 Purpose of Research

The purpose of the research is to determine under what conditions thermal mass is effective at reducing thermal transmission through a building's envelope and therefore reducing the space heating and cooling requirements and the building's energy use. Thermal mass installed in the envelope of a building are given a reduction in required R-value and/or increase in U-factor in the IECC. It is the purpose of this research to determine what R-value or U-factor is required with the "mass wall" to have it perform equal to a no-mass wall with the higher R-value of lower U-factor. In addition, the purpose of this research is to determine the maximum reduction in thermal transmission through "mass walls" as a function of the IECC specified climate zones. Another purpose of this research is to determine a PCM's ability to reduce thermal transmission when installed near or on the exterior of the building's envelope.

CHAPTER 2

THE EFFECTS OF THERMAL MASS ON THERMAL TRANSMISSION

The effects of thermal mass on thermal transmission are climate specific. This chapter investigates the required climate conditions for thermal mass to reduce thermal transmission and the maximum thermal transmission reduction that can be obtained under the climate condition.

BESTEST [2] is a set of qualification tests for building energy use simulation software programs. The qualifications were determined using eight different software programs from five different countries. There are 36 cases in all, 14 qualification tests and 22 diagnostics tests. The weather file used with BESTEST is DRYCOLD TMY (Typical Meteorological Year). DRYCOLD is the same weather data as the Denver-Stapleton EPW (EnergyPlus Weather) file. BESTEST provides a framework to compare annual heating and cooling energy, the maximum heating and cooling load, and the date and time of day of maximum with accepted results. The target maximum and minimum range mean results were obtained from the eight different software programs and the required qualification results were specified.

The 600 and 900 series are the qualification cases. The 600 series are the lightweight cases and the 900 series are the heavyweight cases. The

heavyweight cases are of higher thermal mass building components incorporated in the walls and the floor. The roof components are the same in both the 600 and 900 series. The thermal resistance of the envelope remains the same in both cases.

The simulated building is 8 meters long by 6 meters wide and 2.7 meters high. The long dimension, 8 meters, is in the east-west direction. All of the 600 and 900 series have 12 square meters of windows, either on the south or a combination of east and west. Both series have a heating set point of 20 °C, a cooling set point of 27 °C, with the exception of the 640 and 940 which have setbacks, a 200 watt internal gain, and an infiltration rate of 0.5 ACH, air changes per hour.

The lightweight, 600 series, with the 12 square meters of windows on the south, has a mean annual heating of 5.090 MWH and a mean annual cooling of 6.832 MWH. The heavyweight 900 series which has the same specifications as the 600 series with the exception of different materials with a higher thermal mass, has a mean annual heating of 1.745 MWH and a mean annual cooling of 2.678 MWH. This corresponds to a 66% reduction in heating load and a 61% reduction in cooling load with the addition of the heavyweight materials with a high thermal mass. The reduction in the heating is partially caused by reducing cooling by storing energy in the floor and the wall components. The reduction in cooling includes the interior air temperature dampening of the solar heat gain by the floor and walls [6, 9].

Diagnostic cases 430 and 800 have no windows. Case 430 is lightweight and case 800 is heavyweight. They both have a heating set point of 20°C , a cooling set point of 27°C , an internal gain of 200 watts, and an infiltration rate of 0.5 ACH. The lightweight, 430 case with no windows has a mean annual heating of 6.723 MWH and an annual mean cooling of 0.628 MWH. The heavyweight 800 case, which has the same specifications as the 430 case, with the exception of different materials with a higher thermal mass, has a mean annual heating load of 6.153 MWH and a mean annual cooling load of 0.202 MWH. This corresponds to a reduction in heating of only 8-1/2% and a reduction in cooling of 68% with the addition of the heavyweight materials with a high thermal mass.

2.1 Finite-Difference Model

Figure 2.1 is of the wall configuration used in the finite-difference simulations. The dimensions used are taken from the dimensions specified in BESTEST. BESTEST specifies a wall insulation of fiberglass with a thickness of 0.066 meters, for the lightweight cases and a concrete block thickness of 0.10 meters in the heavyweight case. These dimensions were not changed during the simulations. The node locations and the thickness of each material are shown. The density of the exterior and interior insulation was assumed to be negligible compared to the density of the thermal mass; thus, insulation nodes were placed only on the surface. The thermal mass was modeled with eight nodes. Prior to selecting 8 nodes, the number of nodes was varied until

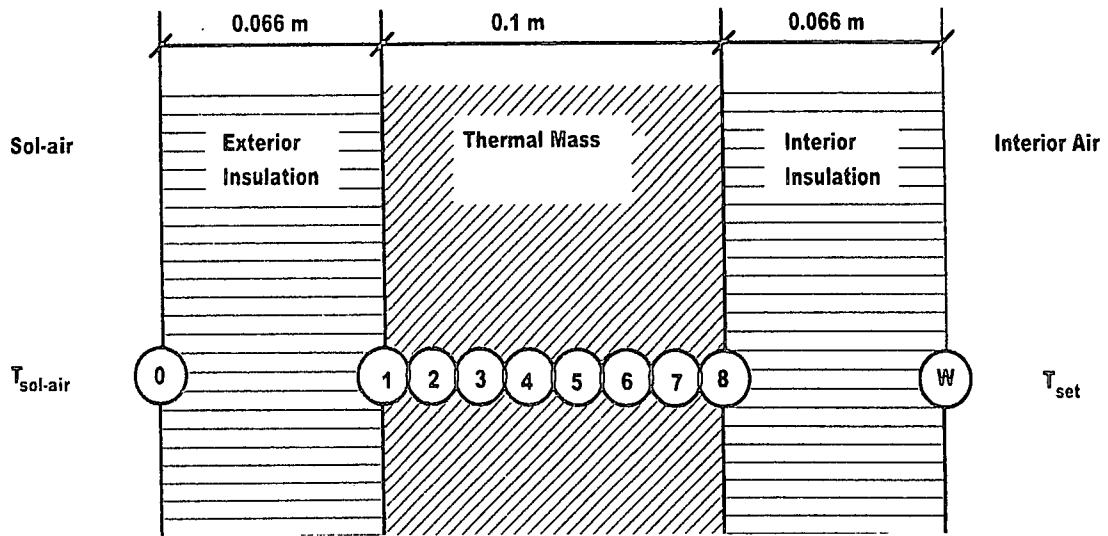


Figure 2.1: Wall configuration used in finite-difference model

there was confidence that the number of nodes did not affect the results. The simulation employed a one-dimensional, forward, explicit solution technique. To eliminate initial conditions, the model was run until solutions converged to at least four significant figures. The same convection coefficients were used as specified in BESTEST, $29.3 \text{ W/m}^2\text{K}$ for the exterior and $8.26 \text{ W/m}^2\text{K}$ for the interior.

Originally the exterior insulation was assigned the thermal conductance value of $0.607 \text{ W/m}^2\text{K}$ as specified in BESTEST. The interior insulation was assigned a thermal conductance value of $79.5 \text{ W/m}^2\text{K}$ which is larger value than that of plasterboard to ensure there appeared to be no insulation on the interior. The thermal conductance of the thermal mass was assigned the value of $5.1 \text{ W/m}^2\text{K}$. The density and specific heat of the thermal mass was considered as a product and varied from 0 to

$1.4 \times 10^6 J/m^3 K$. The values used for this product in the simulations were not representative of any specific materials but used only to gain insight as to the relationship between thermal mass and thermal transmission.

The sol-air temperature was modeled as a sine wave and was assigned a mean temperature and amplitude. Sol-air includes the effect of solar radiation on a building's surface. It is calculated by adding the product of the solar radiation absorptivity of a surface and the global solar irradiance on the surface divided by the convection coefficient to the actual air temperature. The mean and/or amplitude temperatures were changed to represent different possible climate conditions.

2.2: Simulation Results

The finite-difference model was used to complete a matrix of results of the effects of thermal mass on thermal transmission. The mean temperature of the exterior sol-air temperature was varied from $0^\circ C$ to $30^\circ C$. In each case, the amplitude of the exterior sol-air temperature was varied from $0^\circ C$ to the extreme of $40^\circ C$. In each of the combinations of these cases, the thermal mass was varied from 0 to $1.4 \times 10^6 J/m^3 K$. The inside air temperature was held constant at $20^\circ C$. No internal generation, no infiltration, or windows were considered.

The results of the effect of thermal mass on thermal transmission, with exterior sol-air sinusoidal temperature variation and constant inside air temperature, are presented with two mean temperature/amplitude

temperature combinations. In both cases, the inside air temperature is fixed at 20°C and the exterior sol-air temperature varies with an amplitude of 10°C . In the first case, the mean exterior sol-air temperature was 20°C , resulting in an exterior sol-air temperature varying from 10°C to 30°C . In the second case, the mean exterior sol-air temperature was 15°C , resulting in an exterior sol-air temperature varying from 5°C to 25°C .

The first case, with a mean exterior sol-air temperature of 20°C , demonstrates the effect of thermal mass on the time-temperature profile within the thermal mass. Figure 2.2 plots the time-temperature profile over a 24 hour cycle for three points within a hypothetical wall with zero thermal mass. The thermal mass was set to zero by setting the specific heat of the material equal to 0. Node 1 is on the outside surface of the thermal mass. Node 5 is in the mid portion of the thermal mass, and node 8 is on the inside surface of the thermal mass, the side to the constant 20°C air. The thermal mass has a thickness of 0.1 meter and a U-factor of $5.1\text{ W/m}^2\text{K}$. The temperature peaks at hour 15 for all three nodes, which is the hour at which the exterior sol-air temperature peaks. The temperature reduces linearly through the material as expected.

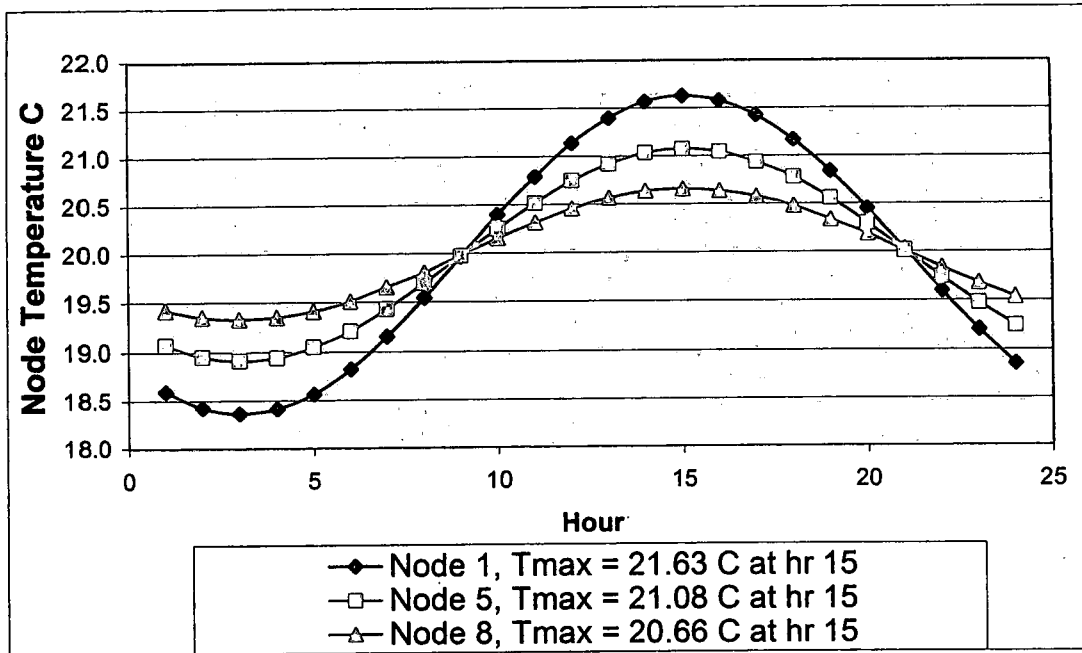


Figure 2.2: Time-temperature profile through thermal mass with interior temperature of 20 °C, exterior sol-air temperature of 20 °C and a temperature amplitude of 10 °C. Thermal mass density-specific heat product set to zero.

Figure 2.3 plots the same nodes as Figure 2.2, but the material has a thermal mass of $1.4 \times 10^5 \text{ J/K} \cdot \text{m}^3$. The peak temperature of node 1 has been reduced from 21.63 °C to 20.85 °C, and its peak temperature hour is now 18, a delay of 3 hours. The peak temperature of node 5 has been reduced from 21.08 °C to 20.53 °C and the peak temperature hour is now 20, a delay of 5 hours [4, 16]. The peak temperature of node 8 has been reduced from 20.66 °C to 20.32 °C and the peak temperature hour is now greater than 20, a delay of greater than 5 hours. The reduction in temperature of node 8 is only 0.34 °C but this reduction represents 52% of the temperature difference between the inner surface of the thermal mass

and the inside air temperature set point of $20\text{ }^{\circ}\text{C}$ and represents a 52% reduction in thermal transmission.

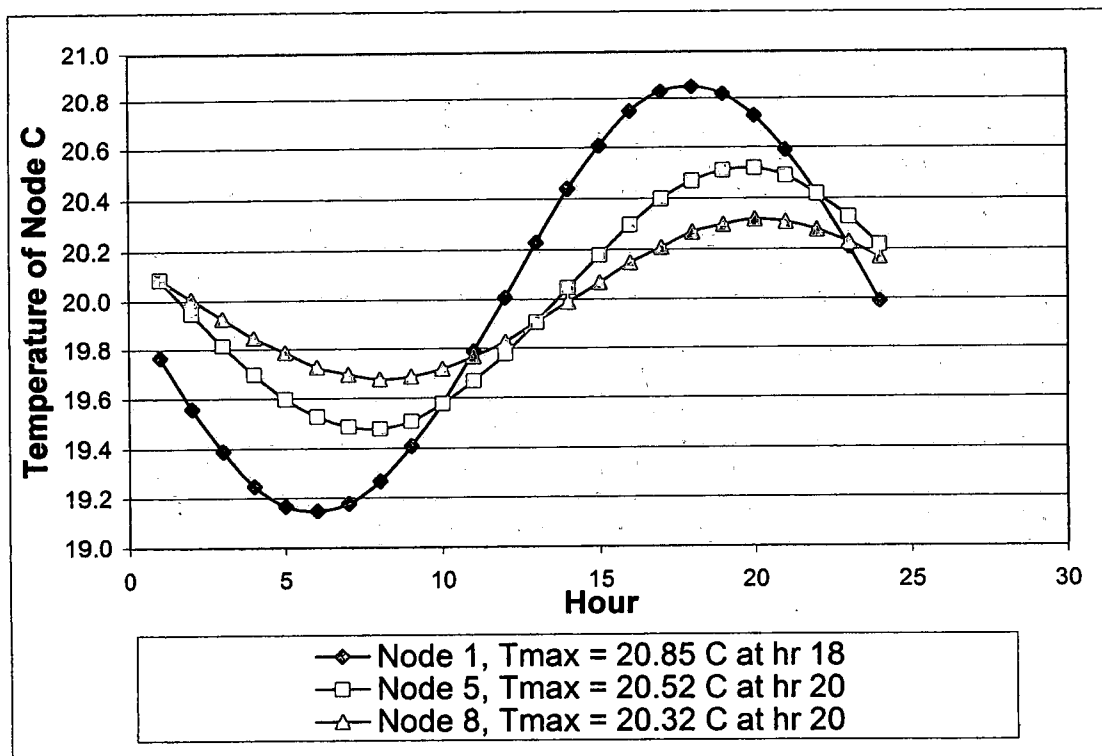


Figure 2.3 Time-temperature profile through thermal mass with interior temperature of $20\text{ }^{\circ}\text{C}$, exterior mean sol-air temperature of $20\text{ }^{\circ}\text{C}$ and a temperature amplitude of $10\text{ }^{\circ}\text{C}$. Thermal mass density-specific heat product set to $1.4 \times 10^6\text{ J/K} \cdot \text{m}^3$

The thermal mass reduces the amplitude of the temperature of each node. The mean, average, temperature of each node remains the same as with no thermal mass and the mean temperature profile through the thermal mass remains linear between the exterior and interior nodes.

Equation (2.1) gives the total heat transferred between node 8 and the inside air over a 24 hour period. Solution of the equation for the zero-mass case, when the amplitude of node 8 is $0.66\text{ }^{\circ}\text{C}$ gives a heat flux of $37.7\text{ WH/m}^2 \cdot \text{day}$. Solution of Equation (2.1) for the high thermal mass case,

when the amplitude of node 8 is 0.32°C , gives a heat flux of $18.3 \text{ WH} / \text{m}^2 \cdot \text{day}$. The reduction in heat load is 52%, which is the identical heat flux and reduction determined from the finite difference solution.

$$Q \left[\frac{\text{WH}}{\text{m}^2 \text{day}} \right] = U \left\{ \left[T_{amp} \int_0^{\pi} \sin \theta d\theta \right] \right\} \frac{1}{2\pi} 24 \frac{\text{hr}}{\text{day}} \quad (2.1)$$

Q is the total heat flux over one 24-hour temperature cycle. T_{amp} is the sol-air temperature amplitude above and below the mean temperature. As the density-specific heat of the thermal mass approached infinity, the temperature amplitude approaches zero and the heat flux approaches zero. Therefore, it can be stated: if the mean cyclic exterior sol-air temperature is equal to the interior temperature set point, the heat flux and thermal loss due to thermal transmission approach zero as the thermal mass approaches infinity. Thus the thermal load is eliminated. The conductance of the interior air film, U , with units of $\text{W} / \text{m}^2 \text{K}$ is between the inner node of the thermal mass 8 and the interior air.

$$U \left[\frac{\text{W}}{\text{m}^2 \text{K}} \right] = \frac{1}{\frac{1}{h_i} + \frac{1}{U_i}} \quad (2.2)$$

$$U \left[\frac{\text{W}}{\text{m}^2 \text{K}} \right] = \frac{1}{\frac{1}{8.26} \frac{\text{m}^2 \text{K}}{\text{W}} + \frac{1}{79.5} \frac{\text{m}^2 \text{K}}{\text{W}}}$$

$$U \left[\frac{\text{W}}{\text{m}^2 \text{K}} \right] = 7.48 \frac{\text{W}}{\text{m}^2 \text{K}}$$

h_i is the interior convection coefficient and U_i is the factor between node 8 and the interior air. Solving Equation (2.1) for a T_{amp} of $0.66\text{ }^{\circ}\text{C}$ gives a heat flux of $37.7\text{ WH}/\text{m}^2\text{day}$. This is the solution for no thermal mass. Solving Equation (2.1) for a T_{amp} of $0.32\text{ }^{\circ}\text{C}$ gives a heat flux of $18.3\text{ WH}/\text{m}^2\text{day}$.

To further demonstrate the effects of thermal mass on thermal transmission, Figure 2.4 plots the time-temperature profile for node 8 with increasing values of the thermal mass. For 0 thermal mass, the heating thermal load is $37.7\text{ WH}/\text{m}^2\text{day}$; when the thermal mass is increased to $5.6 \times 10^6\text{ J/K} \cdot \text{m}^3$, the heating thermal load is reduced to $4.3\text{ WH}/\text{m}^2\text{day}$. The heating thermal load is defined as the quantity of heat that must be added to keep the inside air temperature constant. Similarly, the cooling thermal load is the quantity of cooling required to keep the inside air temperature constant. When the mean outdoor air temperature is the same as the indoor air temperature, as in this case, the heating and cooling thermal loads are equal. The time delay increases from 4 hours to 10 hours and the peak temperatures decrease from $0.66\text{ }^{\circ}\text{C}$, to $0.07\text{ }^{\circ}\text{C}$. Figure 2.5 plots the heating thermal load with increasing thermal mass. The thermal load approaches zero with thermal mass. Figure 2.6 plots the amplitude of node 8 with increasing thermal mass. The amplitude approaches zero with increasing thermal mass. Figure 2.7 plots the temperature time delay of node 8 with respect to the sol-air temperature.

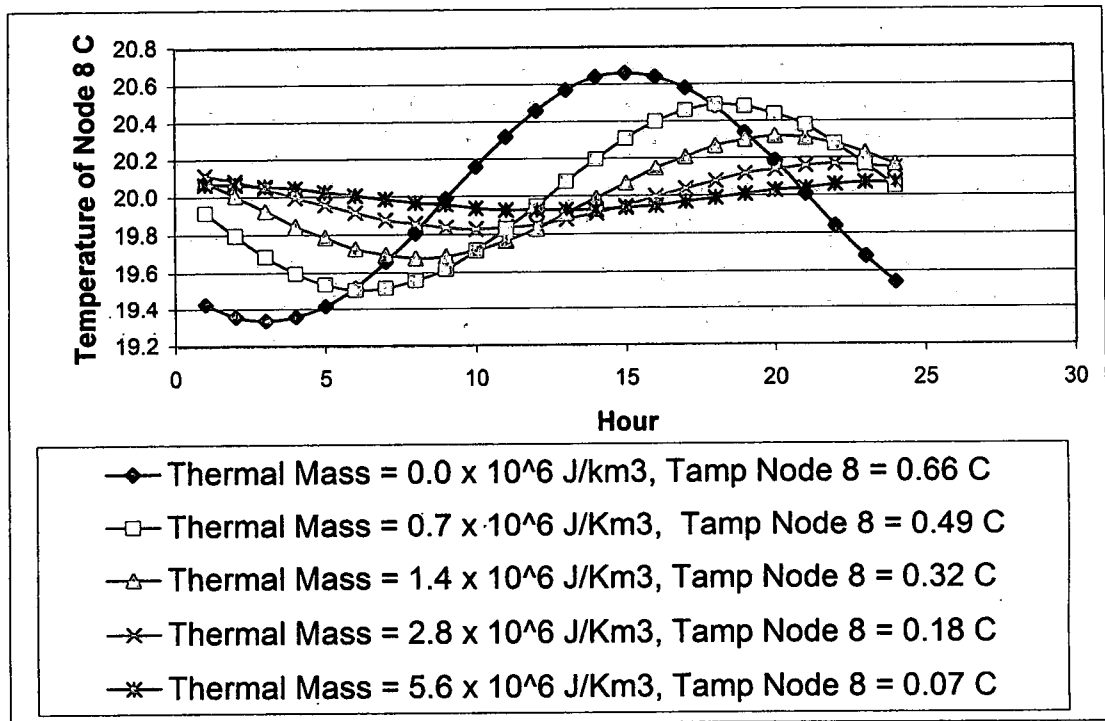


Figure 2.4 Time-temperature profile of node 8 on inner surface of thermal mass with interior temperature of 20°C , exterior mean sol-air temperature of 20°C and a temperature amplitude of 10°C . Thermal mass density-specific heat product increased from to $5.6 \times 10^6 \text{ J/K} \cdot \text{m}^3$.

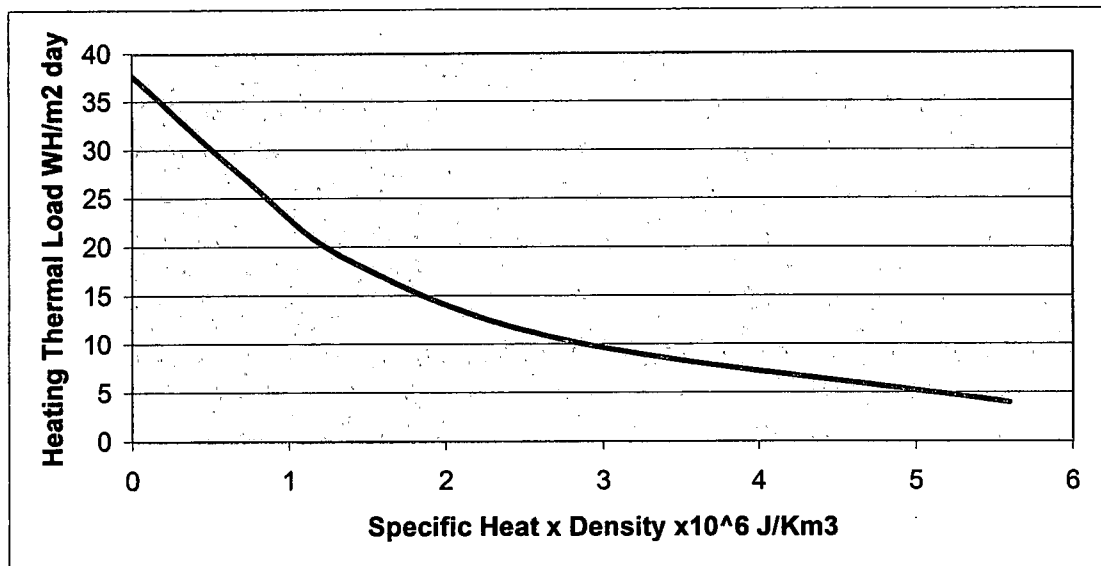


Figure 2.5 Heating thermal load with interior temperature of 20°C , exterior mean sol-air temperature of 20°C and a temperature amplitude of 10°C . Thermal mass density-specific heat product increased from to $5.6 \times 10^6 \text{ J/K} \cdot \text{m}^3$.

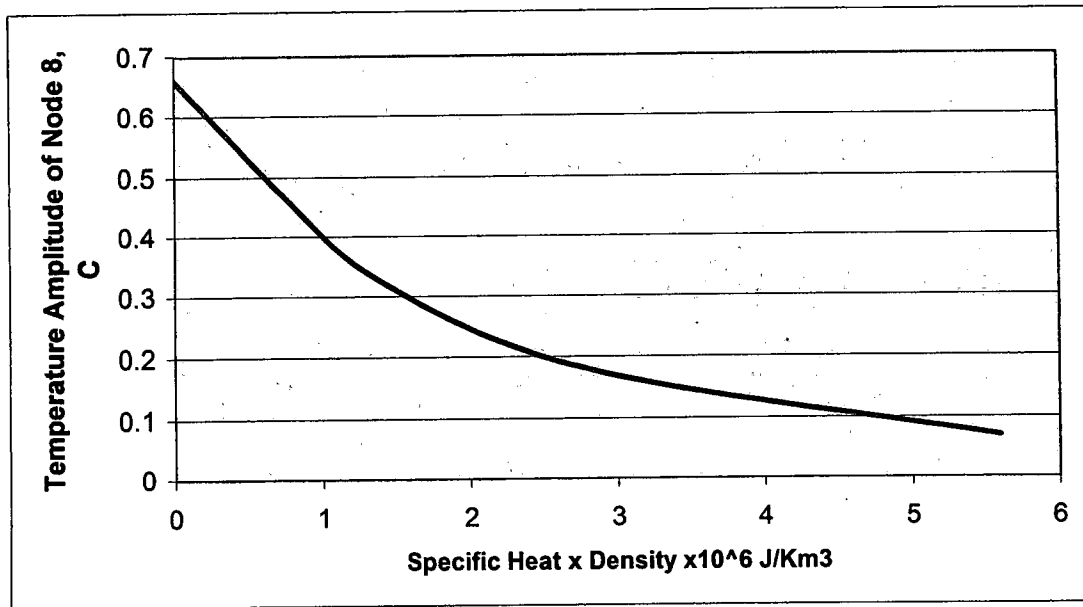


Figure 2.6 Amplitude temperature of node 8 with interior temperature of 20°C , exterior mean sol-air temperature of 20°C and a temperature amplitude of 10°C . Thermal mass density-specific heat product increased from to $5.6 \times 10^6 \text{ J/K} \cdot \text{m}^3$.

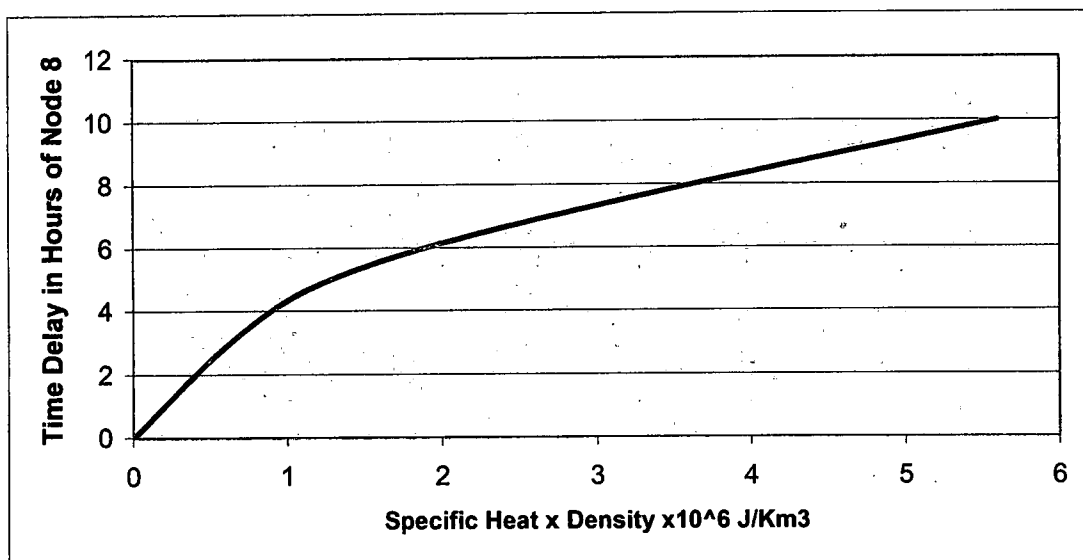


Figure 2.7 Temperature time delay of node 8 with respect to the sol-air temperature with interior temperature of 20°C , exterior mean sol-air temperature of 20°C and a temperature amplitude of 10°C . Thermal mass density-specific heat product increased from to $5.6 \times 10^6 \text{ J/K} \cdot \text{m}^3$.

The second case, with the mean exterior sol-air temperature of 15°C , demonstrates the bounds or conditions under which thermal mass affects

thermal transmission. In addition, it demonstrates the lower limit of net thermal transmission below which increasing thermal mass has no effect on net thermal transmission. Figure 2.8 plots the time-temperature profile of node 8 with increasing values of thermal mass. The mean exterior sol-air temperature is 15°C . The exterior sol-air temperature amplitude is 10°C . The temperature amplitude of node 8 decreases as the value of the thermal mass increases, while the mean temperature of 19.6685°C remains the same. Thus, thermal mass affects only the amplitude and time lag, not the mean temperature. Figure 2.9 plots the heating thermal load with increasing

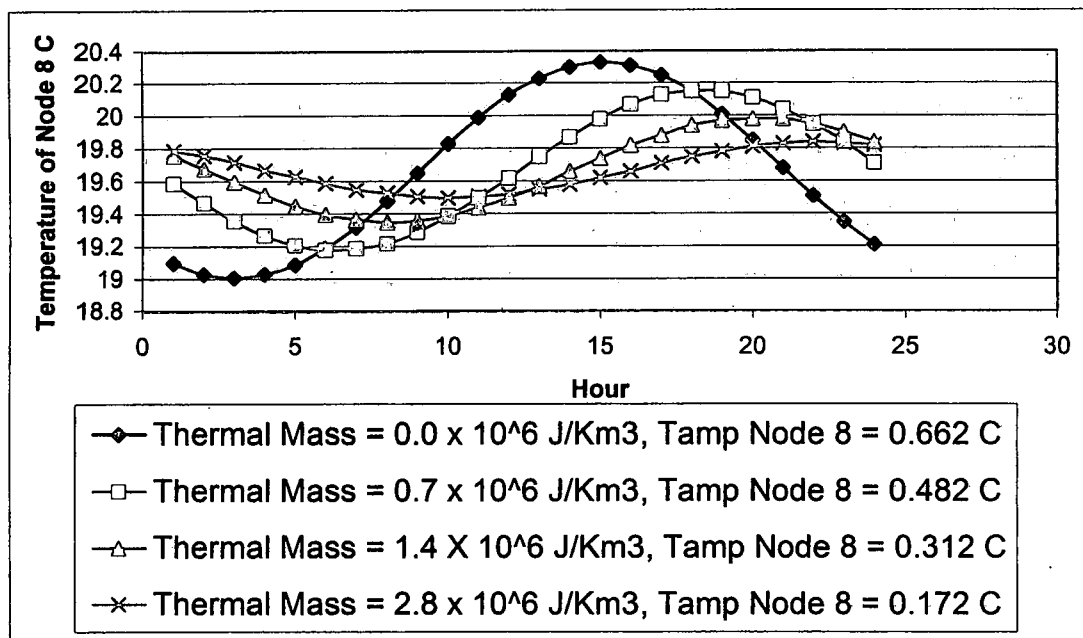


Figure 2.8 Time-temperature profile of node 8 on the inner surface of the thermal mass with interior temperature of 20°C , exterior mean sol-air temperature of 15°C and a temperature amplitude of 10°C . Thermal mass density-specific heat product is varied from 0 to $2.8 \times 10^6 \text{ J/K} \cdot \text{m}^3$

thermal mass. The thermal load reaches a minimum of $59.58 \text{ WH/m}^2\text{day}$ at approximately $1.4 \times 10^6 \text{ J/Km}^3$. At that point, the peak amplitude

temperature is at the interior set point temperature of 20°F . Further increasing thermal mass decreases the amplitude of node 8 but does not decrease the cycle summation of the temperature difference between node 8 and the interior set point. Figure 2.10 plots the amplitude of node 8 with increasing thermal mass. The amplitude approaches zero with increasing thermal mass.

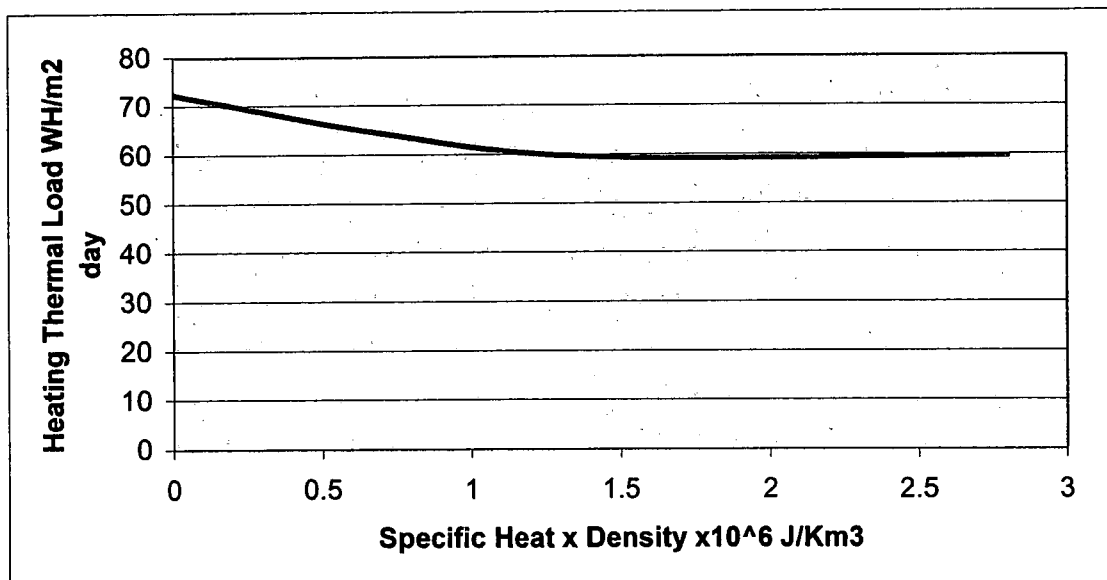


Figure 2.9 Amplitude temperature of node 8 on the inner surface of the thermal mass with interior temperature of 20°C , exterior mean sol-air temperature of 15°C and a temperature amplitude of 10°C . Thermal mass density-specific heat product is varied from 0 to $2.8 \times 10^6 \text{ J/K} \cdot \text{m}^3$

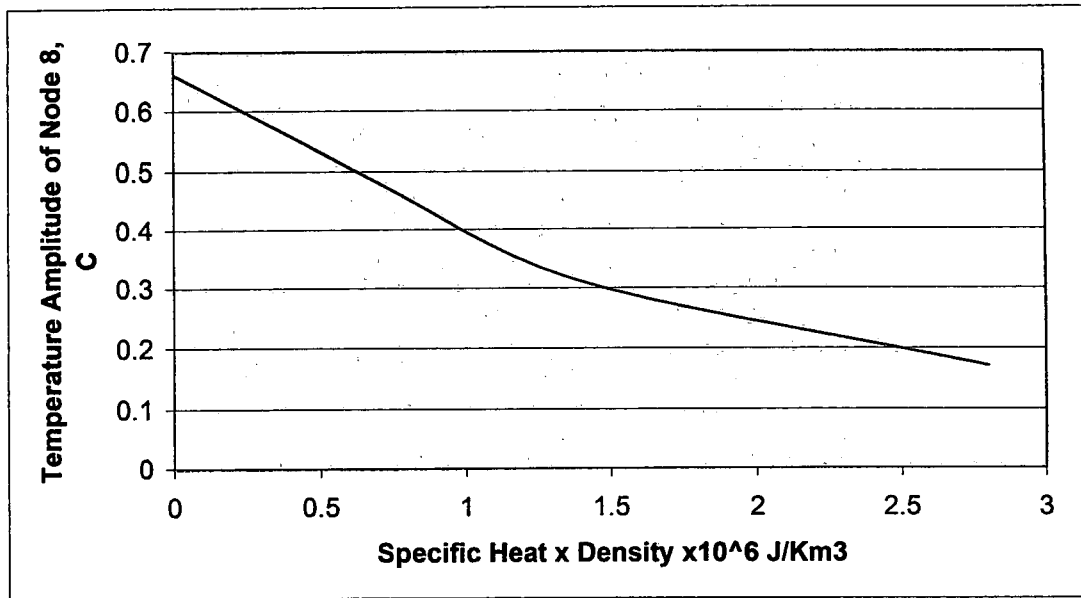


Figure 2.10 Amplitude temperature of node 8 on the inner surface of the thermal mass with interior temperature of 20°C , exterior mean sol-air temperature of 15°C and a temperature amplitude of 10°C . Thermal mass density-specific heat product is varied from 0 to $2.8 \times 10^6 \text{ J/K} \cdot \text{m}^3$

The relation for the thermal load when the mean temperature of node 8 is below the interior air temperature, and the peak temperature of node 8 is above the interior air temperature is shown in Equation (2.3). This equation considers the difference between the interior air temperature and the node 8 temperature; hence, the appropriate U-factor is also between node 8 and the interior air. The equation is also valid if the exterior air mean temperature and amplitude were used with the overall U-factor of the wall. When the mean temperature of node 8 is set to 19.6685°C , Equation (2.3) gives the heating thermal load for zero thermal mass as $72.4 \text{ WH/m}^2\text{day}$. When the thermal mass is increased to $0.7 \times 10^6 \text{ J/K} \cdot \text{m}^3$, the heating thermal load is $64.4 \text{ WH/m}^2\text{day}$. When the thermal mass is approximately $1.4 \times 10^6 \text{ J/K} \cdot \text{m}^3$ the

thermal load reaches a minimum of $59.58 \text{ WH}/m^2\text{day}$. These results are equivalent to the thermal loads determined from the finite-difference simulation.

$$Q_{\text{heat}} \left[\frac{\text{WH}}{m^2 \text{ day}} \right] = U \times \left[\begin{array}{l} T_{\text{set}} - T_{\text{mean node 8}} \\ + \left\{ 2T_{\text{amp node 8}} \cos \left(\sin^{-1} \left(\frac{T_{\text{set}} - T_{\text{mean node 8}}}{T_{\text{amp node 8}}} \right) \right) \right. \\ \left. - 2(T_{\text{set}} - T_{\text{mean node 8}}) \left(\frac{\pi}{2} - \sin^{-1} \left(\frac{T_{\text{set}} - T_{\text{mean node 8}}}{T_{\text{amp node 8}}} \right) \right) \right\} \frac{1}{2\pi} \end{array} \right] \times 24 \frac{\text{hr}}{\text{day}} \quad (2.3)$$

The relation for the thermal transmission when the mean temperature and the peak temperatures of node 8 are below the interior air temperature is shown in Equation (2.4). The amplitude is reduced by additional thermal mass, but the summation of the temperature difference is the same as long as the peak node temperature is less than or equal to the interior air set point. Solving for the thermal load in the above case, with an interior temperature of 20°C and a mean temperature of node 8 of 19.6685°C , the heating thermal load has a minimum value of $59.5 \text{ WH}/m^2\text{day}$.

$$Q_{heating} \left[\frac{WH}{m^2 day} \right] = U \int_0^{24} (T_{set} - T_{node"8"}) dt$$

$$Q_{heating} \left[\frac{WH}{m^2 day} \right] = U (T_{set} - T_{mean node"8"}) \frac{24h}{day} \quad (2.4)$$

$$Q_{heating} \left[\frac{WH}{m^2 day} \right] = 7.48 \frac{W}{m^2 K} (20C - 19.6685C) \frac{24h}{day}$$

$$Q_{heating} \left[\frac{WH}{m^2 day} \right] = 59.5 \frac{WH}{m^2 day}$$

2.3: Maximum Thermal Load Reduction with Thermal Mass

Based on the results presented so far, the following observations about the relationship between thermal mass, thermal transmission, and heating load can be made [17]:

a. When the mean cyclic exterior sol-air temperature is equal to or greater than the interior set point temperature, the heating thermal load can be completely eliminated with thermal mass.

b. When the mean cyclic exterior sol-air temperature is below the interior set point temperature and the peak exterior sol-air temperature is above the interior set point temperature, the heating thermal load can be reduced to a minimum of a variation of Equation (2.4).

$$Q_{heating} \left[\frac{WH}{m^2 \text{ day}} \right] = U_{total} \frac{W}{m^2 C} (T_{set} - T_{mean \text{ exterior air}}) C \frac{24hr}{day}$$

- c. When the mean cyclic exterior sol-air temperature and the peak exterior sol-air temperature are below the interior set point temperature, thermal mass does not reduce the net thermal transmission and the net heating thermal load.

Similarly, the results presented so far support the following observations about the relationship between thermal mass and cooling load:

- d. When the mean cyclic exterior sol-air temperature is equal to or less than the interior set point temperature, thermal transmission and the cooling thermal load can be completely eliminated with thermal mass.
- e. When the mean cyclic exterior air temperature is above the interior set point temperature, and the minimum exterior air temperature is below the interior set point temperature, the cooling thermal load can be reduced to a minimum of variation of Equation (2.4):

$$Q_{cooling} \left[\frac{WH}{m^2 \text{ day}} \right] = U_{total} \frac{W}{m^2 C} (T_{mean \text{ exterior air}} - T_{set}) C \frac{24hr}{day}$$

f. When the mean cyclic exterior sol-air temperature and the peak exterior air temperature are above the interior set point temperature, thermal mass does not reduce the net thermal transmission and the net cooling thermal load.

2.4: Using Weather Files to Determine Maximum Thermal Load Reduction with Thermal Mass

Thermal mass has two effects on the temperature profile within the thermal mass. First, thermal mass reduces the amplitude of the time-temperature profile. As the thermal mass approaches infinity, the amplitude approaches 0 and the temperature approaches the average of the temperature cycle. Thermal mass also delays the time-temperature profile.

When the peak amplitude temperature is above the interior air temperature set point, decreasing the temperature amplitude will also reduce the net thermal transmission and the net thermal load. The average temperature difference between the exterior sol-air temperature and the interior air temperature is reduced. However, when the peak exterior sol-air temperature is below the interior air temperature, reducing the amplitude does not change the average temperature difference between the exterior sol-air temperature and the interior air temperature and there is no reduction in net thermal transmission and net thermal load.

To determine the minimum thermal load and the maximum thermal load reduction, it is only necessary to determine the average temperature of

the exterior sol-air temperature cycle and use this temperature difference between the exterior sol-air temperature and the interior air temperature to calculate the thermal transmission and thermal load for the duration of that cycle. Thus, Equation (2.5) shows the minimum thermal load obtained by increasing thermal mass as a function of exterior air temperature.

$$ThermalLoad_{\text{minimum}} = U \sum_{i=1}^n (T_{\text{set}} - \text{cycle average temperature})_i (\text{period of the cycle})_i \quad (2.5)$$

In many cases an accurate approximation to Equation (2.5) is obtained by using the 24 hour time average of the hourly sol-air temperature to calculate the thermal load of Equation (2.5).

$$ThermalLoad = U \sum_{i=1}^{8760} (T_{\text{set}} - \bar{T}_{24,i})_i \quad (2.6)$$

where

$$\bar{T}_{24,i} = \frac{\sum_{j=-12}^{12} T_{i+j}}{24} \quad (2.7)$$

To demonstrate the accuracy of Equation (2.5) and (2.6), a finite-difference program was created to model BESTEST qualification procedures for heavy and light buildings using the DRYCOLD weather file. The program was qualified with the 600 and 900 series tests. When qualified, the infiltration, internal generation, or windows were all set to zero.

The finite difference program showed a heating load reduction from 4.7 $WH/m^2 year$ to 4.24 $WH/m^2 year$, which is a reduction of 10%. Applying Equation (2.5) with the DRYCOLD weather file resulted in a heating load reduction of 10%, whereas applying Equation (2.6) resulted in a heating load reduction of 9.5%. Similarly, the finite difference program predicted a reduction in cooling load from 1.11 $WH/m^2 year$ to 0.66 $WH/m^2 year$, which is a reduction of 40%.

Application of Equations (2.5) and (2.6) both resulted in a reduction of 40 %. The Minneapolis, Minnesota, weather file with the finite difference program predicted a heating load reduction of 7% and a cooling load reduction of 33%. Equation (2.6) predicts heating load reduction of 6% and a cooling load reduction of 31%. For Phoenix, Arizona, the finite-difference program predicted a heating load reduction of 38% and a cooling load reduction of 12%. Equation (2.6) predicts respectively 28.4% and 10.8%. The 9.2% difference in heating load reduction in Phoenix is attributed to the estimation of the solar average on surfaces when applying Equations (2.5) and (2.6).

2.5: Summary

Thermal mass reduces the magnitude of diurnal temperature variation in walls and building structures. If the maximum temperature of the cyclic exterior air temperature is higher than the interior air temperature, adding thermal mass reduces the net thermal heating load. If the maximum

temperature of the cyclic exterior air temperature is lower than the interior air temperature, adding thermal mass will not reduce the thermal heating load. Similarly, increasing the thermal mass reduces the cooling thermal load only when the minimum exterior air temperature is below the interior air temperature set point.

Equation (2.5) can predict the minimum thermal load that can be obtained with thermal mass. In many cases, Equation (2.5) can approximate the minimum thermal load with good accuracy. In all cases, Equation (2.5) will yield conservative results with a higher thermal load than the true minimum. In addition, the reduction in temperature amplitude, and therefore the peak thermal load, can be closely approximated by Equation (2.6).

CHAPTER 3

THE EFFECTS OF PCM ON THERMAL TRANSMISSION

Phase change material has a specific heat which will result in a reduction of thermal transmission under the same climate conditions as concluded for thermal mass in Chapter 2. This chapter investigates the required climate conditions for the latent heat of phase change material to reduce thermal transmission and the maximum thermal transmission reduction that can be obtained under the climate condition.

Previous work on the effect of PCM on building heating and cooling loop is summarized below. Impregnating phase change material into wall board to dampen interior air temperatures and reduce the required space conditioning energy and the size of space conditioning equipment has been studied [18]. Test cells were constructed and the data collected verified the simulated results [18]. Phase change material with a melting point of 26 °C has been microencapsulated and placed in concrete exterior building walls [19]. Similar test cubicles were constructed. One was constructed with ordinary concrete and the other with the PCM in the concrete in the exterior walls. The interior air temperature was dampened in the cooling season and suggests a reduction in space cooling requirements. However, there was little or no beneficial effect in the heating season because the outdoor air

temperature did not reach up to the melting temperature of 26°C . The use of two PCM with different melting temperatures has been studied in a roof structure [15]. However, both of the melting temperatures were above the interior comfort temperature and served to reduce only summer season interior temperatures and cooling requirements. PCM has also been studied installed in the hollow cores of concrete building blocks [12]. Analysis has been conducted on the installation of PCM in the hollow cores of brick [20]. The temperature of the brick was above the melting temperature the majority of the time simulated.

3.1: Finite-Difference Model for PCM

A sinusoidal function was used to simulate the outside sol-air temperature. Three outside temperature variations are simulated. The first had a mean outside temperature of 20°C and the temperature amplitude was 8°C for a variation from 12°C to 28°C . The second had a mean outside temperature of 15°C and the temperature amplitude was 8°C for a variation from 7°C to 23°C . The third had a mean outside temperature of 10°C and the temperature amplitude was 8°C for a variation from 2°C to 18°C . In each case the indoor temperature remained constant at 20°C . The first simulation was with the latent heat of fusion set to zero, the second with the latent heat set to 180 kJ/kg and the melting point set at 28°C and

the third with the heat of fusion set at 180 kJ/kg and the melting point set at 18°C .

Figure 3.1 is the configuration of the finite-difference model. The insulation thickness is 0.1524 meter or 6-inches and the thickness of the PCM is 0.0762 meter or 3-inches. The inside and outside convection coefficients remain the same as before, $8.26 \text{ W/m}^2\text{K}$ and $29.3 \text{ W/m}^2\text{K}$ respectively. The thermal conductivity of the PCM was 0.24 W/mK and the thermal conductivity of the insulation was 0.17 W/mK . The density of the PCM was 897 kg/m^3 and its specific heat was 1.85 kJ/kgK . The value of 180 kJ/kg was used for the latent heat. The latent heat was simulated in the finite-difference model by adding the 180 kJ/kg to the specific heat at $\pm 1/2^\circ\text{C}$ the melting temperature of the PCM. In this manner the specific heat and the latent heat were examined separately.

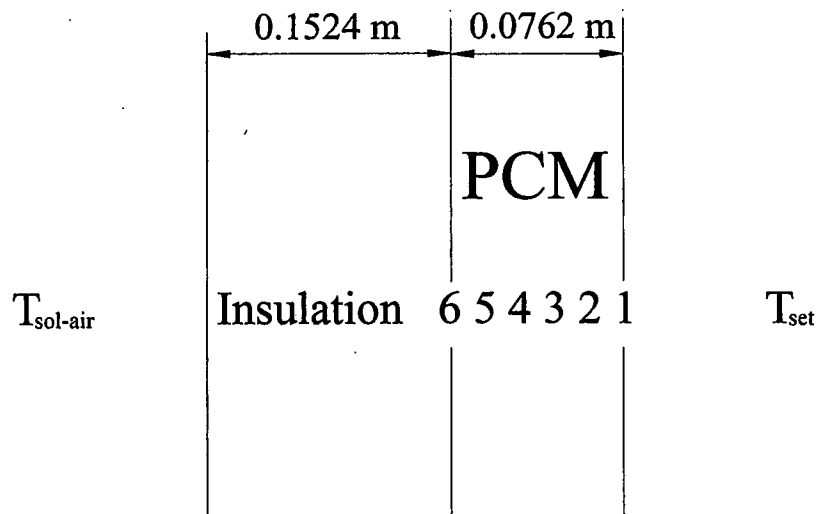


Figure 3.1 Configuration of Finite-Difference Model for PCM

3.2 Simulation Results of PCM

Figure 3.2 below gives the time temperature profile for the nodes of the PCM with the outside sol-air conditions of the average sol-air temperature of 20°C , the amplitude temperature of 8°C , for a sol-air temperature ranging from 12°C to 28°C . The interior set point temperature is constant at 20°C . The melting temperature of the PCM is 28°C . The resulting heating thermal load was determined to be $3.36 \text{ WH}/\text{m}^2\text{day}$ with a time lag of 1.15 hours. With the specific heat set to zero, the heating thermal load was determined to be $9.87 \text{ WH}/\text{m}^2\text{day}$. The resulting $6.51 \text{ WH}/\text{m}^2\text{day}$ per day reduction is due only to the sensible thermal mass of the PCM and not the latent mass.

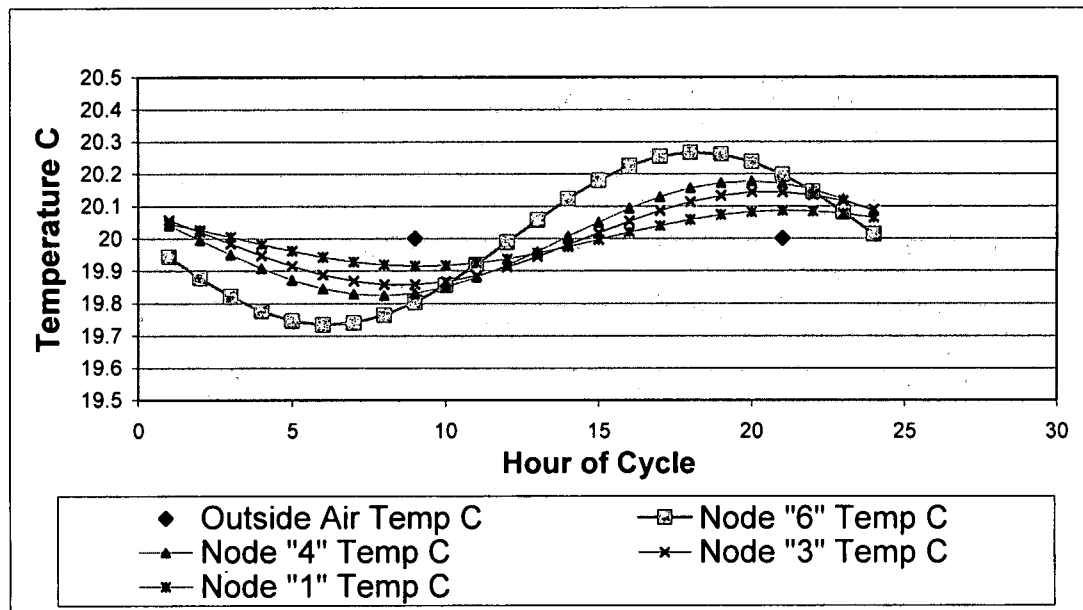


Figure 3.2 Time-temperature profile through PCM with interior temperature of 20°C , exterior sol-air temperature of 20°C and a temperature amplitude of 8°C . Melting temperature of PCM of $28 \pm 1/2^{\circ}\text{C}$. Heating and cooling loads are $3.36 \text{ WH}/\text{m}^2\text{day}$

Figure 3.3 below gives the time temperature profile for the nodes of the PCM with average sol-air temperature of 20°C , with amplitude of 8°C . Thus, the sol-air temperature ranged from 12°C to 28°C . The interior set point temperature is constant at 20°C . The melting temperature of the PCM is now 18°C . The heating and cooling thermal loads remained at $3.36 \text{ WH/m}^2\text{day}$. There was no change in the required thermal load as the PCM temperature did not traverse through its melting temperature in either case.

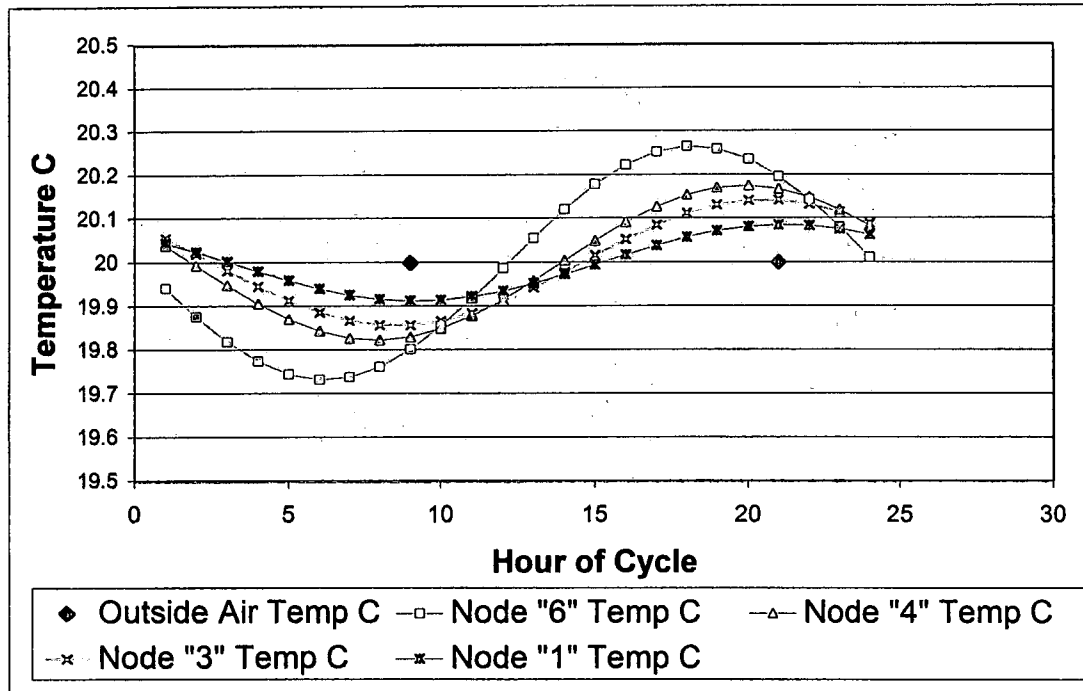


Figure 3.3 Time-temperature profile through PCM with interior temperature of 20°C , exterior sol-air temperature of 20°C and a temperature amplitude of 8°C . Melting temperature of PCM of $18\pm 1/2^{\circ}\text{C}$. Heating and cooling loads are $3.36 \text{ WH/m}^2\text{day}$.

Two simulations with the average sol-air temperature of 15°C and amplitude temperature of 8°C were conducted. The interior set point

temperature is constant at $20\text{ }^{\circ}\text{C}$. The first simulation was with the specific heat of the PCM of 1.85 kJ/kgK and a latent heat of zero. The resulting heating thermal load is $19.38\text{ WH/m}^2\text{day}$ and the cooling thermal load is zero. The second simulation is with specific heat of the PCM 1.85 kJ/kgK and the latent heat of fusion 180 kJ/kg . This simulates $\text{C}_{16}\text{H}_{34}$ with a melting point of $18\text{ }^{\circ}\text{C}$. The heating thermal load was $19.38\text{ WH/m}^2\text{day}$ and a cooling thermal load was zero. The heating and cooling thermal loads remained the same in both of the above simulations because the temperature of the PCM did not traverse through its melting temperature.

None of these simulations resulted in any reduction of thermal transmission. Next paraffin $\text{C}_{16}\text{H}_{34}$ with a melting point of $18\text{ }^{\circ}\text{C}$ and $\text{C}_{18}\text{H}_{38}$ with a melting point of $28\text{ }^{\circ}\text{C}$ were simulated. As before, the PCM temperatures did not go into the melting range.

Next, two simulations were conducted with the insulation located on the inside portion of the wall and the PCM located on the exterior of the wall. The average sol-air temperature was $20\text{ }^{\circ}\text{C}$, with an amplitude temperature of $8\text{ }^{\circ}\text{C}$. Thus, the sol-air temperature ranged from $12\text{ }^{\circ}\text{C}$ to $28\text{ }^{\circ}\text{C}$. The interior set point temperature was constant at $20\text{ }^{\circ}\text{C}$. The first was with the specific heat of the PCM of 1.85 kJ/kgK and a latent heat of fusion of zero. Both the heating and cooling thermal loads were $4.35\text{ WH/m}^2\text{day}$. The specific heat of the PCM resulted in a reduction of the thermal loads from

9.87 WH/m^2day to 4.35 WH/m^2day . Figure 3.4 below gives the time temperature profile for the nodes of the PCM.

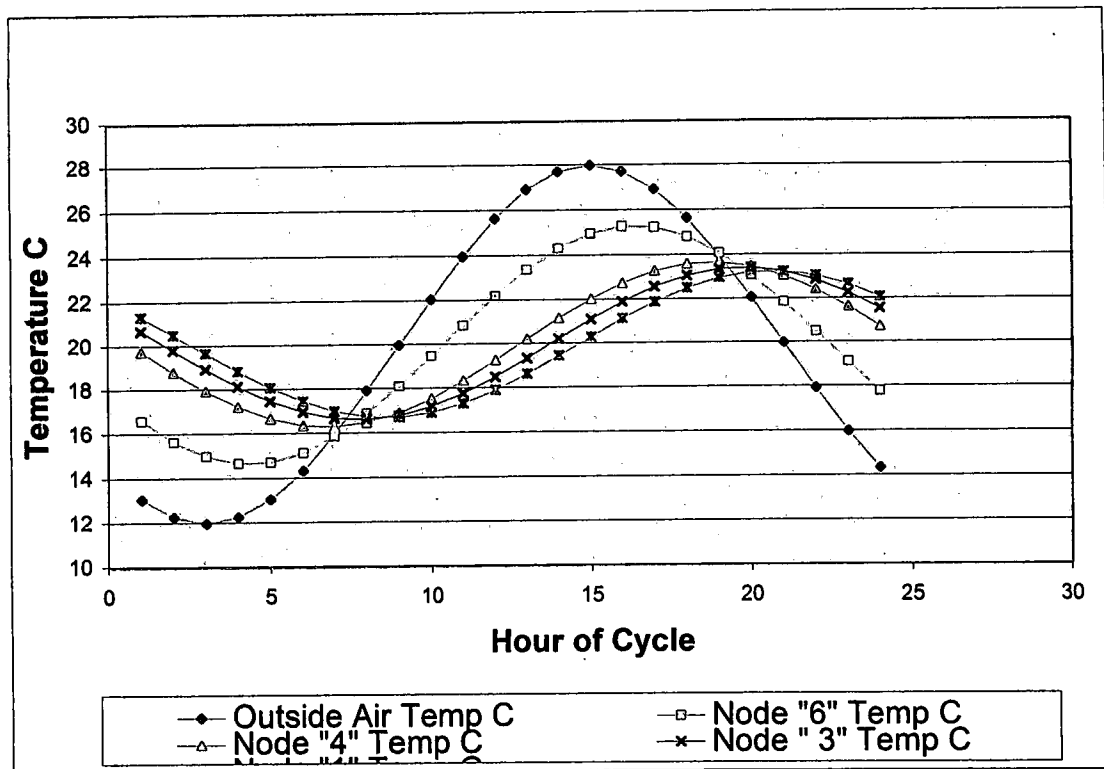


Figure 3.4 Time-temperature profile through PCM with interior temperature of 20 °C, exterior sol-air temperature of 20 °C and a temperature amplitude of 8 °C. Latent heat of PCM zero. Heating and cooling loads are 4.35 WH/m^2day . PCM exterior to insulation.

In the second simulation with the insulation on the interior and the PCM on the exterior, the PCM has a latent heat of 180 kJ/kg at a melting temperature of 18 °C. The time temperature profile is given in Figure 3.5 below. The heating and cooling thermal load was reduced from 4.35 WH/m^2day to 2.47 WH/m^2day . The temperature profile indicates the PCM temperature is now at its melting temperature with a resulting reduction in the thermal loads.

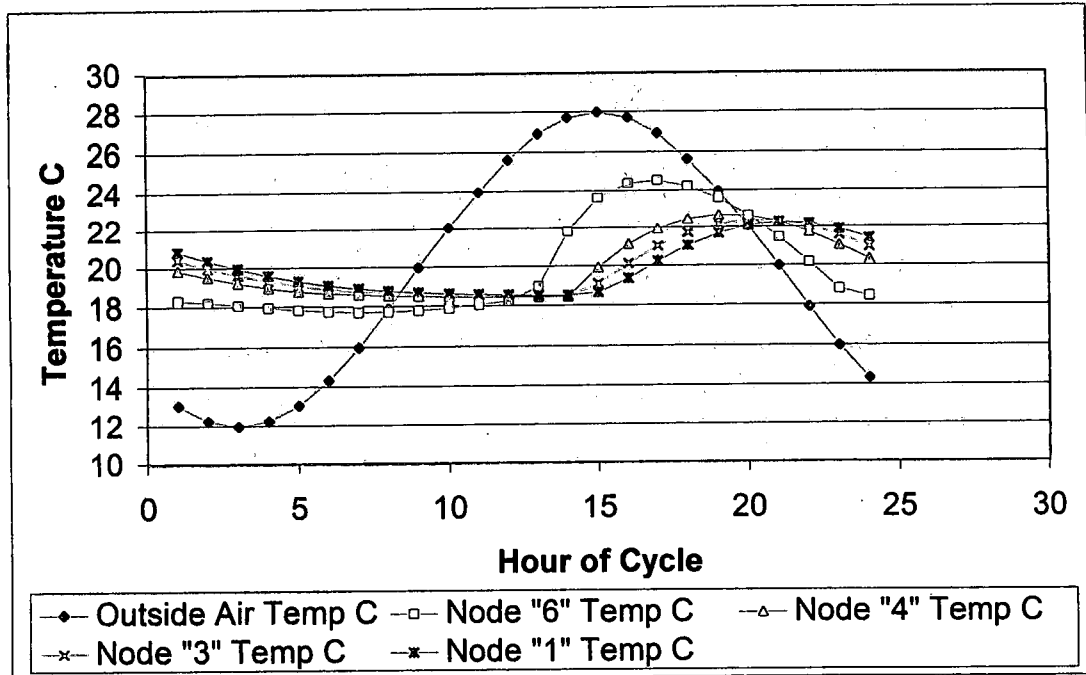


Figure 3.5 Time-temperature profile through PCM with interior temperature of 20°C , exterior sol-air temperature of 20°C and a temperature amplitude of 8°C . Melting temperature of PCM of $18 \pm 1/2^{\circ}\text{C}$. Latent heat of PCM 180 kJ/kg . Heating and cooling loads are $2.47 \text{ WH/m}^2\text{day}$.

Figure 3.5 clearly shows the time-temperature profile is now no longer symmetrical but is flattened at the melting temperature. However, both the heating and cooling thermal loads have been reduced and by the same amount, $1.88 \text{ WH/m}^2\text{day}$. If a comparison is made between the average temperatures over the 24 hour cycle of the simulations with the latent heat of fusion equal to zero and the simulation with the specific heat of 1.85 kJ/kgK and the latent heat of fusion of 180 kJ/kg , it is noted the average temperature of each node over the cycle remains the same. Figure 3.6 below shows this comparison.

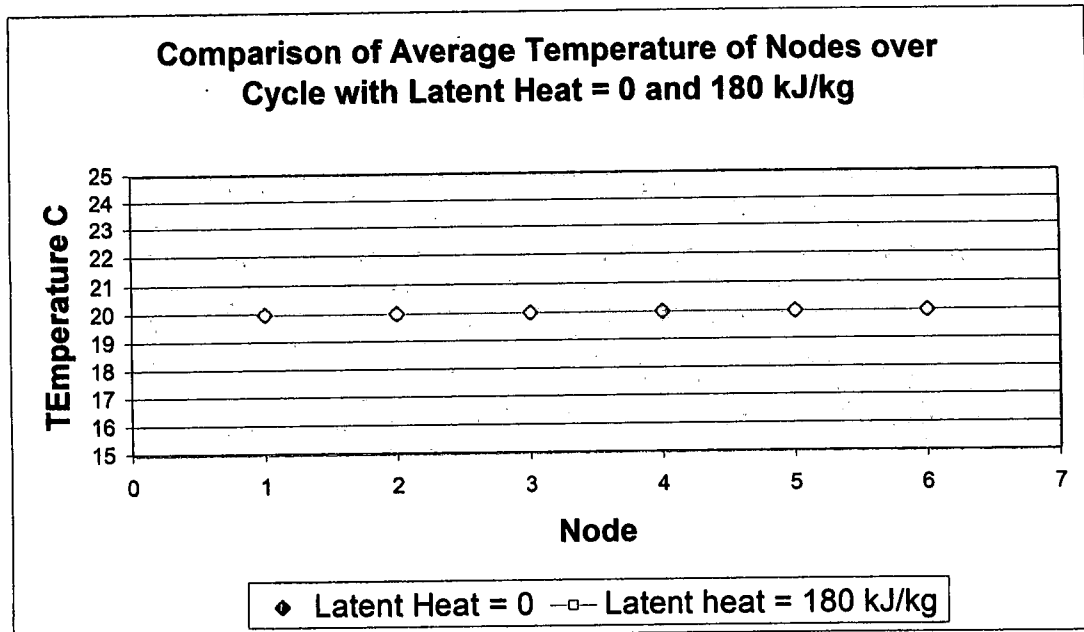


Figure 3.6 Comparison of average node temperatures with latent heat of PCM of 0 kJ/kg and 180 kJ/kg .

3.3 Summary of Effect of PCM on Thermal Load

The conditions under which PCM will affect thermal load are the same as for thermal mass [21]. For a reduction in heating load, the peak cyclic sol-air temperature must be above the interior air set point. For a reduction in cooling load, the minimum cyclic sol-air temperature must be below the interior air temperature set point. However, there is another restriction applied to PCM. The PCM must be installed at a location within the wall that will cause the PCM to pass its melting temperature. If the melting temperature is not traversed, only the sensible thermal mass of the PCM will affect the thermal load and the latent heat of fusion will have no effect on the thermal load.

CHAPTER 4

FINITE-DIFFERENCE MODEL

In the previous finite-difference simulations, the dimensions of the walls were held constant. Properties of thermal mass materials were arbitrarily selected. To proceed and equate the performance of a thermal mass wall with an assigned U-factor to a no-mass wall with another U-factor, it is necessary create finite-difference models under a range of sizes and with properties of standard construction materials such as concrete.

4.1 Finite Difference Model for Concrete

Figure 4.1 is a finite-difference model for concrete. Only the specific heat of the thermal mass indicated by nodes 1 through 6 is considered. The specific heat of the nodes of the two outer and two inner layers is assumed small compared to that of the thermal mass. The thermal mass is initially divided into five equal parts. Next, a study is made to determine the number of divisions required to ensure the solution converges. The required number of divisions is dependent upon the thickness and specific heat of the thermal mass, the amplitude and frequency of the cyclic exterior ambient temperature, and the location of the thermal mass with respect to the insulation and amount of insulation.

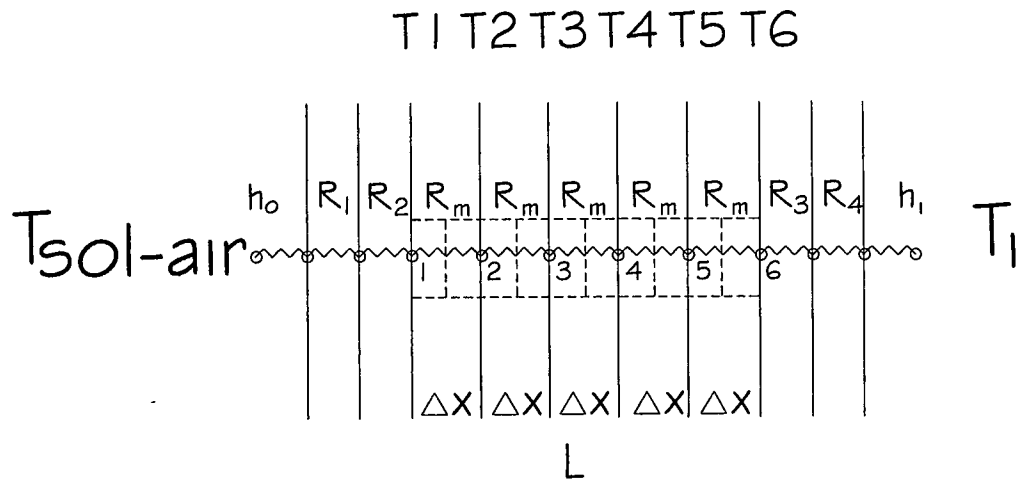


Figure 4.1 Finite-difference model for concrete simulation

4.2 Finite-Difference Equations

An energy balance equation for node 1 is [23]:

$$\frac{(T1 - T_{sol-air})A}{R_{RO}} + \frac{(T1 - T2)A}{R_m} = \rho_m C_{pm} A \frac{\Delta X}{2} \frac{(T1_p - T1)}{\Delta t} \quad (4.1)$$

Rearranging equation (4.1) yields:

$$T1_p = \frac{2\Delta t}{\rho_m C_{pm} \Delta X} \left[\frac{(T1 - T_{sol-air})}{RO} + \frac{(T1 - T2)}{R_m} \right] + T1 \quad (4.2)$$

$$RO = \frac{1}{h_o} + R_1 + R_2 \quad (4.3)$$

$$RI = \frac{1}{h_i} + R_3 + R_4 \quad (4.4)$$

$$R_m = \frac{\Delta X}{k_m} \quad (4.5)$$

Where,

$T1_p$ = Increase in temperature of $T1$ over time interval Δt

$T1$ to $T6$ = Temperature of nodes

R_1, R_2 = Thermal resistances of the exterior materials

R_3, R_4 = Thermal resistances of the interior materials

RO = Total thermal resistance exterior to the thermal mass

RI = Total thermal resistance interior to the thermal mass

ΔX = Thickness of thermal mass between nodes

R_m = Thermal resistance of ΔX

ρ_m = Density of thermal mass

C_{pm} = Specific heat of thermal mass

k_m = Thermal conductivity of thermal mass

h_o = Exterior convection coefficient

h_i = Interior convection coefficient

Δt = Time step

The remaining equations are:

$$T2^p = \frac{\Delta t}{R_m \rho_m C_{pm} \Delta X} (2T2 - T1 - T3) + T2 \quad (4.6)$$

$$T3^p = \frac{\Delta t}{R_m \rho_m C_{pm} \Delta X} (2T3 - T2 - T4) + T3 \quad (4.7)$$

$$T4^p = \frac{\Delta t}{R_m \rho_m C_{pm} \Delta X} (2T4 - T3 - T5) + T4 \quad (4.8)$$

$$T5^p = \frac{\Delta t}{R_m \rho_m C_{pm} \Delta X} (2T5 - T4 - T6) + T5 \quad (4.9)$$

$$T6^p = \frac{2\Delta t}{\rho_m C_{pm} \Delta X} \left[\frac{(T6 - T_i)}{R_i} + \frac{(T6 - T5)}{R_m} \right] + T6 \quad (4.10)$$

4.3 Simulation of Exterior Ambient Temperature with Sinusoidal

A sinusoidal function with a period of 24 hours is used to simulate the cyclic, exterior, ambient temperature. According to The Air Conditioning Contractors of America's, *Manual N Commercial* (Fourth Edition) the highest daily temperature range is 42 °F for Carson City, Nevada [23]. The lowest daily temperature range is 9 °F for Lakeland City Office, Florida. These temperature ranges will be used in the following simulations.

The 2009 International Energy Conservation Code (IECC) specifies the interior design temperatures used for heating and cooling load calculations shall be a maximum of 72 °F (22 °C) for heating and a minimum of 75 °F (24 °C) for cooling [2]. Therefore, in the analysis to determine the required number of divisions for the thermal mass and/or the interior set point temperature is 23 °C. The mean temperature of the outside ambient temperature is 23 °C.

The equation for the sinusoidal simulation of the cyclic, ambient temperature is:

$$T_o = T_{o,mean} + T_{amp} \left[\frac{2\pi \sin(hr-1-9)}{24} \right] + \left[\frac{T_{amp}N}{3600/\Delta t} \left(\sin\left(\frac{2\pi(hr-8)}{24}\right) - \sin\left(\frac{2\pi(hr-1-8)}{24}\right) \right) \right] \quad (4.11)$$

hr from 1 to 24

and

N from 1 to $3600/\Delta t$

The first term is the selected mean temperature, the second term is algebraic addition to the temperature on the hour and the third term is algebraic addition to the temperature between the hours. This results in the selection of a time step, Δt for convergence. The first selection of the time step is 15 seconds or 15/3600 hour. The resulting outside, cyclic, temperature profile is given in Figure 4.2.

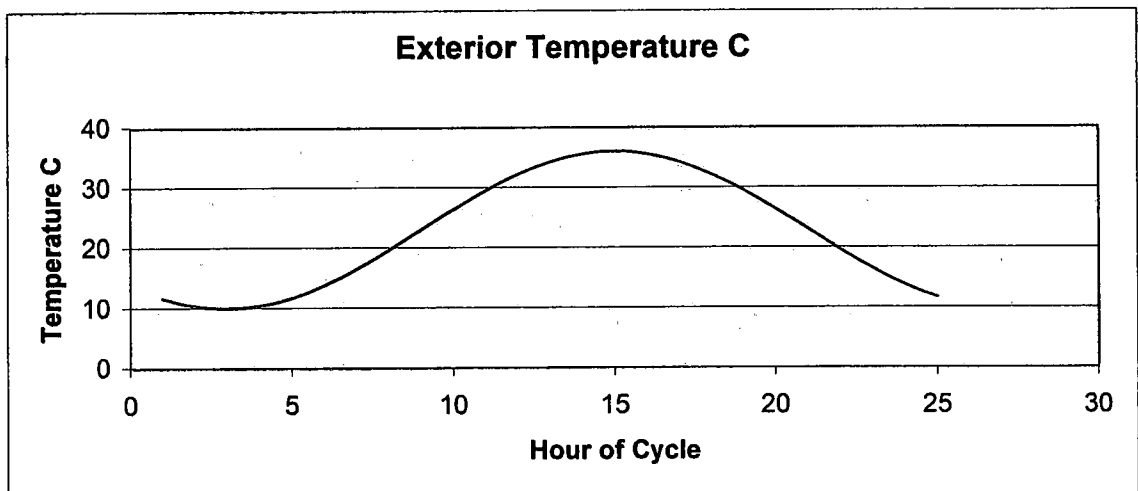


Figure 4.2 Sinusoidal simulation cyclic ambient temperatures

The maximum temperature occurs at 3:00 pm, 1500 hours, which is consistent with the normal time of high daily temperature. This profile will merge with solar data from TMY2 weather files.

4.4 Determination of Required Number of Nodes with Concrete as Thermal Mass

Stone concrete is a standard building material which serves as a thermal mass. Therefore, the properties of concrete are used to determine the required number of nodes for the simulated amount heat transfer through the wall per day to converge. Concrete has a specific heat of $880 \text{ J/kg}\cdot\text{K}$, $0.20 \text{ Btu/lb}_m\text{F}$, a thermal conductivity of $1.4 \text{ W/m}\cdot\text{K}$, $1.04 \text{ Btu/hr}\cdot\text{ft}\cdot\text{F}$ and a density of 2300 kg/m^3 , $144 \text{ lb}_m/\text{ft}^3$. Standard concrete wall thicknesses in the United States range in thickness from 3 inches to 12 inches. Therefore, concrete thicknesses of 3 inch, 6 inch, 9 inch and 12 inch, 0.0762 m, 0.1524 m, 0.2286 m and 0.3048 m respectively, are examined.

The 2009 IECC allows for different R-value tradeoffs for the incorporation of thermal mass into the wall structure depending upon whether the thermal mass is on the exterior or interior of the wall insulation. Therefore, concrete is examined with no insulation, with 1-inch, 3-1/2-inch and 6-inch thick insulation positioned on both the interior and exterior of the thermal mass. The value of thermal conductivity of the insulation is

$0.027 \text{ W/m}\cdot\text{K}$ The wall is covered by $\frac{1}{2}$ -inch thick gypsum board with a thermal conductivity of $0.17 \text{ W/m}\cdot\text{K}$. This range of insulation thicknesses and the thermal conductivity value provide a range of thermal resistances consistent with the 2009 IECC. Convection coefficients for the interior and exterior surfaces of the wall are taken from BESTEST. The exterior convection coefficient is $29.3 \text{ W/m}^2\cdot\text{K}$, $5.16 \text{ Btu/ft}^2\cdot\text{F}$, and the interior convection coefficient is $8.26 \text{ W/m}^2\cdot\text{K}$, $1.45 \text{ Btu/ft}^2\cdot\text{F}$.

Figure 4.3 shows the values of the thermal transmission through a 12-inch thick concrete wall with the different insulation arrangements in Wh/Day for an increasing number of nodes. The difference between the simulated Wh/Day for 12 nodes and 15 nodes is 0.2 %. The 12-inch thick concrete case requires the highest number of nodes for the simulated Wh/Day to converge.

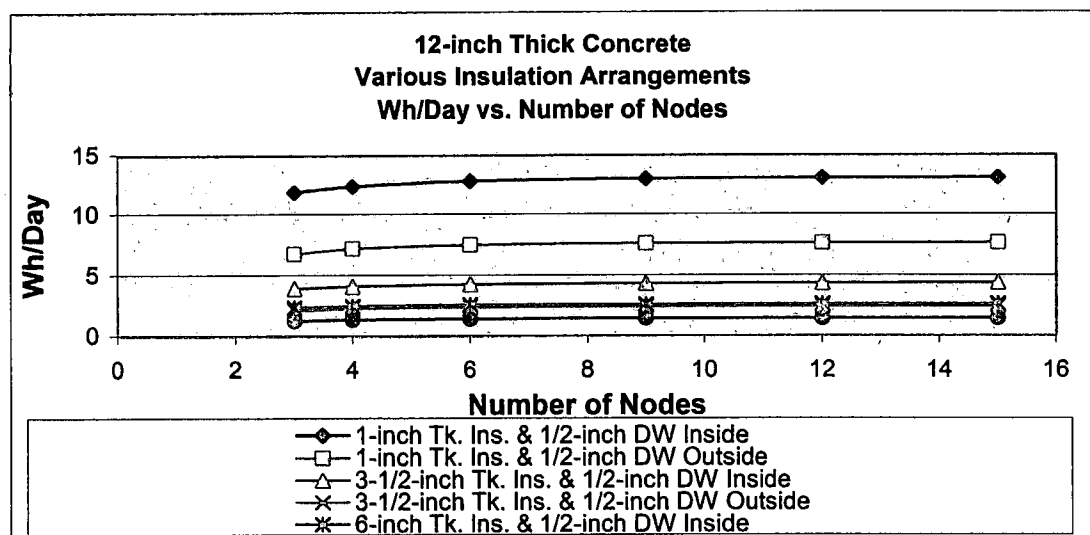


Figure 4.3 Number of nodes vs. insulation arrangements for 12-inch thick concrete

Table 4.1 lists the values in Figure 4 and the percentage difference in the WH / Day obtained by increasing the number of nodes.

Table 4.1

12-inch Thick Concrete Wh/Day vs. Number of Nodes								
Number of Nodes	No Insulation	1-inch tk. Insulation & 1/2-inch DW Inside	1-inch tk. Insulation & 1/2-inch DW Outside	3-1/2-inch tk. Insulation & 1/2-inch DW Inside	3-1/2-inch tk. Insulation & 1/2-inch DW Outside	6-inch tk. Insulation & 1/2-inch DW Inside	6-inch tk. Insulation & 1/2-inch DW Outside	% Change in Wh/Day with Increasing Number of Nodes
3	85.634	11.871	6.777	3.942	2.136	2.363	1.268	
4	85.337	12.370	7.228	4.130	2.293	2.479	1.362	7.40%
6	86.726	12.807	7.521	4.288	2.393	2.575	1.423	4.50%
9	87.498	12.988	7.632	4.353	2.430	2.614	1.445	1.60%
12	87.762	13.046	7.666	4.373	2.442	2.627	1.452	0.50%
15	87.880	13.072	7.681	4.382	2.447	2.632	1.455	0.20%

Number of nodes and percentage change in WH / Day

The simulated Wh / Day for the 1-inch thick insulation with 1/2-inch gypsum board on the inside of the concrete was fit to the curve:

$$\frac{Wh}{Day} = 13.119 - \frac{2.854}{0.254X^2} \quad (4.12)$$

$X = \text{number of nodes}.$

The fitted curve and the simulated data are shown in Figure 4.4. Substituting 1000 nodes into the equation (4.12) yields 13.119 WH / Day . Using this as the simulated solution for an infinite number of nodes allows an estimated simulation error of 0.36 % for 15 nodes, 0.6 % error using 12 nodes, 1.0 % for 9 nodes and 2.4 % for 6 nodes. Actual weather conditions may result in greater temperature changes per unit of time than are given by the sinusoidal

simulation weather; therefore 15 nodes are used in the finite difference model.

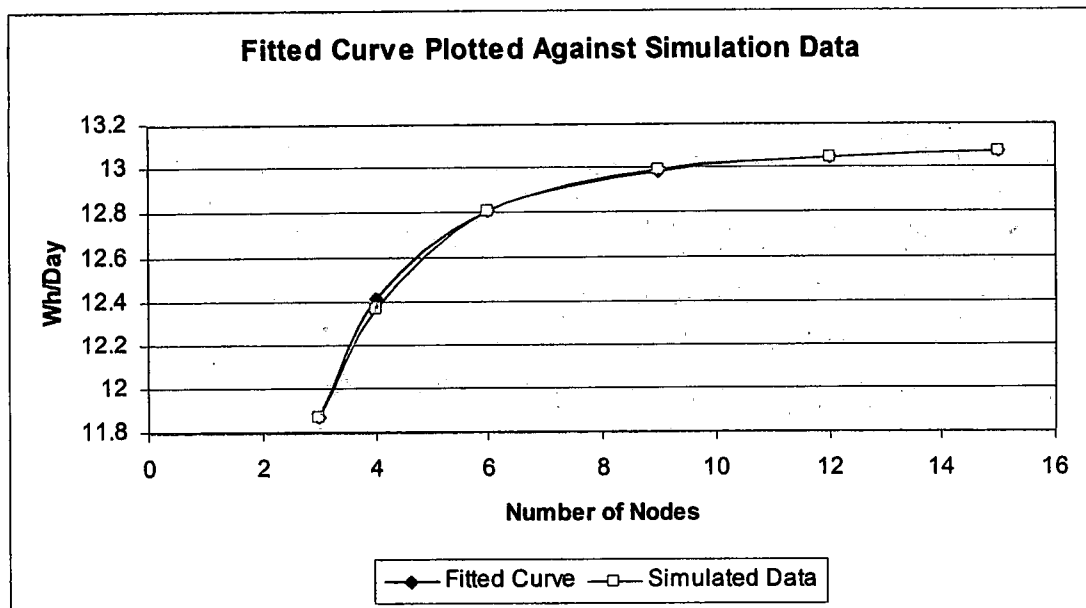


Figure 4.4 Fitted curve of WH / Day vs. simulated WH / Day

Thermal mass wall structure results in a reduction of thermal transmission through the wall under specific cyclic exterior temperature conditions, but it always results in a time lag between the exterior cyclic temperature profile and the temperature profile at the interior of the wall. This time lag is examined relative to the number of nodes.

Figure 4.5 shows the required heating and cooling requirements for a 12-inch thick concrete wall with 1-inch thick insulation and ½-inch gypsum board. The maximum heating requirement is at approximately 1300 hours. The lowest temperature of the sinusoidal temperature simulation is 10 °C at 300 hours. This is a 10 hour time lag.

To estimate this time lag more accurately the intersection of the heating/cooling curve with $Y = 0$ is determined. This intersection is shown in Figure 4.6. The peak heating requirements are 6 hours before this intersection at 1,276 hours. Therefore, the time lag is 9.76 hours.

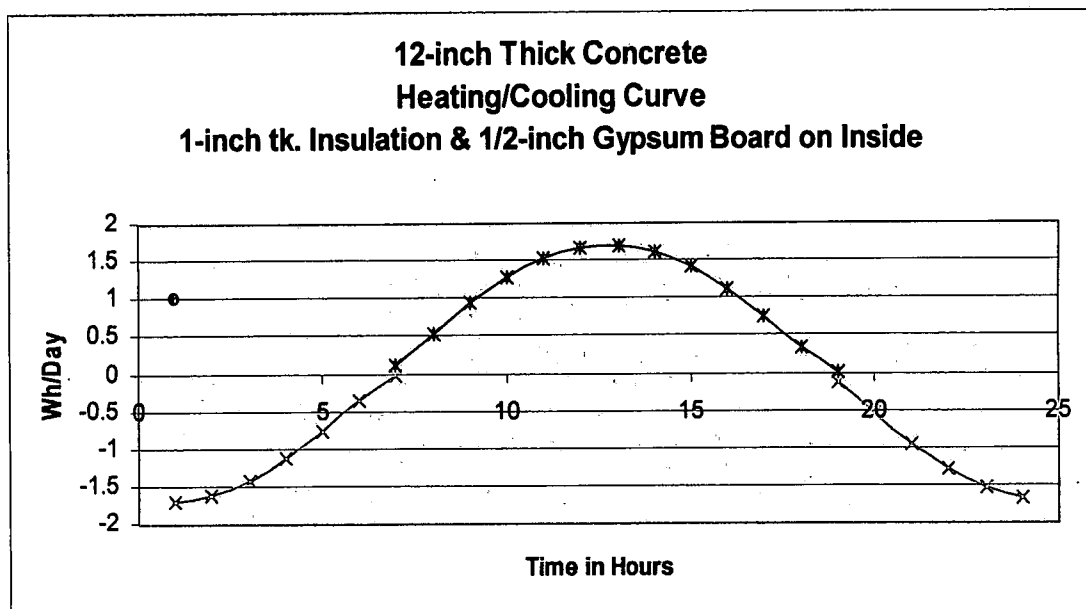


Figure 4.5 Lag time of inner concrete wall

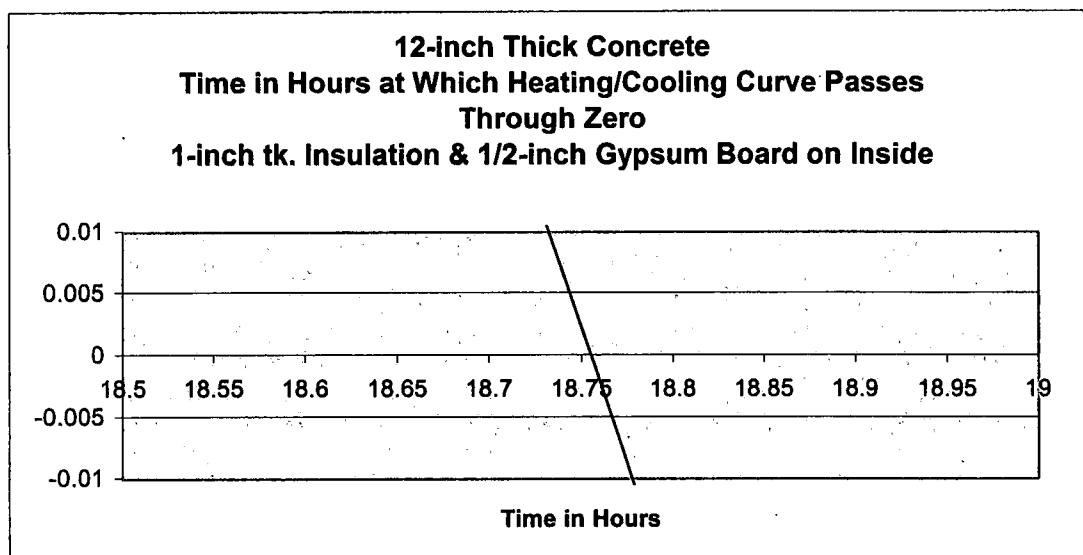


Figure 4.6 Intersection of WH / Day curve with the X axis

Table 4.2 shows the time lag as a function of the number of nodes for 12-inch thick concrete with 1-inch thick insulation and ½-inch thick gypsum board. 15 nodes resulted in an increase of 0.11% from 12 nodes. Therefore, 15 nodes will yield acceptably accurate results for the estimated time lag.

Table 4.2

12-inch Thick Concrete Time Lag in Hours vs. Number of Nodes								
Number of Nodes	No Insulation	1-inch Tk. Insulation & 1/2-inch DW Inside	1-inch Tk. Insulation & 1/2-inch DW Outside	3-1/2-inch Tk. Insulation & 1/2-inch DW Inside	3-1/2-inch Tk. Insulation & 1/2-inch DW Outside	6-inch Tk. Insulation & 1/2-inch DW Inside	6-inch Tk. Insulation & 1/2-inch DW Outside	% Change in Time Lag with Increasing Number of Nodes
3	7.95	9.13	10.46	9.25	10.6	9.27	10.6	
4	8.42	9.5	10.62	9.63	10.74	9.65	10.77	3.08%
6	8.7	9.69	10.67	9.8	10.78	9.83	10.82	1.38%
9	8.78	9.73	10.68	9.84	10.78	9.85	10.82	0.27%
12	8.81	9.76	10.68	9.87	10.82	9.87	10.83	0.23%
15	8.9	9.76	10.69	9.87	10.8	9.88	10.82	0.11%

Time lag vs. percentage change between nodes

4.5 Determination of Required Time Step with Concrete as Thermal Mass

Figure 4.7 shows the $WH / m^2 day$ required for 12-inch thick concrete with 1-inch thick insulation and ½-inch thick gypsum board versus time step, dt . The thermal transmission through the wall is $13.072 WH / m^2 day$ at a time step of 15 seconds, and 13.060 at a time step of zero seconds. Therefore, the estimated error for a time step of 15 seconds is 0.09 %. Figure 4.8 is the time lag vs. the length of the time step. The value of the thermal

transmission converges to 9.76 hours at a time step of 20 seconds.

Therefore, a time step of 15 seconds is used in the simulations.

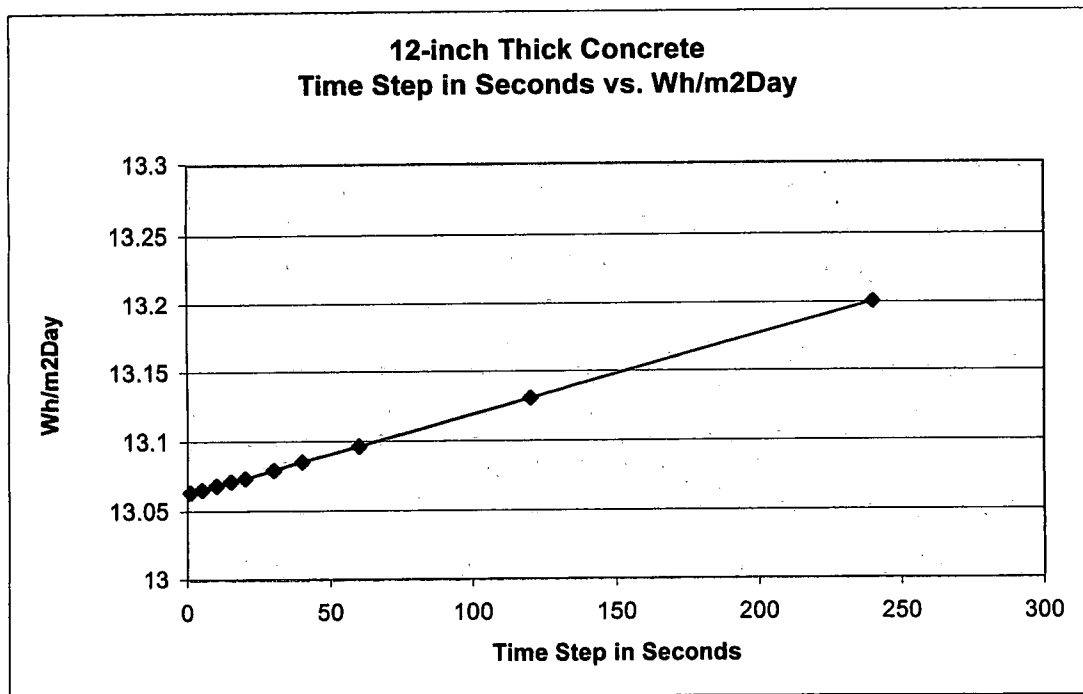


Figure 4.7 Time step, seconds vs. $WH / m^2 day$

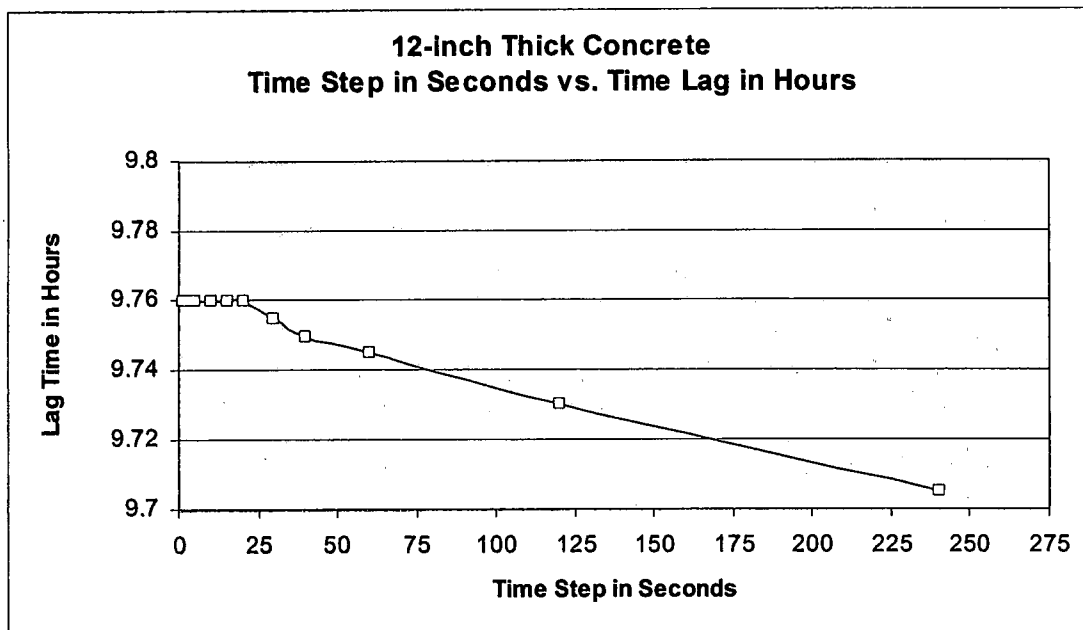


Figure 4.8 Time step vs. lag time in hours

CHAPTER 5

THERMAL MASS AND THE IECC

Chapter 1 states that the IECC allows a reduction in R-value and increase in U-factor with the incorporation of a "mass wall." This chapter offers research to support the IECC definition of "mass wall." This chapter also offers research to support the allowed reduction and increase according to the IECC defined climate zones. However, this chapter will demonstrate the amount of allowed reduction R-value and increase in U-factor are too large. U-factors are offered for the "mass wall" which will demonstrate equal thermal performance between the "mass wall" and the no-mass wall.

The IECC, International Energy Conservation Code, allows a reduction in insulation R-value or an increase in U-factor of the exterior envelope wall of a residential building with the incorporation of a "mass wall." The IECC's definition of a "mass wall" is not readily available. These determinations are left up to the local code officials and/or engineers. Documentation about the amount of R-value reduction or increase in U-factor that will correspond to an annually thermal transmission through a "mass wall" equivalent to that of a non-mass wall have not been identified.

REScheckTM is residential energy code compliance demonstration software supported by the DOE. In the REScheckTM Software User's Guide a

definition of mass wall is given as[24].

“NOTE: Concrete, masonry, and "qualifying" log walls receive a mass wall credit in some locations. In order to qualify for this credit, the heat capacity of the exterior wall must be greater than or equal to 6 Btu/ft² °F [123 kJ/m² °K] of exterior wall area. Masonry and concrete walls having a mass greater than or equal to 30 lb/ft² of exterior wall area (146 kg/m²) will meet this requirement. Masonry and concrete walls with lesser mass should be entered as wood-framed walls. For log walls, the heat capacity will be dependent on the specified wood species and nominal width. The insulating value of the logs themselves is accounted for in the software. You should only enter a cavity R-value if there is additional insulation being used.”

5.1: IECC R-Values and U-Factors

The IECC requirements for energy code compliance are climate specific. The R-values and U-factors for the building envelope and the Fenestration U-factors and solar heat gain coefficients change with geographic location. The climate zones as defined by the IECC are shown in Figure 5.1 below.

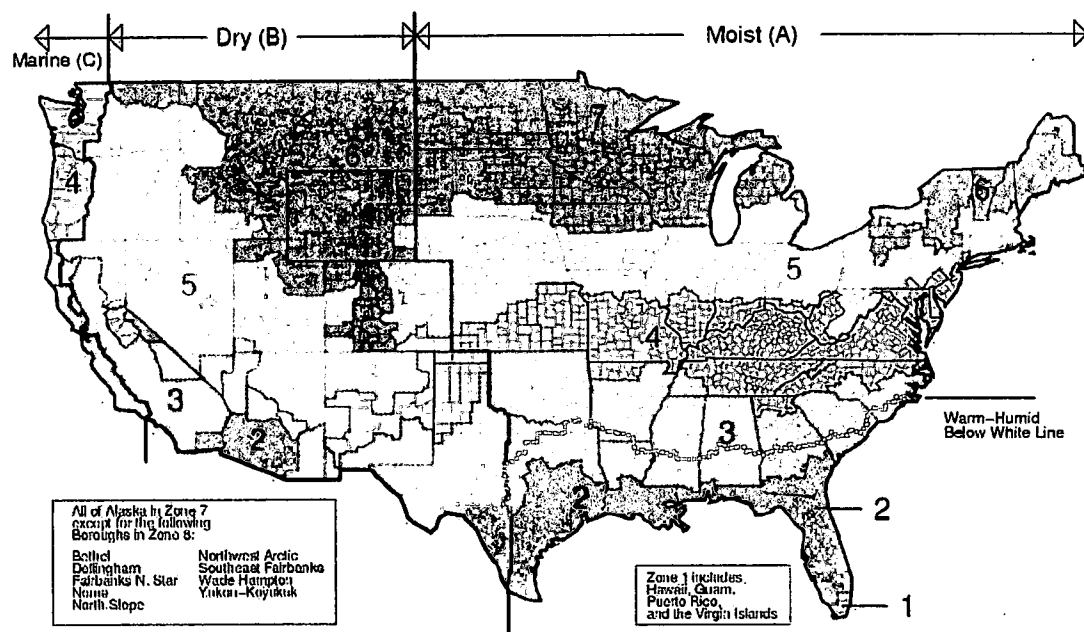


Figure 5.1 Climate Zones

The IECC has two methods of listing envelope insulation requirements. The first is to list the required insulation R-value that is to be installed in the insulation cavity of a wall. These requirements are listed according to climate zone. In some climate zones a requirement may be listed with the R-values. For example, 19 or 13+5. This approach offers two methods of compliance: insulation with an R-value of 19 in the wall cavity; or insulation with an R-value of 13 in the wall cavity and sub-siding with an R-value of 5 over the exterior of the wall. The 2006 IECC requirements for installed R-values in envelope walls are given in Table 5.1 below.

**2006 IECC
INSULATION AND FENESTRATION REQUIREMENTS BY COMPONENT**

CLIMATE ZONE	FENESTRATION U-FACTOR	SKYLIGHT U-FACTOR	GLAZED FENESTRATION SHGC	CEILING R-VALUE	WOOD FRAME WALL R-VALUE	MASS WALL R-VALUE	FLOOR R-VALUE	BASEMENT WALL R-VALUE	SLAB R-VALUE & DEPTH	CRAWL SPACE WALL R-VALUE
1	1.20	0.75	0.40	30	13	3	13	0	0	0
2	0.75	0.75	0.40	30	13	4	13	0	0	0
3	0.65	0.65	0.40	30	13	5	19	0	0	5 / 13
4 except Marine	0.40	0.60	NR	38	13	5	19	10 / 13	10, 2ft	10 / 13
5 and Marine 4	0.35	0.60	NR	38	19 or 13+5	13	30	10 / 13	10, 2 ft	10 / 13
6	0.35	0.60	NR	49	19 or 13+5	15	30	10 / 13	10, 4 ft	10 / 13
7 and 8	0.35	0.60	NR	49	21	19	30	10 / 13	10, 4 ft	10 / 13

Table 5.1

The 2006 IECC requirements for installed U-factors of envelope walls are given in Table 5.2 below. The primary difference between the two tables is that the listed R-values are for wall cavity insulation and the U-factors are for the exterior wall. This includes the interior air films, framing fraction, and

interior and exterior sheathing. This is verified in the REScheck™ Software User's Guide.

“Cavity Insulation R-Value – Enter the R-value of any insulation to be installed in the cavities between above-grade wall structural members. The insulating values of other parts of the building assembly (e.g., gypsum board and air films) are accounted for by the program and should not be included.”

2006 IECC EQUIVALENT U-FACTORS

CLIMATE ZONE	FENESTRATION U-FACTOR	SKYLIGHT U-FACTOR	CEILING U-FACTOR	FRAME WALL U-FACTOR	MASS WALL U-FACTOR	FLOOR U-FACTOR	BASEMENT WALL U-FACTOR	CRAWL SPACE WALL U-FACTOR
1	1.20	0.75	0.035	0.082	0.197	0.064	0.360	0.477
2	0.75	0.75	0.035	0.082	0.165	0.064	0.360	0.477
3	0.65	0.65	0.035	0.082	0.141	0.047	0.360	0.136
4 except Marine	0.40	0.60	0.030	0.082	0.141	0.047	0.059	0.065
5 and Marine 4	0.35	0.60	0.030	0.060	0.082	0.033	0.059	0.065
6	0.35	0.60	0.026	0.060	0.06	0.033	0.059	0.065
7 and 8	0.35	0.60	0.026	0.057	0.057	0.033	0.059	0.065

Table 5.2

Table 5.3 below lists the envelope R-value requirements of the 2009 IECC. The R-value specification of 13/17 in Zone 5 allows a reduction of cavity insulation to R-13 with a “mass wall,” but only a reduction to R-17 if over half of the thermal resistance of the insulation is on the interior of the mass.

**2009 IECC
INSULATION AND FENESTRATION REQUIREMENTS BY COMPONENT**

CLIMATE ZONE	FENESTRATION U-FACTOR ^b	SKYLIGHT ^b U-FACTOR	GLAZED FENESTRATION ^{b,e} SHGC	CEILING R-VALUE	WOOD FRAME WALL R-VALUE	MASS WALL R-VALUE ⁱ	FLOOR R-VALUE	BASEMENT ^c WALL R-VALUE	SLAB ^d R-VALUE & DEPTH	CRAWL SPACE ^c WALL R-VALUE
1	1.20	0.75	0.30	30	13	3/4	13	0	0	0
2	0.65 ^j	0.75	0.30	30	13	4/6	13	0	0	0
3	0.50 ^j	0.65	0.30	30	13	5/8	19	5/13 ^f	0	5/13
4 except Marine	0.35	0.60	NR	38	13	5/10	19	10/13	10, 2ft	10/13
5 and Marine 4	0.35	0.60	NR	38	20 or 13+5 ^h	13/17	30 ^g	10/13	10, 2 ft	10/13
6	0.35	0.60	NR	49	20 or 13+5 ^h	15/19	30 ^g	15/19	10, 4 ft	10/13
7 and 8	0.35	0.60	NR	49	21	19/21	38 ^g	15/19	10, 4 ft	10/13

Table 5.3

Table 5.4 below lists the required envelope U-factors. When more than half the insulation is on the interior, the “mass wall” U-factors must be a maximum of 0.017 in Zone 1, 0.14 in Zone 2, 0.12 in Zone 3, 0.10 in Zone 4 except Marine, and the same as the frame U-factor in Marine Zone 4 and Zones 5 through 8. 2009 IECC also accounts for the compression of R-19, 6-inch thick fiberglass insulation, into a 5-1/2-inch thick 2x6 wall by reducing the R-value by R-1 or more and therefore requires an R-20.

5.2: Finite-Difference Model for Concrete

The heat transfer through a wall component is proportional to the U-factor and inversely proportional to the R-value. As outlined previously, thermal mass in a wall component subjected to a cyclic load, under certain conditions will result in a decrease in thermal transmission through the wall component [21,22]. The IECC allows for a reduction in insulation and/or an increase in U-factor with the addition of thermal mass in an exterior wall component. The IECC refers to this as a "mass wall." Therefore, the finite-difference model simulates heat transfer through the exterior wall with no thermal mass and with the U-factor required by the IECC in that Climate Zone using the TMY2 file for a location in that Zone and records the annual heat transfer. The heat transfer to the exterior is recorded as heating requirement and heat transfer to the interior is recorded as cooling requirements. The model then simulates the wall with the addition of concrete as thermal mass with a thickness varying from 1-inch to 12-inches and records the annual heating and cooling requirements. As the concrete is added to the wall, the added thermal resistance of the concrete is considered and the insulation reduced to maintain the U-factor the same with or without the concrete. This avoids crediting a reduction of total heat transfer with the addition of concrete due to the thermal resistance of the concrete to the reduction resulting from thermal mass of the concrete.

The IECC also allows for a smaller reduction in R-value and smaller increase in U-factor depending on the location of the thermal mass in the

mass wall. Therefore, the model allows for different locations of the thermal mass within the wall and assigns an equivalent U-factor.

The equivalent U-factor is defined as the steady-state U-factor which will result in the equivalent total annual cooling and heating loads as produced by a "mass wall." The equivalent U-factor is Climate Zone specific and different equivalent U-factors are obtained for cooling and heating considered separately. The total annual cooling and heating loads are considered when assigning the equivalent U-factor.

Figure 5.3 is the schematic of the model. The U-factor is held constant with the addition of concrete to the wall to remove the effects of additional thermal resistance of the concrete. This insures the reduction is due only to the thermal mass.

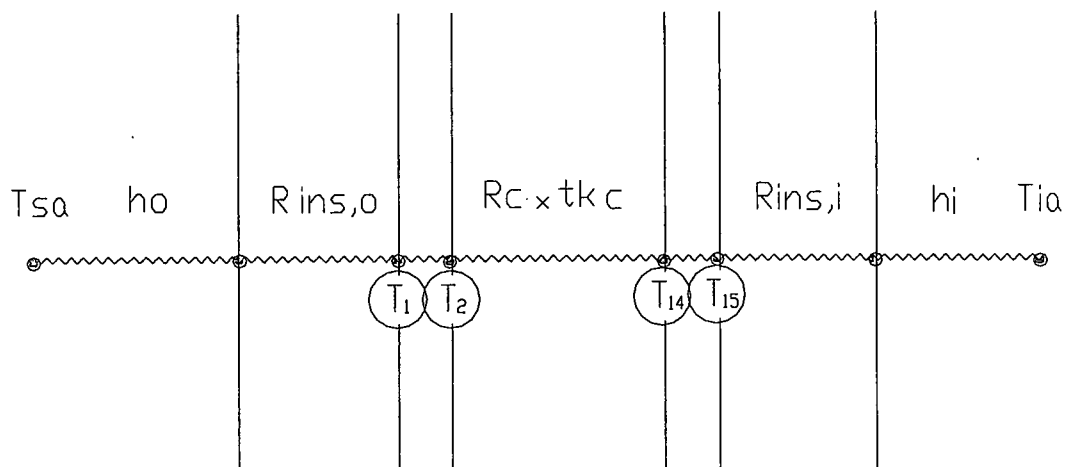


Figure 5.3 Model of wall

$$U - Factor = \frac{1}{R_o + R_c \times tk_{c,m} + R_i} \quad (5.1)$$

$$RO = \frac{1}{h_o} + \%R_{ins,o} \quad (5.2)$$

$$RI = \frac{1}{h_i} + \%R_{ins,i} \quad (5.3)$$

$$R_{ins,tot} = \%R_{ins,o} + \%R_{ins,i} \quad (5.4)$$

$$U - Factor = \frac{1}{\frac{1}{h_o} + R_{ins,tot} + \frac{1}{h_i} + R_c \times tk_{c,in}} \quad (5.5)$$

$$R_{ins,tot} = \frac{1}{U - Factor} - \frac{1}{h_o} - \frac{1}{h_i} - R_c \times tk_{c,in} \quad (5.6)$$

Where,

RO = Total thermal resistance exterior to the concrete

RI = Total thermal resistance interior to the concrete

R_c = Thermal resistance per inch of concrete

$\%R_{ins,o}$ = Percentage of total insulation resistance exterior to concrete

$\%R_{ins,i}$ = Percentage of total insulation resistance interior to concrete

$R_{ins,tot}$ = Total insulation thermal resistance

tk_c = Thickness of concrete in inches

h_o = Exterior convection coefficient

h_i = Interior convection coefficient

T_{sa} = Temperature sol-air

T_{ia} = Interior air temperature

There are fifteen nodes and fourteen sections across the concrete. For simplicity, only nodes 1, 2, 14, and 15 are shown. The finite-difference model reads time, air temperature and solar radiation data from a TMY2 file and calculates the solar radiation on the north, east, south, and west vertical surfaces. It then calculates the sol-air temperature at each surface. It then averages the four sol-air temperatures and uses the averaged sol-air temperature as the exterior temperature. The interior air temperatures are set as required by the IECC. The model calculates the heat transfer through the wall for each of 8,760 hours for the year. It iterates the temperature through the thermal mass time step of 5/3600 of an hour for concrete thicker than 1-inch and 1/3600 of an hour for 1-inch thick or less. The model iterates through the year until the temperatures for the nodes converge on hour 1 on January 1. The equations through the nodes are:

$$T1_p = T1 + 2 \times D \times \left(\left(\frac{T_{solavg} - T1}{RO} \right) + (T2 - T1) \times U \right) \quad (5.7)$$

$$T2_p = T2 + D \times U \times (T1 + T3 - 2 \times T2) \quad (5.8)$$

$$T3_p = T3 + D \times U \times (T2 + T4 - 2 \times T3) \quad (5.9)$$

•
•
•

$$T13_p = T13 + D \times U \times (T12 + T14 - 2 \times T13) \quad (5.10)$$

$$T14_p = T14 + D \times U \times (T13 + T15 - 2 \times T14) \quad (5.11)$$

$$T15_p = T15 + 2 \times D \times \left(\left(\frac{T_i - T15}{RI} \right) + (T14 - T15) \times U \right) \quad (5.12)$$

Where,

T_{13} = Node temperature at iteration n

T_{13_p} = Node temperature at iteration n+1

$$D = \frac{dt}{(dx \times Denconc \times Cpconc)} \quad (5.13)$$

dx = Distance between nodes in thermal mass, concrete

$Denconc$ = Density of concrete

$Cpconc$ = Specific heat of concrete

$$U = \frac{kconc}{dx} \quad (5.14)$$

$kconc$ = Thermal conductivity of concrete

5.3: Values and Constants used in IECC Mass Wall

CHAPTER 4 of the 2009 IECC, RESIDENTIAL ENERGY EFFICIENCY, states that the calculation of the U-factor shall use a series-parallel path calculation method.

$$U - Factor = \frac{1}{R - Value(Total)} \quad (5.15)$$

$$R - Value(Tot.) = \frac{1}{\frac{\% area insulation cavity}{R through insulation cavity} + \frac{\% area stud space}{R through stud space}} \quad (5.16)$$

Table 5.5, from an Excel spreadsheet, uses equation (5.16) to calculate the total R-value and U-factor. The U-factor of 0.082 for a 2x4 wood wall construction with R-13 in the cavity is consistent with the corresponding values in the IECC. As alternate construction methods, framing methods, can

result in varying percentages of insulation cavity and stud spaces, only U-factors are used in the model simulations.

R-Value of non-insulating Sheeting =	0
R-Value on Insulating Sheeting =	0
R-Value of 1/2-inch Dry Wall =	0.45
R-Value of 2X4 =	4.38
R-Value of 2X6 =	0
R-Value of Cavity Insulation =	13
R-Value of Outside Air Film =	0.17
R-Value of Inside Air Film =	0.68
Percentage of Cavity Space =	89.00%
Percentage of Stud Space =	11.00%
R-Value through Cavity =	14.3
R-Value through Stud Space =	5.68
R-Value of Wall =	12.25431
U-Factor =	0.082

Table 5.5 Calculation of U-factor

ASHRAE *Handbook of Fundamentals* gives an interior air film resistance as $0.17 \text{ hr} \cdot \text{ft}^2 \cdot ^\circ\text{F} / \text{Btu}$ in the winter season and 0.25 in the summer [25]. The interior air film resistance of $0.17 \text{ hr} \cdot \text{ft}^2 \cdot ^\circ\text{F} / \text{Btu}$ is used. ASHRAE also gives the interior vertical surface air film resistance as $0.68 \text{ hr} \cdot \text{ft}^2 \cdot ^\circ\text{F} / \text{Btu}$ which is used. The American Concrete Institute give standard gravel concrete a density between 140 and $150 \text{ lb}_m / \text{ft}^3$. The value of $145 \text{ lb}_m / \text{ft}^3$ is used. The thermal conductivity of concrete is $1.04 \text{ Btu} / \text{hr} - \text{ft} - ^\circ\text{F}$ and the specific heat is $0.2 \text{ Btu} / \text{lb}_m - ^\circ\text{F}$.

There are three methods of demonstrating energy code compliance in the IECC: prescriptive path, UA tradeoff, and simulation. The 2009 IECC in SECTION 302, DESIGN CONDITIONS, lists interior design temperatures

used for heating and cooling load calculation shall be a maximum of $72^{\circ}F$ for heating and a minimum of $75^{\circ}F$ for cooling. In SECTION 406 of the 2009 IECC, SIMULATED PERFORMANCE ALTERNATIVE, TABLE 405.5.2 list a thermostat cooling set point = $75^{\circ}F$ and a heating set point = $72^{\circ}F$. These are the set points used in the simulation model. TABLE 405.5.2 also list an above grade wall solar absorptance = 0.75.

5.4: Detailed Investigation of Mass Wall in Dayton

TMY2 93815 for Dayton, Ohio, was used in this simulation. To receive credit for a mass wall, the wall must have a heat capacity of $6 \text{ Btu/ft}^2\text{ }^{\circ}F$. For concrete in the exterior wall to qualify, it must be a minimum of $30 \text{ lb}_m/\text{ft}^2$. Using a conservative specific heat of $0.20 \text{ Btu/lb}_m\text{ }^{\circ}F$, this equates to only 2-1/2 inches thick of concrete.

Dayton, Ohio, is in CLIMATE ZONE 5 and is required to have a U-factor of 0.057 in a non-mass exterior wall. The simulated cooling load for a no mass exterior wall with a U-factor of 0.057 is $916 \text{ Btu/ft}^2\text{ yr}$. The simulated cooling load requirements for a mass wall with 2-1/2-inches of concrete in the interior and the IECC allowed U-factor of 0.082 is $450 \text{ Btu/ft}^2\text{ yr}$. It is $353 \text{ Btu/ft}^2\text{ yr}$ for 6-inches of concrete in the interior. Figure 5.4 plots $\text{Btu/ft}^2\text{ yr}$ cooling load against the concrete thickness.

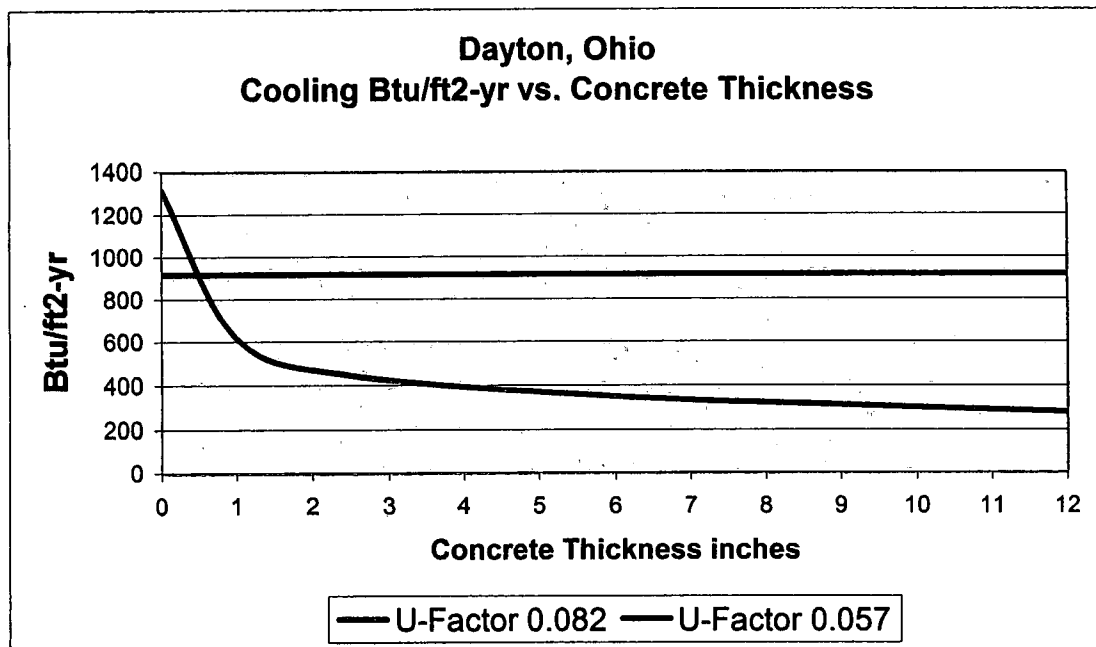


Figure 5.4 Cooling vs. Concrete Thickness, Dayton, Ohio

Figure 5.5 plots the cooling load against U-factor for 2-1/2-inches of concrete in the interior. The horizontal line at 916 $Btu/ft^2 \cdot yr$ is the cooling load for the U-factor of 0.057. The lines intersect at approximately 0.16. This indicates a 2-1/2-inch concrete "mass wall" will transmit the same amount heat as a 0.057 wall with a U-factor of only 0.16.

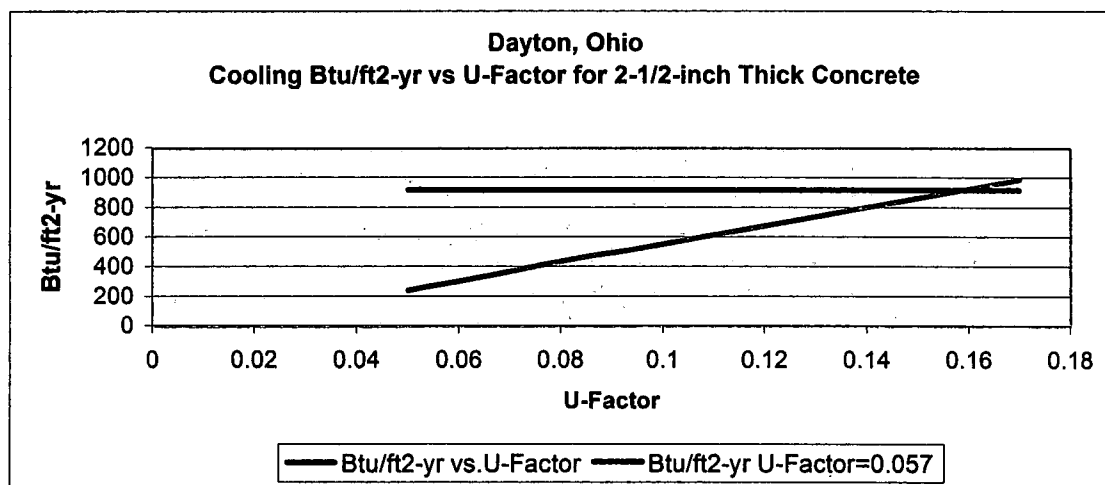


Figure 5.5 Comparison of U-factor "mass wall" to U-factor no-mass wall, 2-1/2-inch thick concrete, cooling

Figure 5.6 plots the cooling load against U-factor for 6-inches of concrete in the interior. The horizontal line at 916 $Btu/ft^2\text{-yr}$ is the cooling load for the U-factor of 0.057. The lines intersect at approximately 0.195. This indicates a 6-inch concrete “mass wall” will perform the same as a 0.057 wall with a U-factor of only 0.195.

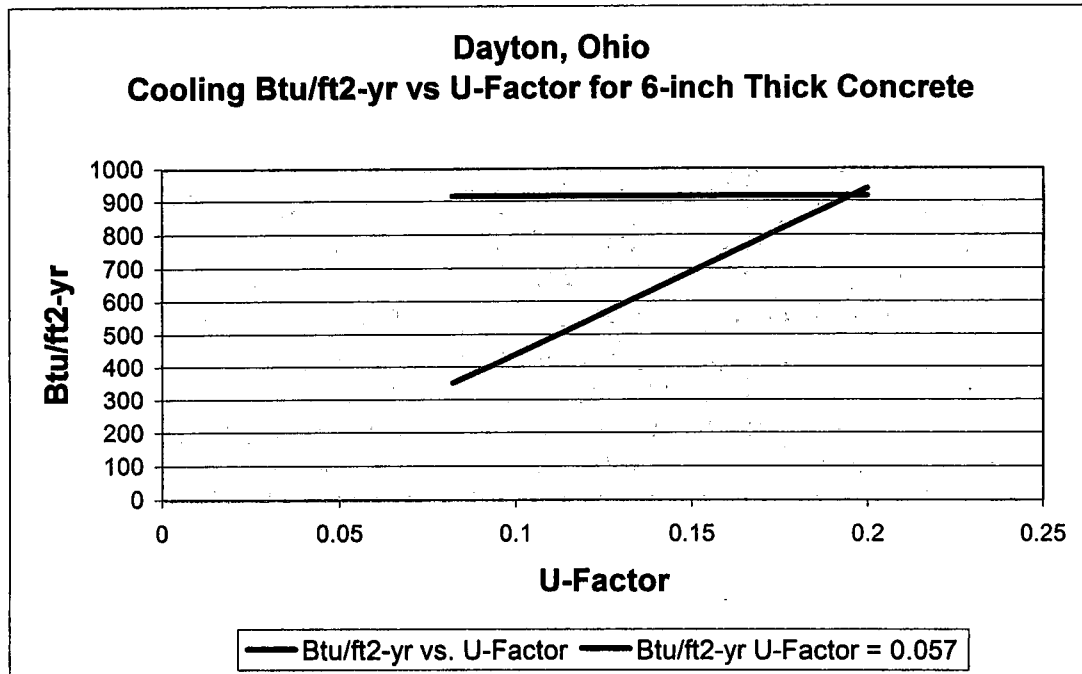


Figure 5.6 Comparison of U-factor mass wall to U-factor no-mass wall, 6-inch thick concrete, cooling

Because the cooling load for a no-mass wall is proportional to the U-factor, the 2-1/2-inch concrete “mass wall” performs the same as a no-mass wall with a U-factor of 0.28. The 6-inch concrete “mass wall” performs the same as a no-mass wall with a U-factor of 0.22. The 2-1/2 inch concrete “mass wall” with a U-factor of 0.082, as allowed by the 2009 IECC, reduces the cooling load from the U-factor 0.57 no-mass wall by approximately 50%.

The 6-inch concrete “mass wal” with a U-factor of 0.082 will reduce the cooling load by approximately 60%.

Figure 5.7 plots the Btu/ft^2yr heating load against concrete thickness. The heating load for the U-factor 0.057 no-mass wall is 10,018 Btu/ft^2yr . The “mass wall” with the U-factor of 0.082, as allowed by the 2009 IECC, does not approach the 10,010 Btu/ft^2yr and generates 35% more heating load.

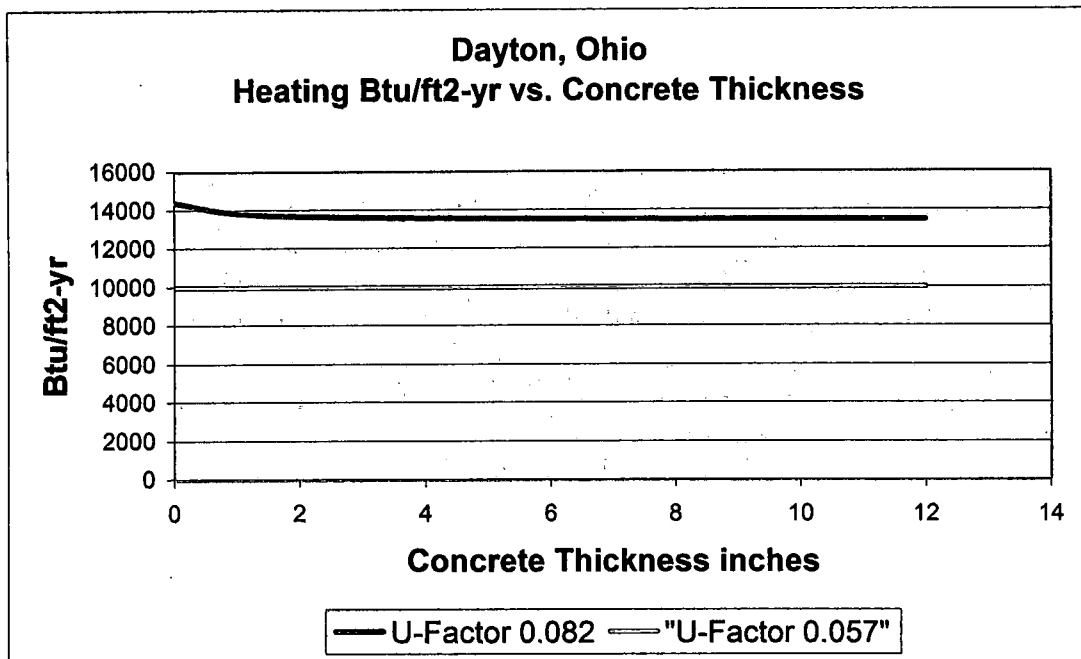


Figure 5.7 Heating vs. concrete thickness, Dayton, Ohio

Figure 5.8 plots the 2-1/2-inch concrete “mass wall” heating load against U-factor to determine the required U-factor for the “mass wall” to perform the same as a 0.057 no-mass wall. The lines cross at approximately a U-factor of 0.061, which is less than the 0.082 allowed by the IECC. Figure

5.9 plots show result with 6-inches of concrete. The results are approximately the same as for 2-1/2 inches of concrete.

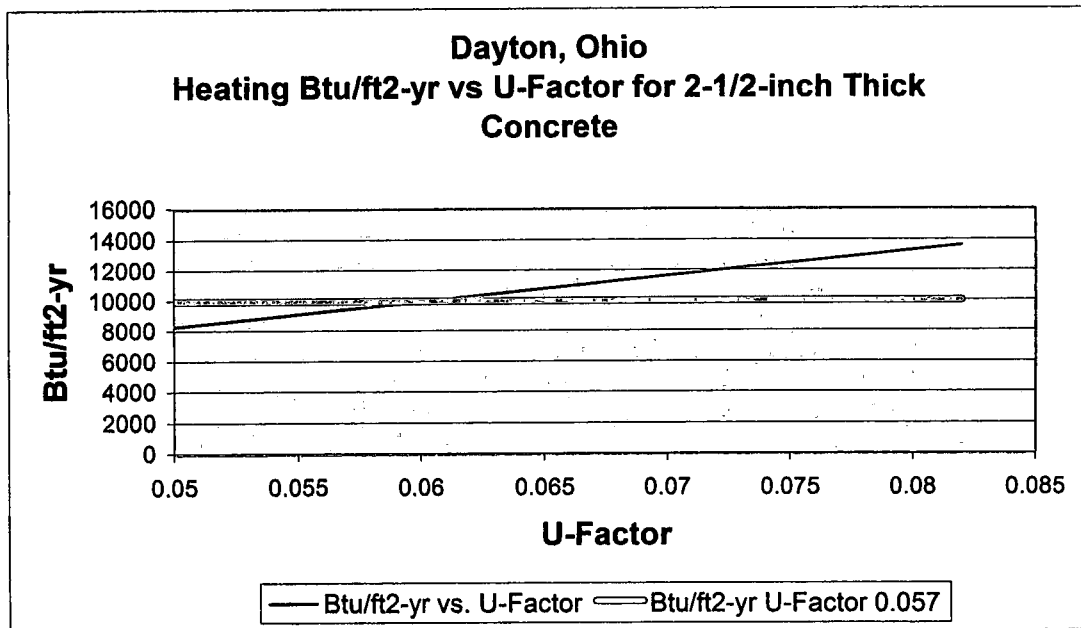


Figure 5.8 Comparison of U-factor "mass wall" to U-factor no-mass wall, 2-1/2-inch thick concrete, heating

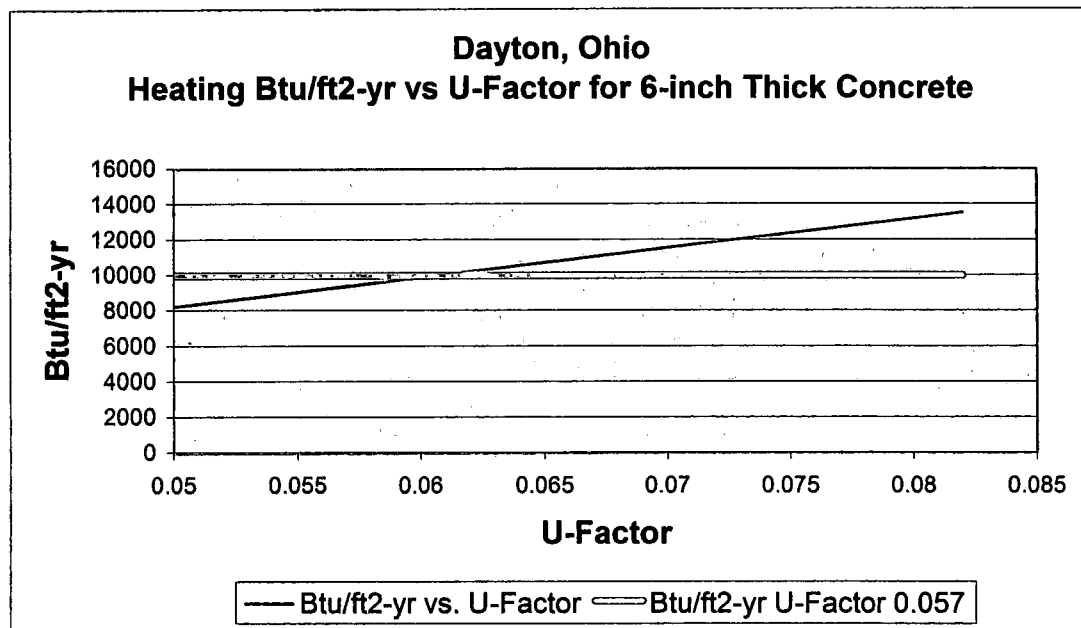


Figure 5.9 Comparison of U-factor "mass wall" to U-factor no-mass wall, 6-inch thick concrete, heating

Figure 5.10 plots the total annual cooling and heating against concrete thickness of a “mass wall” with a U-factor of 0.082. The total annual cooling and heating with the no-mass wall with a U-factor of 0.057 is 10,929 $Btu/ft^2\text{-yr}$. The “mass wall” annual $Btu/ft^2\text{-yr}$ starts at 15,722 $Btu/ft^2\text{-yr}$ at 0-inch thick and flattens at approximately 14,093 $Btu/ft^2\text{-yr}$ at 2-1/2-inches thick and remains approximately 29% greater than the 0.057 no-mass wall.

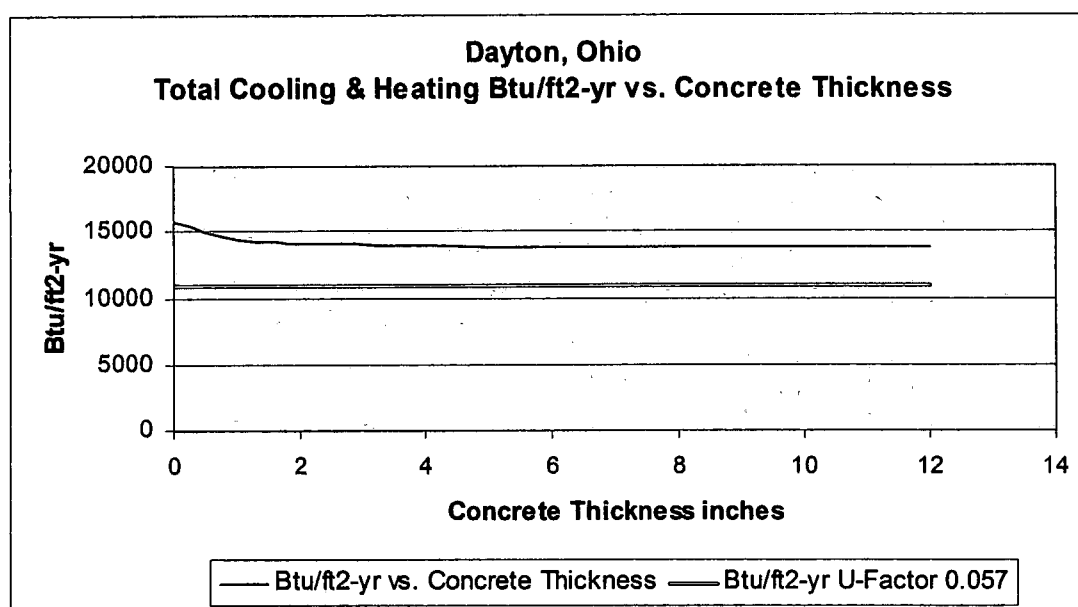


Figure 5.10 Total heating and cooling vs. concrete thickness, Dayton, Ohio

Figure 5.11 plots the 2-1/2-inch “mass wall” against U-factor to determine the U-factor for which the “mass wall” which will perform annually as the no-mass U-factor 0.057 wall. The lines cross at approximately 0.064 which is lower than the 0.082 allowed by the IECC.

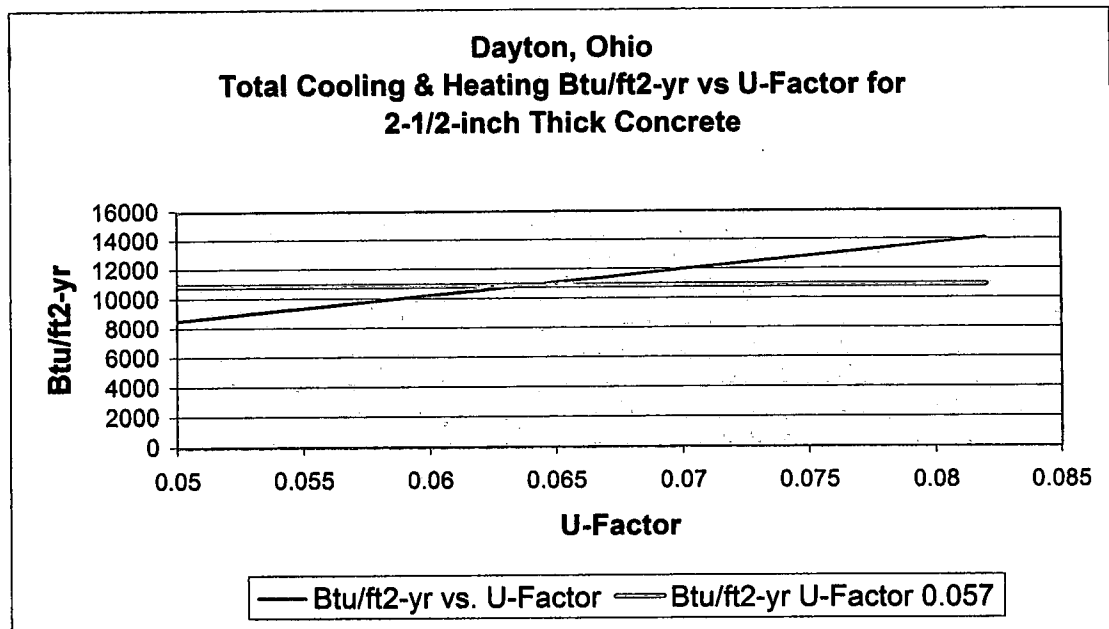


Figure 5.11 Comparison of U-factor “mass wall” to U-factor no-mass wall, 6-inch thick concrete, total heating and cooling

The IECC requires a reduction in U-factor if the mass is positioned in the wall with more than one half of the insulation on the interior. Figure 5.12 plots the total annual cooling and heating loads for a 6-inch thick concrete mass wall with a U-factor of 0.082 positioned at different locations within the wall.

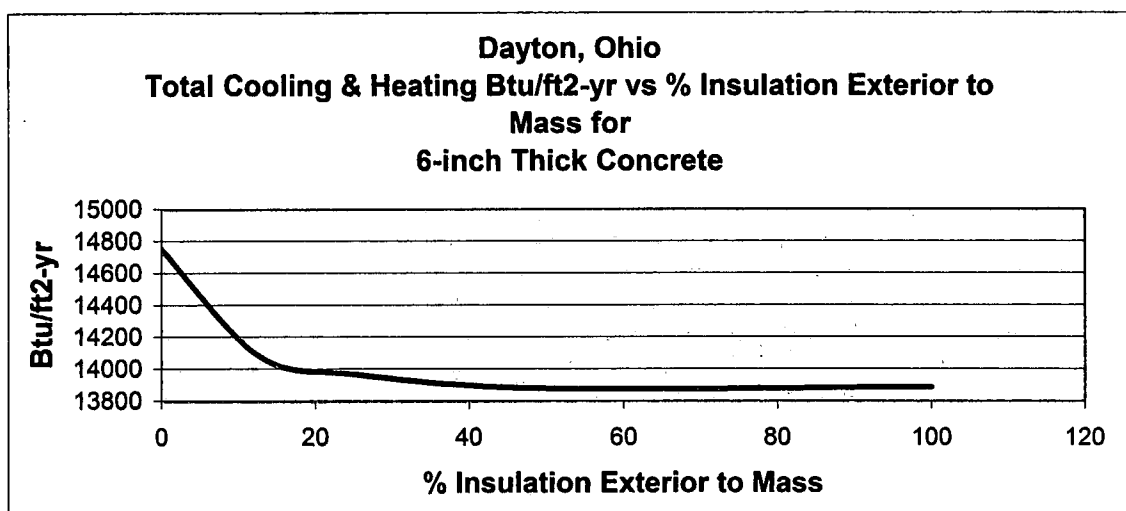


Figure 5.12 Total heating and cooling vs. location of insulation, Dayton, Ohio

With 25% of the insulation on the exterior of the concrete, the total annual cooling heating loads increase less than 1% from the interior position. Moreover, the mass performs better when positioned in the center of the insulation.

5.5: Analysis of Other Locations in Climate Zone 5 and Marine 4

Dayton, Ohio, Boulder, Colorado, and Portland, Oregon, are in Climate Zone 5 and Marine 4 in the IECC. Dayton, Ohio, has an average annual temperature of $50.7^{\circ}F$, an annual sol-air temperature of $54.4^{\circ}F$, annual heating degrees of days of 6,088, and annual cooling degrees of days of 880. Boulder, Colorado, has an average annual temperature of $49.8^{\circ}F$, an annual sol-air temperature of $54.6^{\circ}F$, annual heating degrees days of 6,472, and annual cooling degree days of 922. Portland, Oregon, has an average annual temperature $53.1^{\circ}F$, an annual sol-air temperature of $56.4^{\circ}F$, annual heating degree days of 4,813, and annual cooling degree days of 486.

The IECC requires a U-Factor of $0.057 \text{ Btu/hr} \cdot \text{ft}^2 \cdot ^{\circ}F$ for a standard no-mass wall and allows a U-factor reduction to $0.082 \text{ Btu/hr} \cdot \text{ft}^2 \cdot ^{\circ}F$ for a “mass wall” having $6 \text{ Btu/ft}^2 \cdot ^{\circ}F$

5.5.1: Boulder, Colorado

Figure 5.13 plots the $\text{Btu/ft}^2 \text{ yr}$ cooling load for a concrete “mass wall” with a U-factor of $0.082 \text{ Btu/hr} \cdot \text{ft}^2 \cdot ^{\circ}F$ with increasing concrete thickness.

The concrete is on the interior of the wall. The $Btu/ft^2 \cdot yr$ cooling load for a standard no-mass wall with a U-factor of $0.057 \text{ } Btu/hr \cdot ft^2 \cdot ^\circ F$ is plotted as a horizontal line. The "mass wall" cooling load requirements cross the no-mass wall cooling load requirements at approximately a concrete thickness of less than 1-inch. The reduction of cooling load for the U-factor $0.082 \text{ } Btu/hr \cdot ft^2 \cdot ^\circ F$ "mass wall" reduces 75% with 2-1/2-inches of concrete and 81% with 6-inches of concrete.

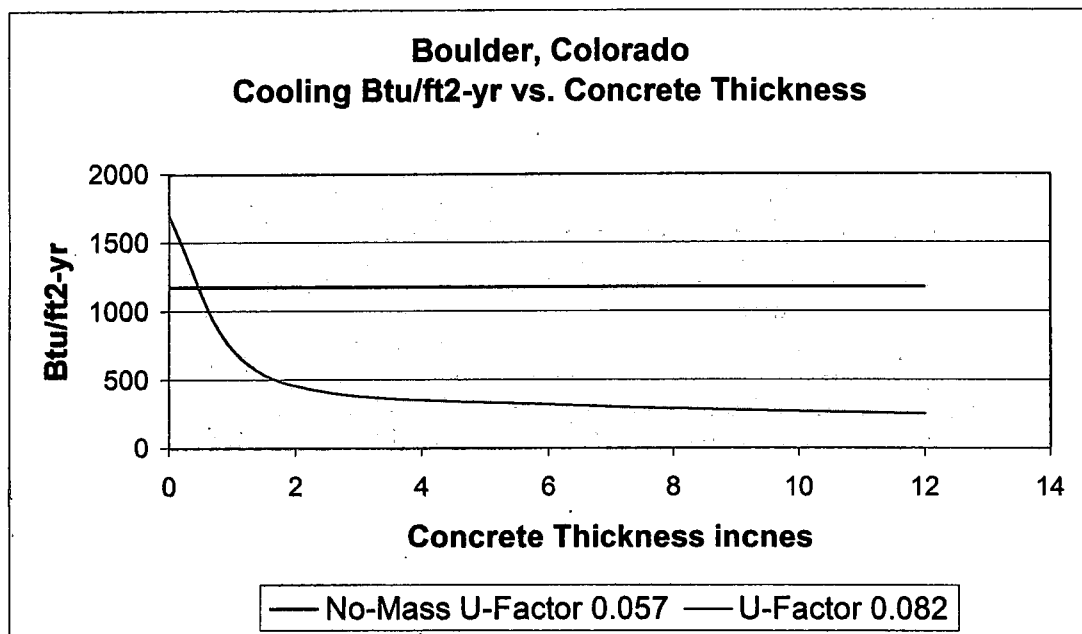


Figure 5.13 Cooling load vs. concrete thickness, Boulder, Colorado

Figure 5.14 plots the $Btu/ft^2 \cdot yr$ heating load for a concrete "mass wall" with a U-factor of $0.082 \text{ } Btu/hr \cdot ft^2 \cdot ^\circ F$ with increasing concrete thickness. The concrete is on the interior of the wall. The $Btu/ft^2 \cdot yr$ heating load for a standard no-mass wall with a U-factor of $0.057 \text{ } Btu/hr \cdot ft^2 \cdot ^\circ F$ is plotted as a horizontal line. The "mass wall" heating load requirements do not

cross the no-mass wall with a U-factor of $0.057 \text{ Btu/hr} \cdot \text{ft}^2 \cdot ^\circ\text{F}$. The reduction of heating load for the U-factor $0.082 \text{ Btu/hr} \cdot \text{ft}^2 \cdot ^\circ\text{F}$ "mass wall" reduces approximately 9% with both 2-1/2-inches and 6-inches of concrete but remains approximately 20% above the no-mass wall.

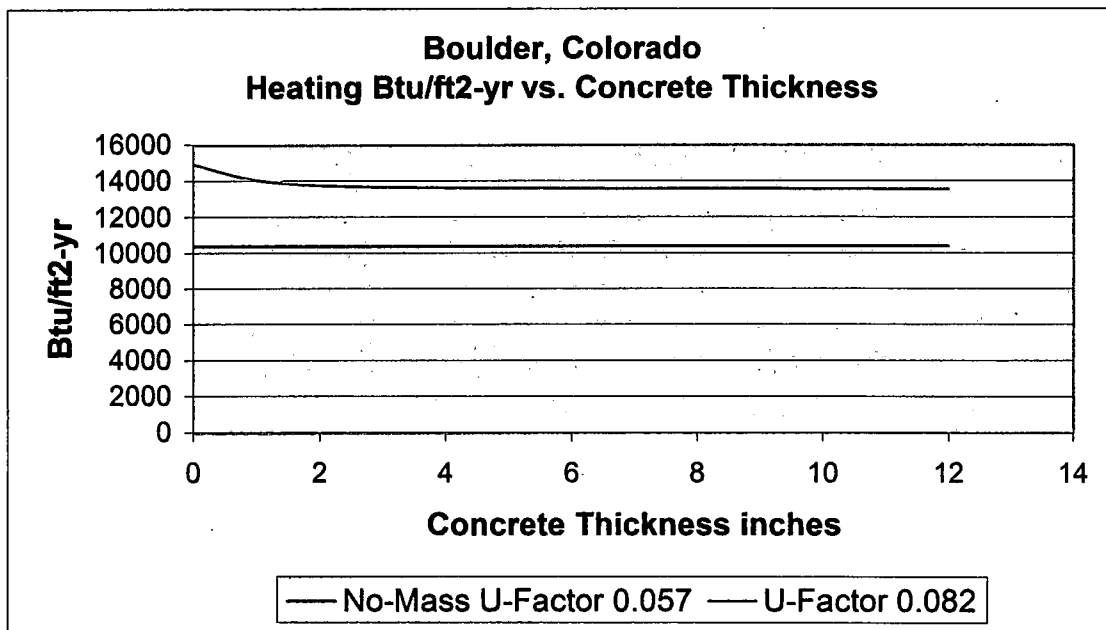


Figure 5.14 Heating vs. concrete thickness, Boulder, Colorado

Figure 5.15 plots the $\text{Btu/ft}^2\text{yr}$ total cooling and heating load for a concrete "mass wall" with a U-factor of $0.082 \text{ Btu/hr} \cdot \text{ft}^2 \cdot ^\circ\text{F}$ with increasing concrete thickness. The $\text{Btu/ft}^2\text{yr}$ total cooling and heating load for a standard no-mass wall with a U-factor of $0.057 \text{ Btu/hr} \cdot \text{ft}^2 \cdot ^\circ\text{F}$ is plotted as a horizontal line. The "mass wall" heating load requirements do not cross the no-mass wall load requirements with a U-factor of $0.057 \text{ Btu/hr} \cdot \text{ft}^2 \cdot ^\circ\text{F}$.

The reduction of total cooling and heating load for the U-factor 0.082 $Btu/hr \cdot ft^2 \cdot ^\circ F$ "mass wall" reduces approximately 15% with both 2-1/2-inches and 6-inches of concrete but remains approximately 21% above the no-mass wall.

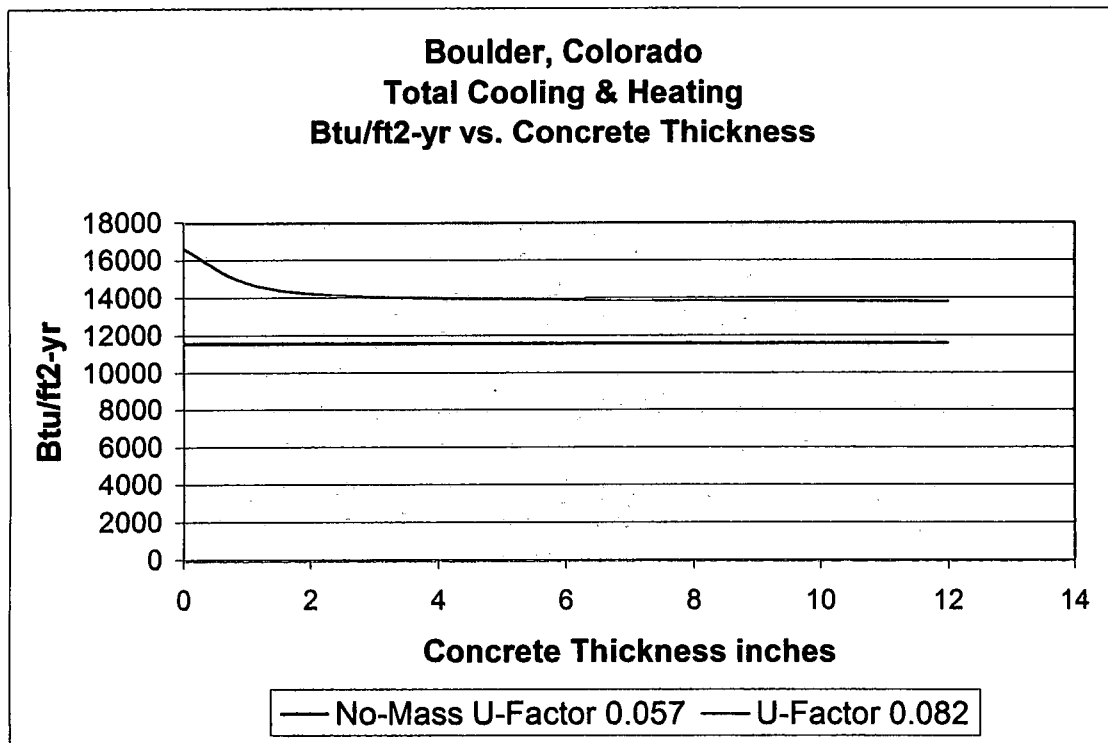


Figure 5.15 Total cooling and heating vs. concrete thickness, Boulder, Colorado

Figure 5.16 plots $Btu/ft^2 \cdot yr$ cooling load requirements with increasing U-factors on the exterior of 2-1/2-inch concrete. The cooling load requirement of the no-mass wall with a U-factor of 0.057 $Btu/hr \cdot ft^2 \cdot ^\circ F$ is plotted as a horizontal line. The two requirements cross at an approximate U-factor of 0.17 $Btu/hr \cdot ft^2 \cdot ^\circ F$. This indicates a 2-1/2-inch thick "mass wall" with a U-

factor of $0.17 \text{ Btu/hr} \cdot \text{ft}^2 \cdot ^\circ\text{F}$ will perform as well in the cooling season as the no-mass wall with the U-factor of $0.057 \text{ Btu/hr} \cdot \text{ft}^2 \cdot ^\circ\text{F}$.

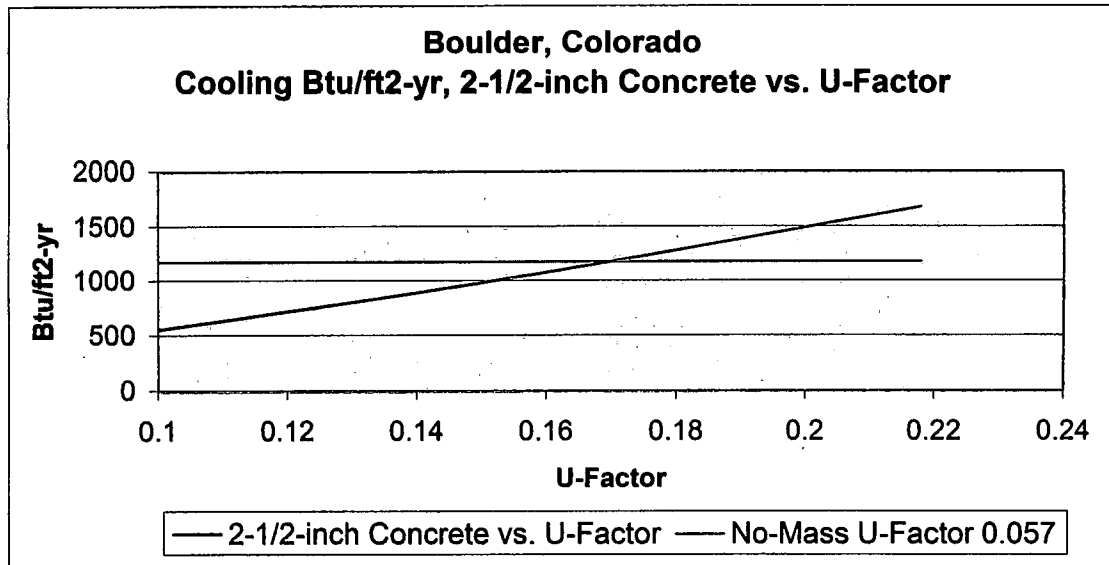


Figure 5.16 Cooling vs. U-factor of "mass wall" compared to U-factor of no-mass wall

Figure 5.17 plots $\text{Btu/ft}^2\text{yr}$ heating load requirements with increasing U-factors on the exterior of 2-1/2-inch concrete. The heating load requirement of the no-mass wall with a U-factor of $0.057 \text{ Btu/hr} \cdot \text{ft}^2 \cdot ^\circ\text{F}$ is plotted as a horizontal line. This indicates the 2-1/2-inch thick "mass wall" would require a U-factor of approximately $0.061 \text{ Btu/hr} \cdot \text{ft}^2 \cdot ^\circ\text{F}$ to perform as well in the heating season as the no-mass wall with a U-factor $0.057 \text{ Btu/hr} \cdot \text{ft}^2 \cdot ^\circ\text{F}$.

The cooling load requirements are reduced by 75% for the "mass wall" of 2-1/2-inches of concrete with the U-factor of $0.082 \text{ Btu/hr} \cdot \text{ft}^2 \cdot ^\circ\text{F}$ and reduces the cooling load below that of the no-mass wall with a U-factor of

$0.57 \text{ Btu/hr} \cdot \text{ft}^2 \cdot ^\circ\text{F}$. The heating load requirements are reduced by 9% for the “mass wall” with the U-factor of $0.082 \text{ Btu/hr} \cdot \text{ft}^2 \cdot ^\circ\text{F}$ but do not perform as well as the no-mass wall.

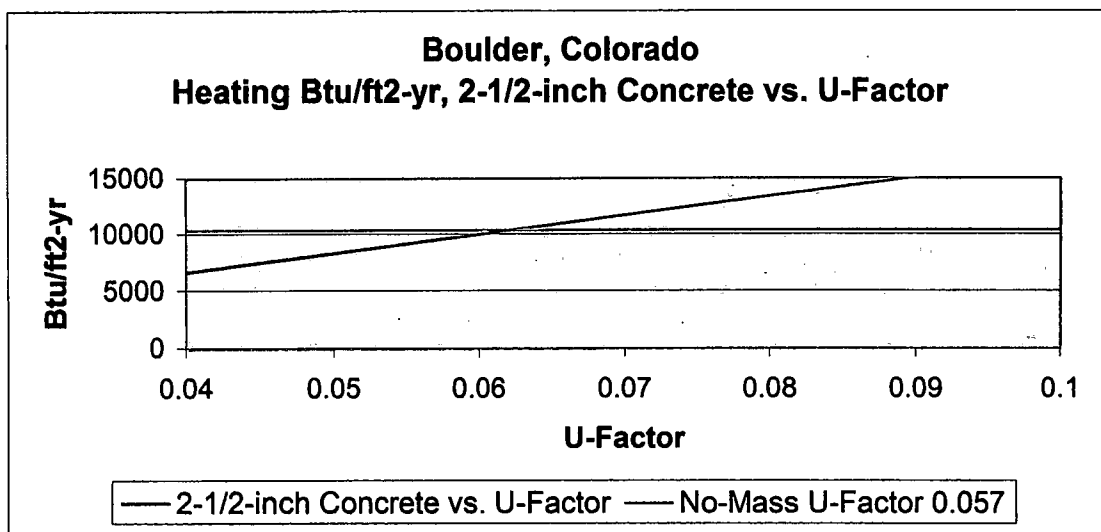


Figure 5.17 Heating vs. U-factor of “mass wall” compared to U-factor of no-mass wall

Figure 5.18 plots the total cooling and heating requirements with increasing U-factor for the 2-1/2 thick concrete “mass wall” with the U-factor of $0.082 \text{ Btu/hr} \cdot \text{ft}^2 \cdot ^\circ\text{F}$ to determine the U-factor for which it will perform as well as the no-mass wall with the U-factor of $0.057 \text{ Btu/hr} \cdot \text{ft}^2 \cdot ^\circ\text{F}$. The lines cross at approximately $0.068 \text{ Btu/hr} \cdot \text{ft}^2 \cdot ^\circ\text{F}$. This is the required U-factor for the IECC “mass wall” to perform and the IECC no-mass wall.

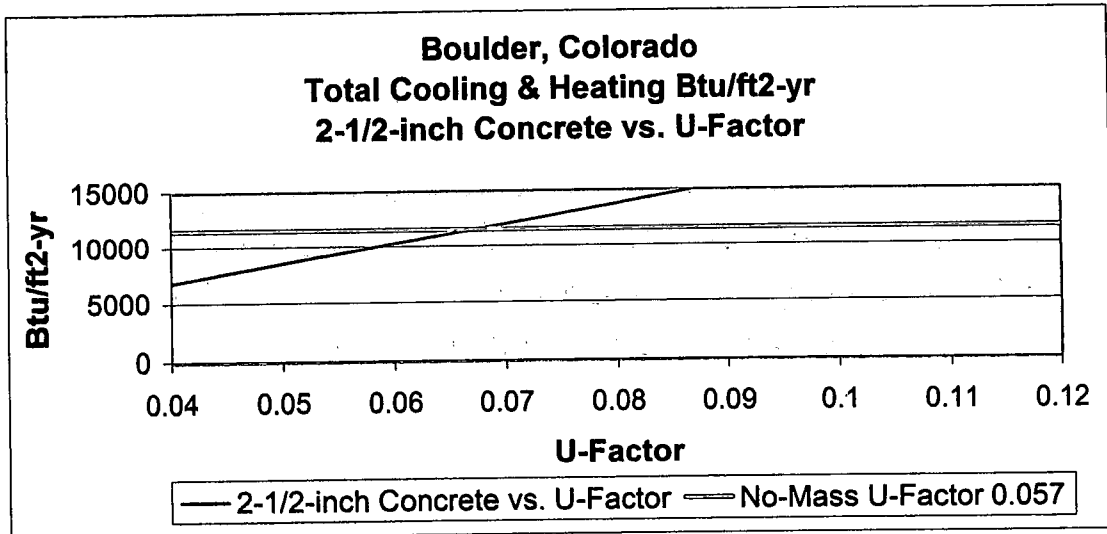


Figure 5.18 Total cooling and heating vs. U-factor of "mass wall" compared to U-factor of no-mass wall

5.5.2 Portland, Oregon

Figure 5.19 plots the $Btu/ft^2 \cdot yr$ cooling load for a concrete "mass wall" with a U-factor of $0.082 \text{ Btu/hr} \cdot ft^2 \cdot ^\circ F$ with increasing concrete thickness. The cooling reduces to zero with 8-inches thick concrete but is reduced by 90% at 2-1/2-inch thick concrete. The $Btu/ft^2 \cdot yr$ cooling load for a standard no-mass wall with a U-factor of $0.057 \text{ Btu/hr} \cdot ft^2 \cdot ^\circ F$ is plotted as a horizontal line.

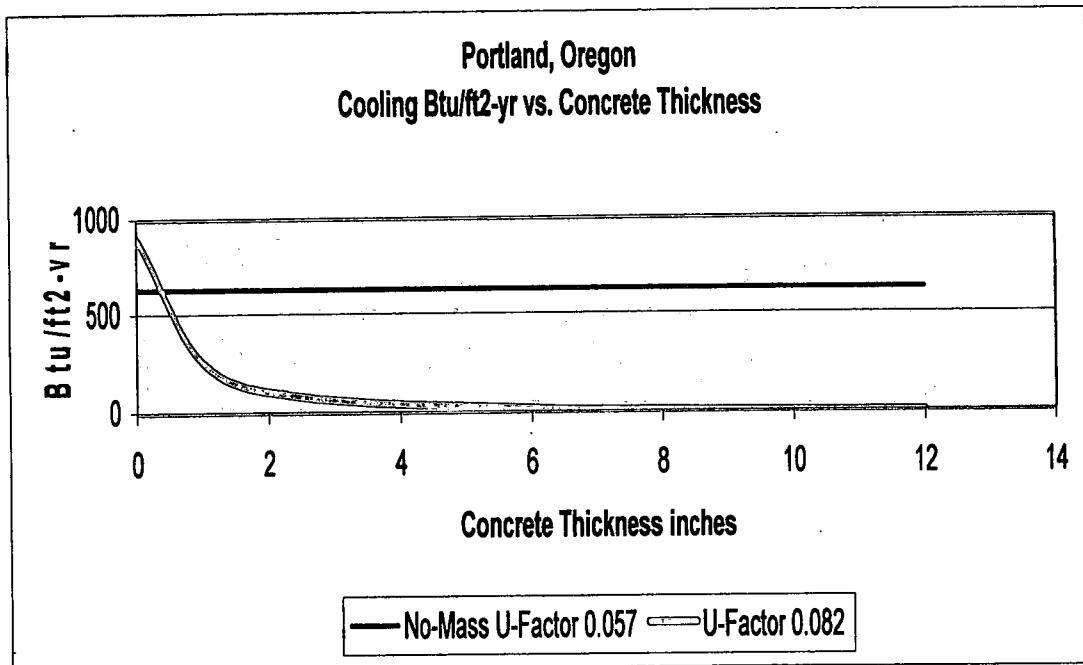


Figure 5.19 Cooling vs. concrete thickness, Portland, Oregon

Figure 5.20 plots the $Btu/ft^2 \cdot yr$ heating load for a concrete "mass wall" with a U-factor of $0.082 \text{ Btu/hr} \cdot ft^2 \cdot ^\circ F$ with increasing concrete thickness. The $Btu/ft^2 \cdot yr$ heating load for a standard no-mass wall with a U-factor of $0.057 \text{ Btu/hr} \cdot ft^2 \cdot ^\circ F$ is plotted as a horizontal line. The heating load is only reduced by 7% at a thickness of 2-1/2-inches. The horizontal line is the heating load for the no-mass wall with a U-factor of 0.057.

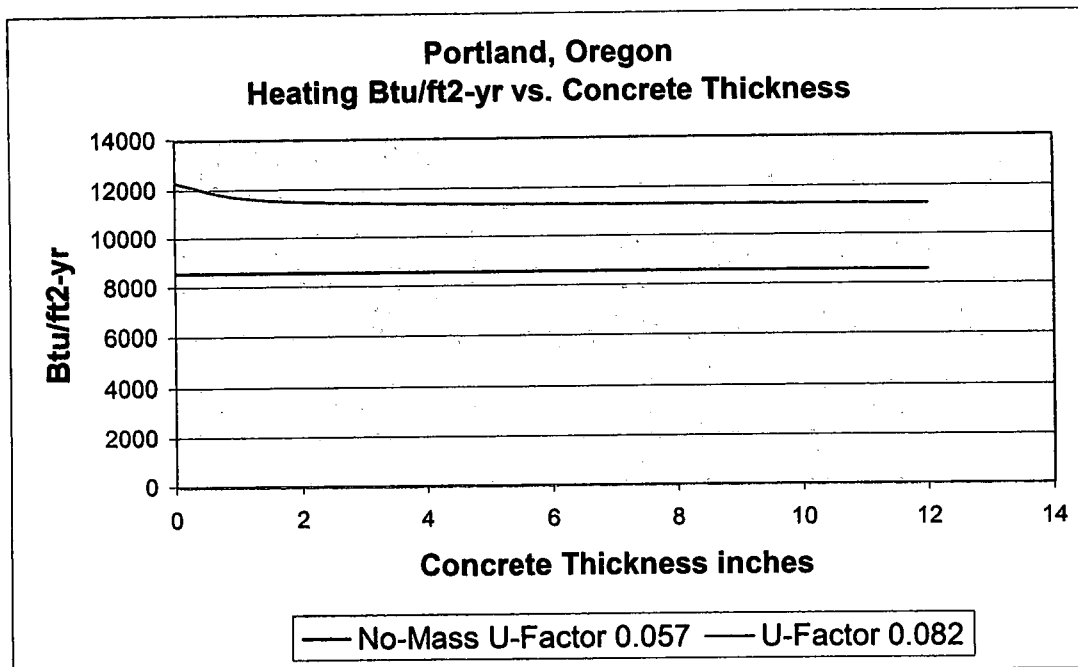


Figure 5.20 Heating vs. concrete thickness, Portland, Oregon

Figure 5.21 plots the $Btu/ft^2 \cdot yr$ total cooling and heating load for a concrete "mass wall" with a U-factor of $0.082 Btu/hr \cdot ft^2 \cdot ^\circ F$ with increasing concrete thickness. The $Btu/ft^2 \cdot yr$ total cooling and heating load for a standard no-mass wall with a U-factor of $0.057 Btu/hr \cdot ft^2 \cdot ^\circ F$ is plotted as a horizontal line. The reduction of the total cooling and heating loads is 12-1/2% at a thickness of 2-1/2-inches of concrete. Figure 5.22 plots the total cooling and heating requirements with increasing U-factor for the 2-1/2 thick concrete "mass wall" with the U-factor of $0.082 Btu/hr \cdot ft^2 \cdot ^\circ F$ to determine the U-factor for which it will perform as well as the no-mass wall with the U-factor of $0.057 Btu/hr \cdot ft^2 \cdot ^\circ F$. The lines cross at approximately 0.066

$Btu/hr \cdot ft^2 \cdot ^\circ F$. This is the required U-factor for the IECC "mass wall" to perform and the IECC no-mass wall.

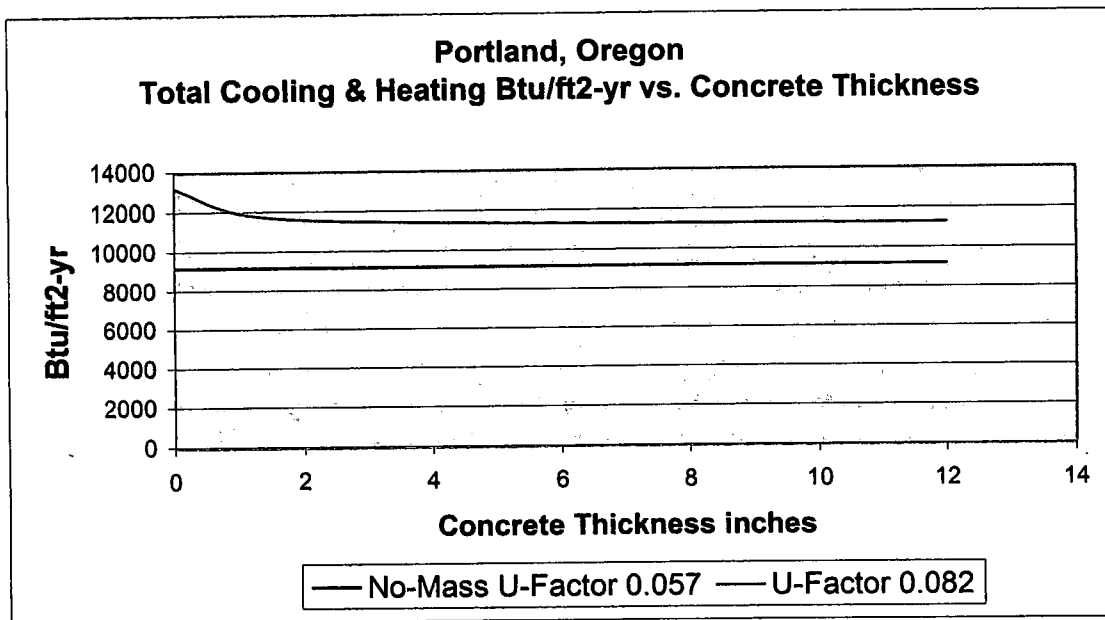


Figure 5.21 Total cooling and heating vs. concrete thickness, Portland, Oregon

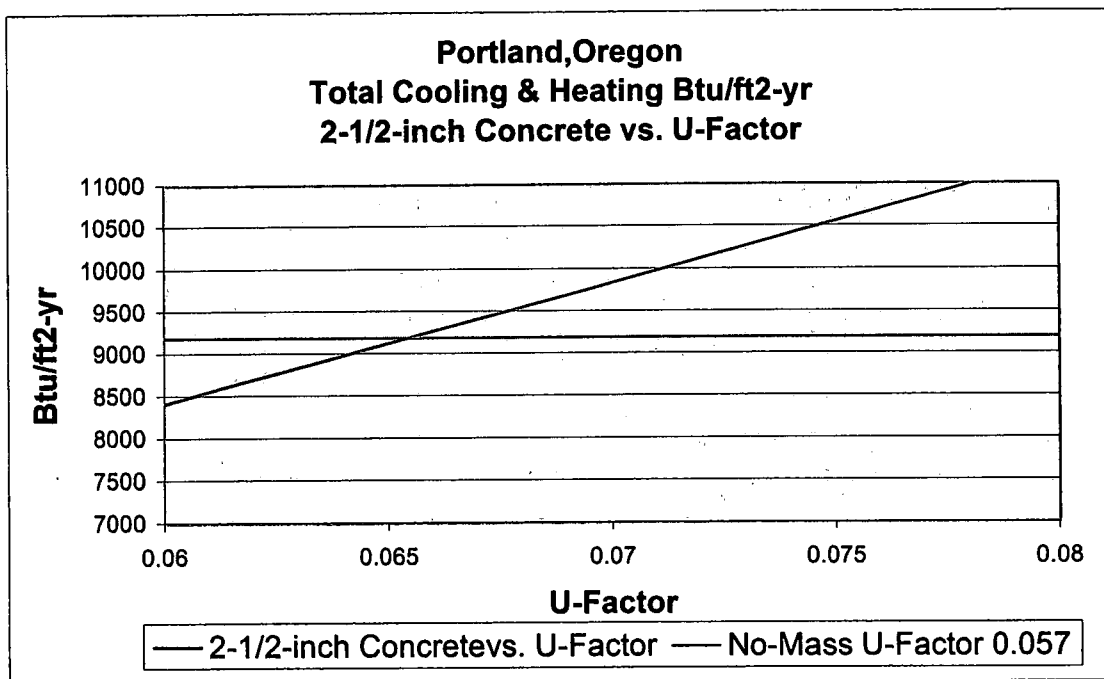


Figure 5.22 Total cooling and heating vs. U-factor of "mass wall" compared to U-factor of no-mass wall

5.5.3 Summary of Climate Zone 5 and Marine 4

The annual cooling load is reduced between 35% and 90% with 2-1/2-inch thick "mass wall" with a U-factor of $0.082 \text{ Btu/hr} \cdot \text{ft}^2 \cdot ^\circ\text{F}$ positioned on the interior of the wall. The annual heating load is reduced between 5% and 8%. However, for the "mass wall," defined as having $6 \text{ Btu/ft}^2 \cdot ^\circ\text{F}$, the required U-factor for it to perform as a standard no-mass wall with a U-factor of 0.057 as in the 2009 IECC varies between 0.064 to $0.068 \text{ Btu/hr} \cdot \text{ft}^2 \cdot ^\circ\text{F}$.

5.6: Analysis of Locations in Climate Zone 2

Both Tampa, Florida, and San Antonio, Texas, are in Climate Zone 2 of the IECC. Tampa, Florida, has an average annual temperature of $71.4 ^\circ\text{F}$, an annual sol-air temperature of $75.6 ^\circ\text{F}$, annual heating degrees of days of 906, and annual cooling degrees of days of 3,260. San Antonio, Texas, has an average annual temperature of $68.1 ^\circ\text{F}$, an annual sol-air temperature of $72.3 ^\circ\text{F}$, annual heating degrees days of 1,873, and annual cooling degree days of 2,975. The IECC requires a U-Factor of $0.082 \text{ Btu/hr} \cdot \text{ft}^2 \cdot ^\circ\text{F}$ for a standard no-mass wall and allows a U-factor reduction to $0.165 \text{ Btu/hr} \cdot \text{ft}^2 \cdot ^\circ\text{F}$ for a "mass wall" having $6 \text{ Btu/ft}^2 \cdot ^\circ\text{F}$.

5.6.1: Tampa, Florida

Figure 5.23 plots the $Btu/ft^2 \cdot yr$ cooling load for a concrete "mass wall" with a U-factor of $0.165 Btu/hr \cdot ft^2 \cdot ^\circ F$ with increasing concrete thickness. The concrete is on the interior of the wall. The $Btu/ft^2 \cdot yr$ cooling load for a standard no-mass wall with a U-factor of $0.082 Btu/hr \cdot ft^2 \cdot ^\circ F$ is plotted as a horizontal line. The "mass wall" cooling load requirements do not cross the no-mass wall cooling load requirements. The reduction of cooling load for the U-factor $0.165 Btu/hr \cdot ft^2 \cdot ^\circ F$ "mass wall" reduces 27% with 2-1/2-inches of concrete and 30% with 6-inches of concrete. However, the "mass wall" cooling load remains approximately 48% above the no-mass wall with a U-factor of $0.082 Btu/hr \cdot ft^2 \cdot ^\circ F$ as allowed in the IECC.

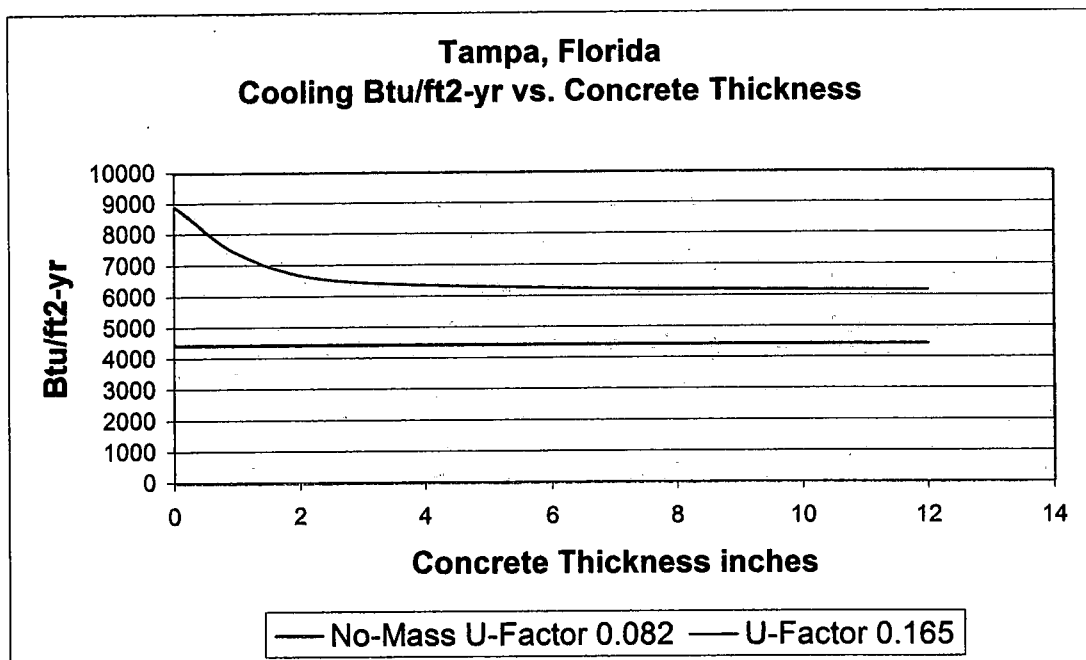


Figure 5.23 Cooling vs. concrete thickness, Tampa, Florida

Figure 5.24 plots the $Btu/ft^2 \cdot yr$ heating load for a concrete "mass wall" with a U-factor of $0.165 Btu/hr \cdot ft^2 \cdot ^\circ F$ with increasing concrete thickness. The $Btu/ft^2 \cdot yr$ heating load for a standard "no mass" wall with a U-factor of $0.082 Btu/hr \cdot ft^2 \cdot ^\circ F$ is plotted as a horizontal line. The "mass wall" heating load requirements do not cross the no-mass wall with the U-factor of $0.082 Btu/hr \cdot ft^2 \cdot ^\circ F$. The reduction of heating load for the U-factor $0.165 Btu/hr \cdot ft^2 \cdot ^\circ F$ "mass wall" reduces approximately 29% with 2-1/2-inches of concrete and approximately 34% with 6-inches of concrete. The 2-1/2 inch concrete remains approximately 43% above the no-mass wall.

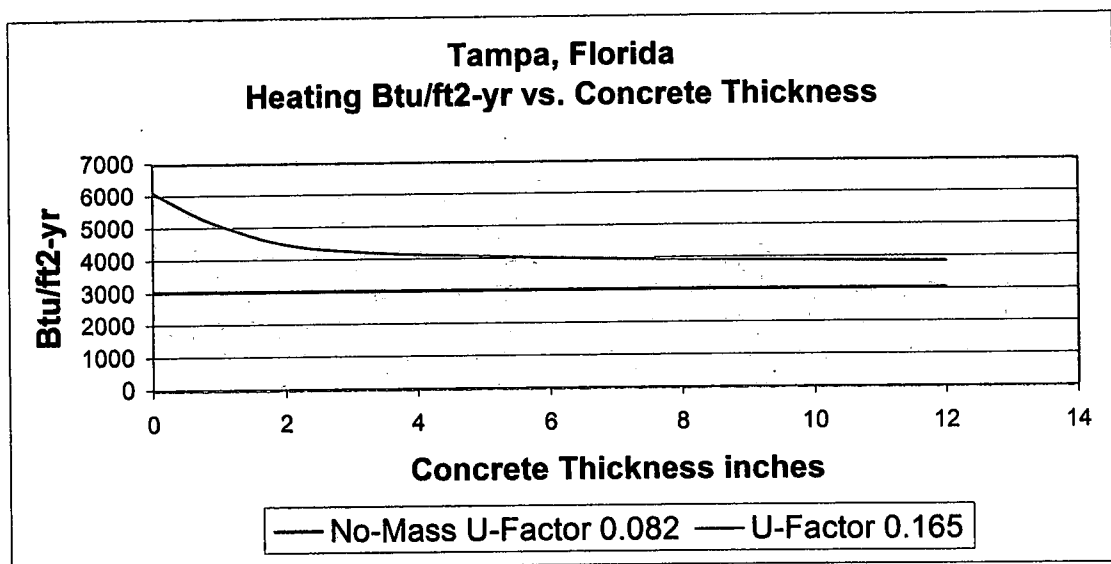


Figure 5.24 Heating vs. concrete thickness, Tampa, Florida

Figure 5.25 plots the $Btu/ft^2 \cdot yr$ total cooling and heating load for a concrete "mass wall" with a U-factor of $0.165 Btu/hr \cdot ft^2 \cdot ^\circ F$ with increasing concrete thickness. The $Btu/ft^2 \cdot yr$ total cooling and heating load for a

standard no-mass wall with a U-factor of $0.082 \text{ Btu/hr} \cdot \text{ft}^2 \cdot ^\circ\text{F}$ is plotted as a horizontal line. The "mass wall" heating load requirements do not cross the no-mass wall load requirements with a U-factor of $0.082 \text{ Btu/hr} \cdot \text{ft}^2 \cdot ^\circ\text{F}$. The reduction of total cooling and heating load for the U-factor $0.165 \text{ Btu/hr} \cdot \text{ft}^2 \cdot ^\circ\text{F}$ "mass wall" reduces approximately 28% with 2-1/2-inches of concrete and approximately 32% with 6-inches of concrete but remains respectively approximately 46%% and 36% above the no-mass wall.

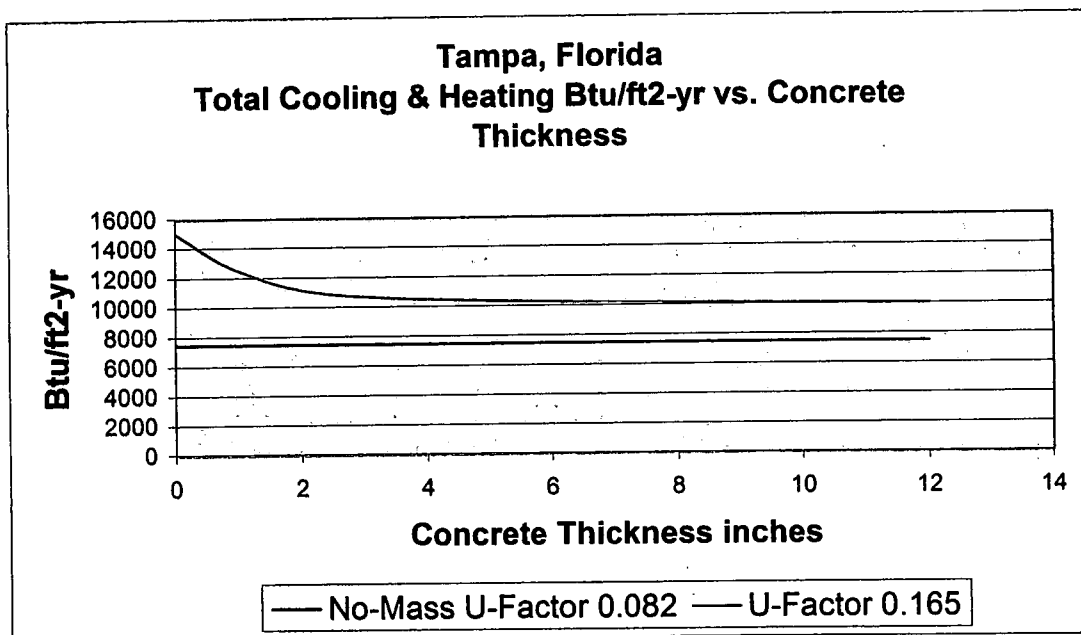


Figure 5.25 Total cooling and heating vs. concrete thickness, Tampa, Florida

Figure 5.26 plots the total cooling and heating requirements with increasing U-factor for the 2-1/2 thick concrete "mass wall" with the U-factor of $0.165 \text{ Btu/hr} \cdot \text{ft}^2 \cdot ^\circ\text{F}$ to determine the U-factor for which it will perform as well as the no-mass wall with the U-factor of $0.082 \text{ Btu/hr} \cdot \text{ft}^2 \cdot ^\circ\text{F}$. The lines cross at approximately $0.116 \text{ Btu/hr} \cdot \text{ft}^2 \cdot ^\circ\text{F}$. This is the required U-

factor for the 2-1/2-inch thick IECC "mass wall" to perform as the IECC no-mass wall. To determine the dependence on the location of the concrete within the wall Figure 5.27 plots the total $Btu/ft^2\text{-yr}$ cooling and heating load for 2-1/2-inches of concrete against the location within the wall. The mass remains 95% effective with only 25% of the insulation exterior to it.

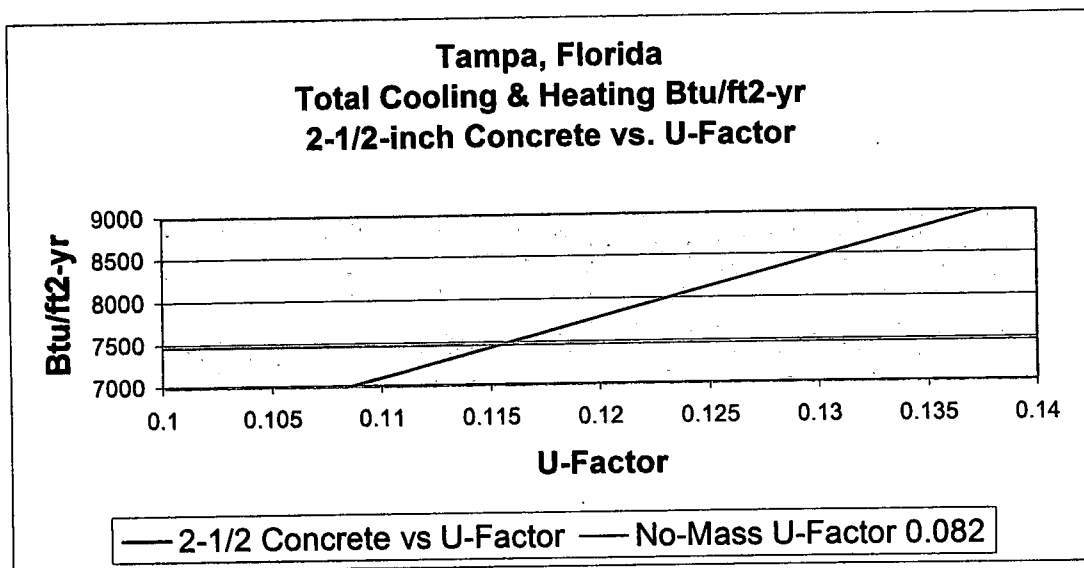


Figure 5.26 Total cooling and heating vs. U-factor of "mass wall" compared to U-factor of no-mass wall

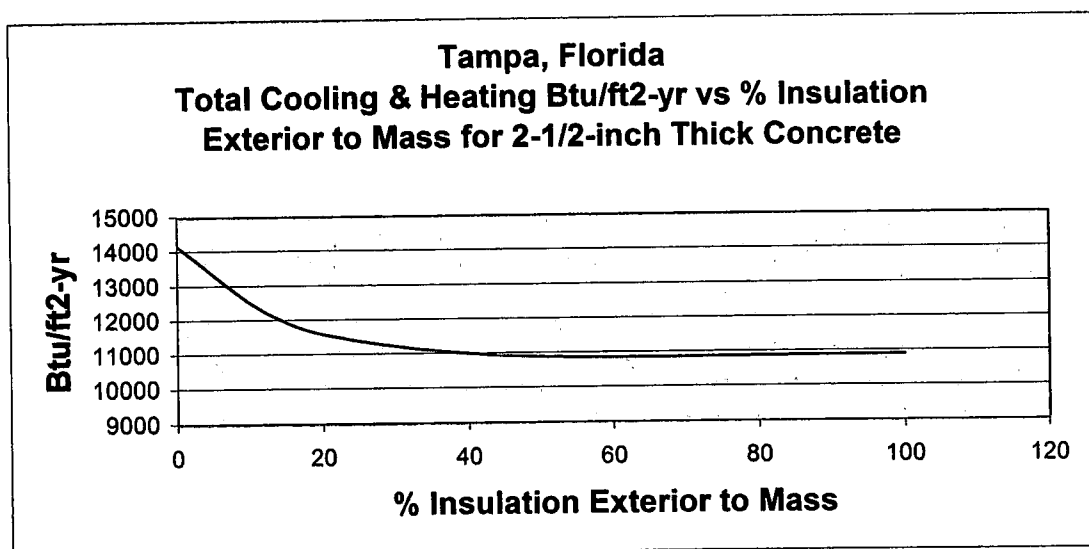


Figure 5.27 Total cooling and heating vs. insulation location, Tampa, Florida

5.6.2: San Antonio, Texas

Figure 5.28 plots the $Btu/ft^2\text{-yr}$ total cooling and heating load for a concrete "mass wall" with a U-factor of $0.165 \text{ Btu/hr} \cdot \text{ft}^2 \cdot ^\circ\text{F}$ with increasing concrete thickness. The $Btu/ft^2\text{-yr}$ total cooling and heating load for a standard no-mass wall with a U-factor of $0.082 \text{ Btu/hr} \cdot \text{ft}^2 \cdot ^\circ\text{F}$ is plotted as a horizontal line. The "mass wall" total cooling and heating load requirements does not cross the no-mass wall, with a U-factor of $0.082 \text{ Btu/hr} \cdot \text{ft}^2 \cdot ^\circ\text{F}$, load requirements. The reduction of total cooling and heating load for the U-factor $0.165 \text{ Btu/hr} \cdot \text{ft}^2 \cdot ^\circ\text{F}$ "mass wall" reduces approximately 20% with 2-1/2-inches of concrete but remains respectively approximately 62% above the no-mass wall with a U-factor of $0.082 \text{ Btu/hr} \cdot \text{ft}^2 \cdot ^\circ\text{F}$.

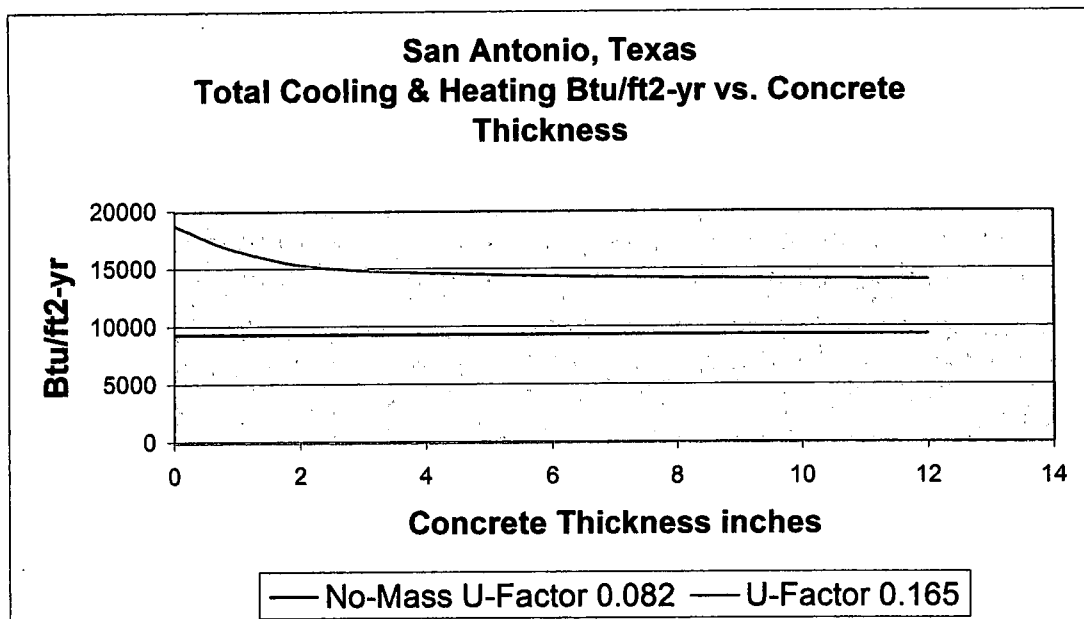


Figure 5.28 Total cooling and heating vs. concrete thickness, San Antonio, Texas

Figure 5.29 plots the total cooling and heating requirements with increasing U-factor for the 2-1/2 thick concrete “mass wall” with the U-factor of $0.165 \text{ Btu/hr} \cdot \text{ft}^2 \cdot ^\circ\text{F}$ to determine the U-factor for which it will perform as well as the no-mass wall with the U-factor of $0.082 \text{ Btu/hr} \cdot \text{ft}^2 \cdot ^\circ\text{F}$. The lines cross at approximately $0.103 \text{ Btu/hr} \cdot \text{ft}^2 \cdot ^\circ\text{F}$. This is the required U-factor for the 2-1/2-inch thick IECC “mass wall” to perform and the IECC no-mass wall.

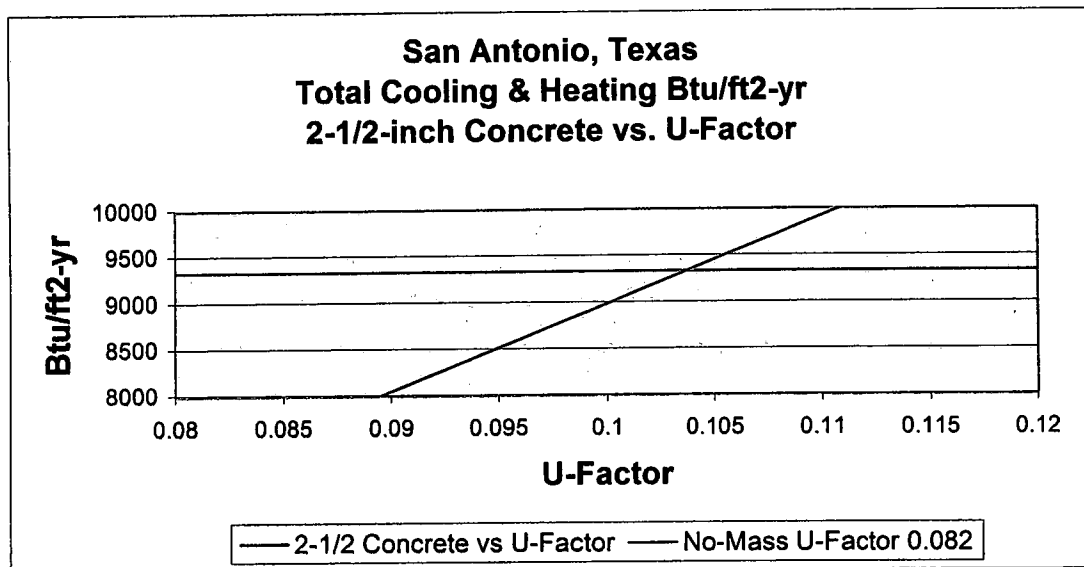


Figure 5.29 Total cooling and heating vs. U-factor of “mass wall” compared to U-factor of no-mass wall

5.6.3: Summary of Climate Zone 2

The annual cooling load is reduced between 20% and 28% with 2-1/2-inch thick “mass wall” with a U-factor of $0.165 \text{ Btu/hr} \cdot \text{ft}^2 \cdot ^\circ\text{F}$ positioned on the interior of the wall. The annual heating load is reduced between 24% and

27%. However, for the “mass wall,” defined as having $6 \text{ Btu/ft}^2 \cdot ^\circ F$, the required U-factor for it to perform as a standard no-mass wall with a U-factor of 0.082 as in the 2009 IECC varies between 0.103 to $0.116 \text{ Btu/hr} \cdot \text{ft}^2 \cdot ^\circ F$.

5.7 Analysis of Locations in Climate Zone 3

Both Tulsa, Oklahoma, and Topeka, Kansas, are in Climate Zone 3 of the IECC. Tulsa, Oklahoma, has an average annual temperature of $59.5 \text{ }^\circ F$, an annual sol-air temperature of $63.6 \text{ }^\circ F$, annual heating degrees of days of 4063, and annual cooling degrees of days of 2,044. Topeka, Kansas, has an average annual temperature of $53.9 \text{ }^\circ F$, an average annual sol-air temperature of $57.9 \text{ }^\circ F$, annual heating degrees days of 5,515, and annual cooling degree days of 1,461. The IECC requires a U-Factor of 0.082 $\text{Btu/hr} \cdot \text{ft}^2 \cdot ^\circ F$ for a standard no-mass wall and allows a U-factor reduction to $0.141 \text{ Btu/hr} \cdot \text{ft}^2 \cdot ^\circ F$ for a “mass wall” having $6 \text{ Btu/ft}^2 \cdot ^\circ F$.

5.7.1: Tulsa, Oklahoma

Figure 5.30 plots the $\text{Btu/ft}^2 \text{ yr}$ cooling load for a concrete “mass wall” with a U-factor of $0.141 \text{ Btu/hr} \cdot \text{ft}^2 \cdot ^\circ F$ with increasing concrete thickness. The $\text{Btu/ft}^2 \text{ yr}$ cooling load for a standard no-mass wall with a U-factor of $0.082 \text{ Btu/hr} \cdot \text{ft}^2 \cdot ^\circ F$ is plotted as a horizontal line. The “mass wall” cooling load requirements do not cross the no-mass wall cooling load

requirements. The reduction of cooling load for the U-factor 0.165 $Btu/hr \cdot ft^2 \cdot ^\circ F$ "mass wall" reduces 27% with 2-1/2-inches of concrete and 31% with 6-inches of concrete.

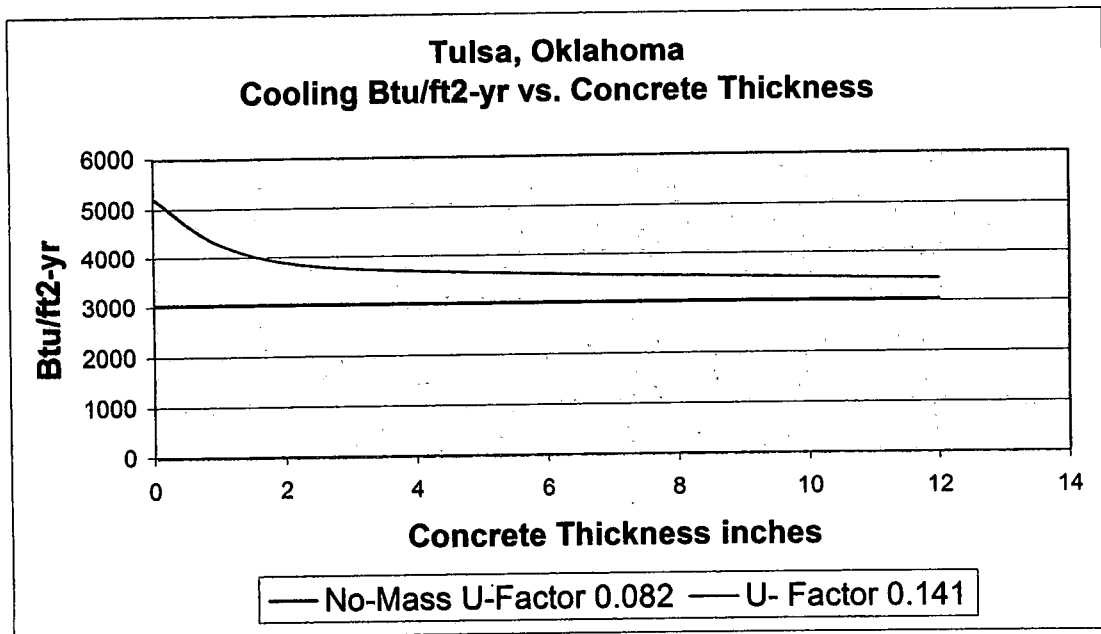


Figure 5.30 Cooling vs. concrete thickness, Tulsa, Oklahoma

However, the "mass wall" cooling load remains approximately 19% above the no-mass wall with a U-factor of 0.082 $Btu/hr \cdot ft^2 \cdot ^\circ F$ as allowed in the IECC. Figure 5.31 plots the $Btu/ft^2 \cdot yr$ heating load for a concrete "mass wall" with a U-factor of 0.141 $Btu/hr \cdot ft^2 \cdot ^\circ F$ with increasing concrete thickness. The $Btu/ft^2 \cdot yr$ heating load for a standard no-mass wall with a U-factor of 0.082 $Btu/hr \cdot ft^2 \cdot ^\circ F$ is plotted as a horizontal line. The "mass wall" heating load requirements do not cross the no-mass wall with the U-factor of 0.082 $Btu/hr \cdot ft^2 \cdot ^\circ F$. The reduction of heating load for the U-factor 0.141 $Btu/hr \cdot ft^2 \cdot ^\circ F$ "mass wall" is only approximately 7% with 2-

1/2-inches of concrete and approximately 9% with 6-inches of concrete. The 2-1/2 inch concrete remains approximately 60% above the no-mass wall.

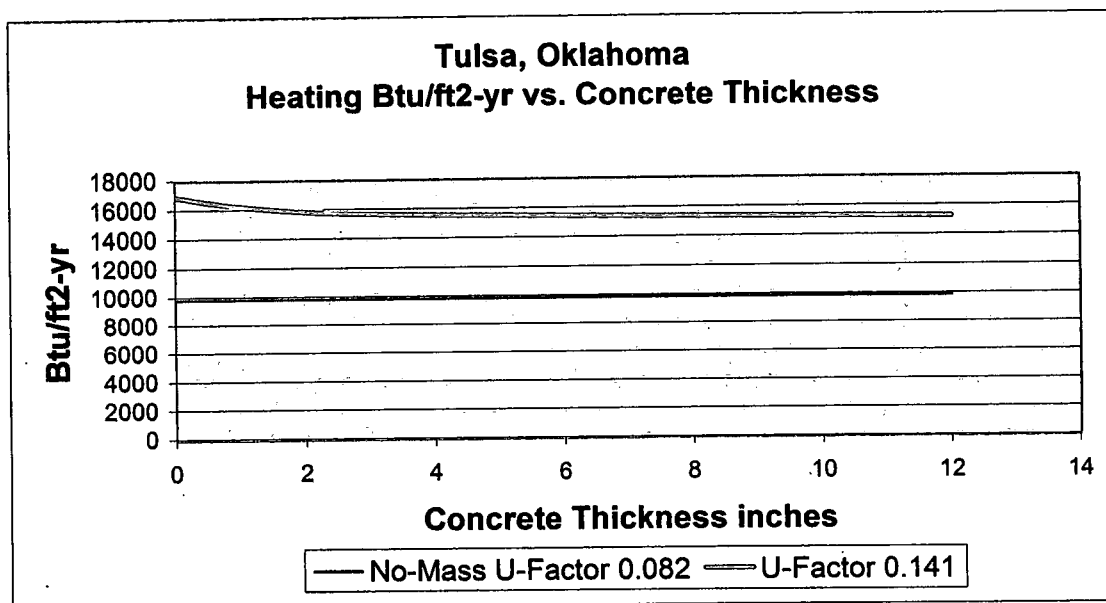


Figure 5.31 Heating vs. concrete thickness, Tulsa, Oklahoma

Figure 5.32 plots the $Btu/ft^2 \cdot yr$ total cooling and heating load for a concrete "mass wall" with a U-factor of $0.141 Btu/hr \cdot ft^2 \cdot ^\circ F$ with increasing concrete thickness. The $Btu/ft^2 \cdot yr$ total cooling and heating load for a standard no-mass wall with a U-factor of $0.082 Btu/hr \cdot ft^2 \cdot ^\circ F$ is plotted as a horizontal line. The "mass wall" total load requirements do not cross the no-mass wall load requirements with a U-factor of $0.082 Btu/hr \cdot ft^2 \cdot ^\circ F$. The reduction of total cooling and heating load for the U-factor $0.165 Btu/hr \cdot ft^2 \cdot ^\circ F$ "mass wall" reduces approximately 28% with 2-1/2-inches of concrete and approximately 32% with 6-inches of concrete but remains respectively approximately 46%% and 36% above the no-mass wall.

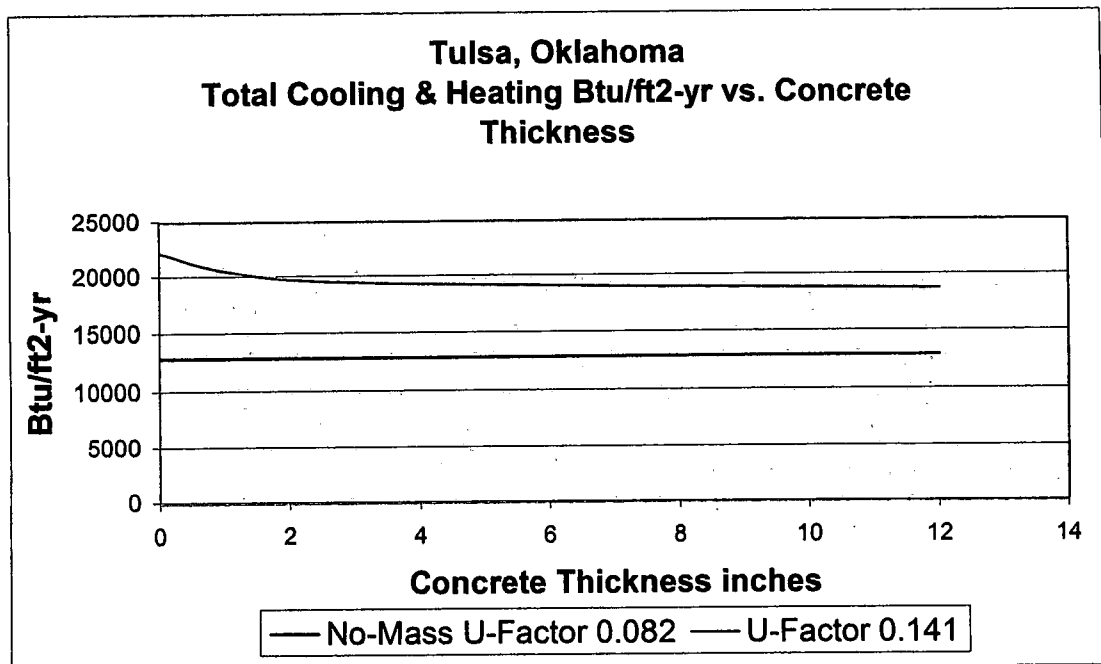


Figure 5.32 Total cooling and heating vs. concrete thickness

Figure 5.33 plots the total cooling and heating requirements with increasing U-factor for the 2-1/2 thick concrete “mass wall” with the U-factor of $0.141 \text{ Btu/hr} \cdot \text{ft}^2 \cdot ^\circ\text{F}$ to determine the U-factor for which it will perform as well as the no-mass wall with the U-factor of $0.082 \text{ Btu/hr} \cdot \text{ft}^2 \cdot ^\circ\text{F}$. The lines cross at approximately $0.094 \text{ Btu/hr} \cdot \text{ft}^2 \cdot ^\circ\text{F}$. This is the required U-factor for the 2-1/2-inch thick IECC “mass wall” to perform and the IECC no-mass wall.

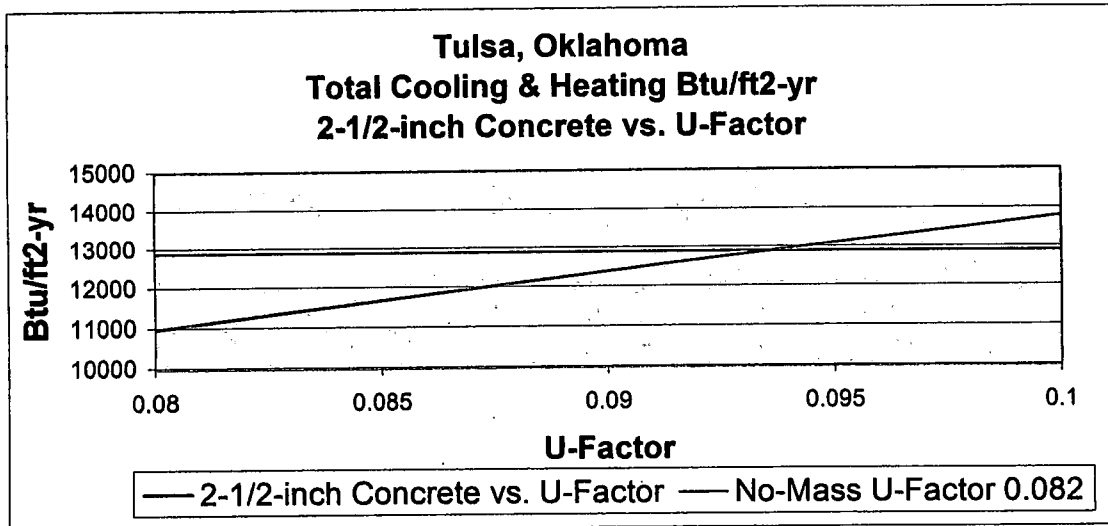


Figure 5.33 Total cooling and heating vs. U-factor of "mass wall" compared to U-factor of no-mass wall

5.7.2: Topeka, Kansas

Figure 5.34 plots the $Btu/ft^2 - yr$ total cooling and heating load for a concrete "mass wall" with a U-factor of $0.165 Btu/hr \cdot ft^2 \cdot ^\circ F$ with increasing concrete thickness. The $Btu/ft^2 yr$ total cooling and heating load for a standard no-mass wall with a U-factor of $0.082 Btu/hr \cdot ft^2 \cdot ^\circ F$ is plotted as a horizontal line. The "mass wall" total cooling and heating load requirements do not cross the no-mass wall, with a U-factor of $0.082 Btu/hr \cdot ft^2 \cdot ^\circ F$, load requirements. The reduction of total cooling and heating load for the U-factor $0.141 Btu/hr \cdot ft^2 \cdot ^\circ F$ "mass wall" reduces approximately 10% with 2-1/2-inches of concrete but remains approximately 55% above the no-mass wall with a U-factor of $0.082 Btu/hr \cdot ft^2 \cdot ^\circ F$.

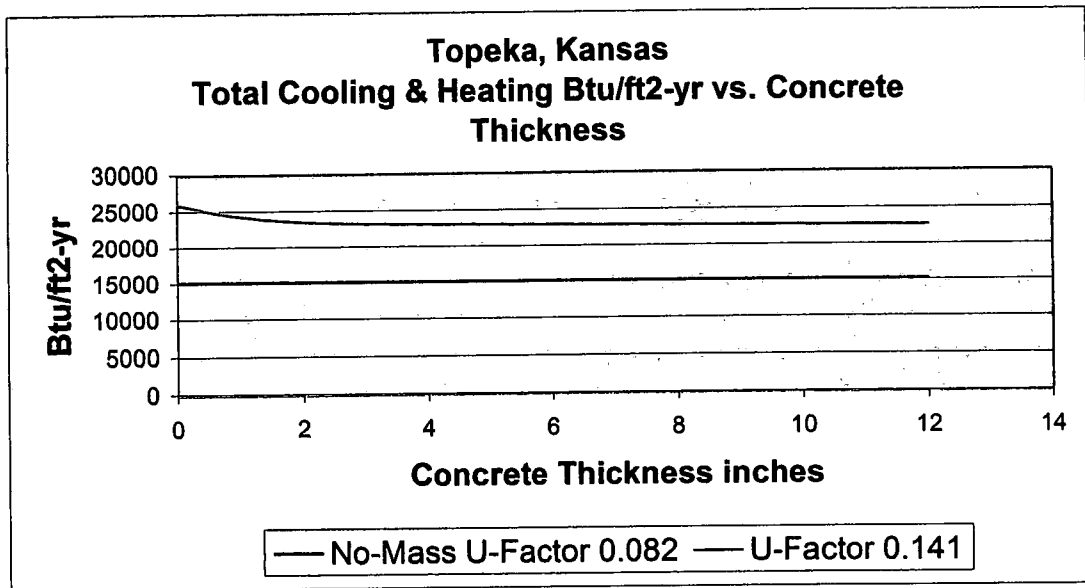


Figure 5.34 Total cooling and heating vs. concrete thickness, Topeka, Kansas

Figure 5.35 plots the total cooling and heating requirements with increasing U-factor for the 2-1/2 thick concrete “mass wall” with the U-factor of $0.141 \text{ Btu/hr} \cdot \text{ft}^2 \cdot ^\circ\text{F}$ to determine the U-factor for which it will perform as well as the no-mass wall with the U-factor of $0.082 \text{ Btu/hr} \cdot \text{ft}^2 \cdot ^\circ\text{F}$. The lines cross at slightly greater than $0.091 \text{ Btu/hr} \cdot \text{ft}^2 \cdot ^\circ\text{F}$.

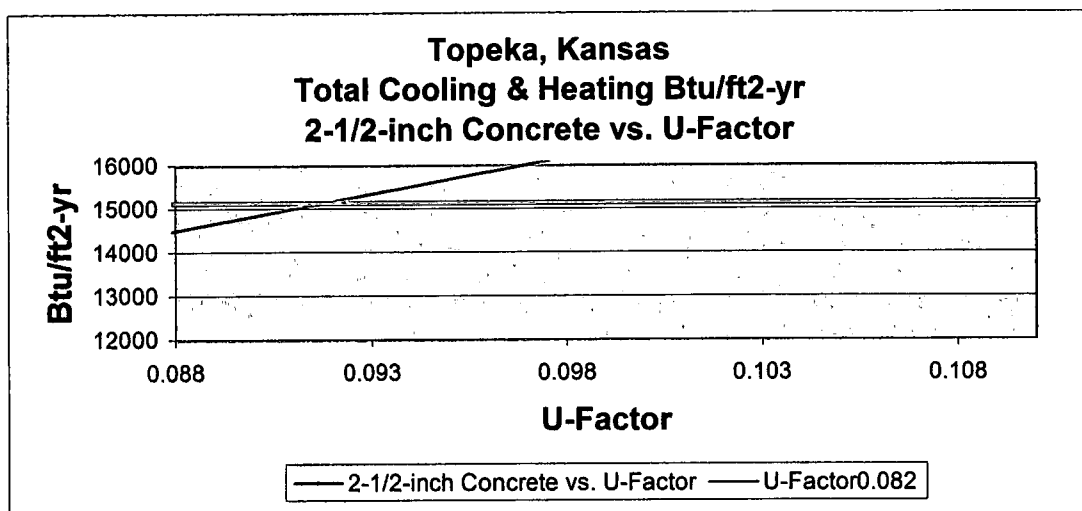


Figure 5.35 Total cooling and heating vs. U-factor of “mass wall” compared to U-factor of no-mass wall

5.7.3: Summary of Climate Zone 3

The annual cooling load is reduced between 27% and 38% with 2-1/2-inch thick "mass wall" with a U-factor of 0.141 positioned on the interior of the wall. The annual heating load is reduced between 5% and 7%. However, for the "mass wall," defined as having $6 \text{ Btu/ft}^2 \cdot ^\circ\text{F}$, the required U-factor for it to perform as a standard no-mass wall with a U-factor of 0.082 as in the 2009 IECC varies between 0.091 to $0.094 \text{ Btu/hr} \cdot \text{ft}^2 \cdot ^\circ\text{F}$.

5.8 Summary

The results of the climate zones studied are shown in table 5.6. The climate zone is shown in the first column, the IECC U-factor for the no-mass wall is shown in the second column, the IECC U-factor for the "mass wall" is shown in the third column, and the final column shows the U-factor required for the "mass wall" to transmit the same amount of heat as the IECC no-mass wall.

	FRAME WALL	MASS WALL	MASS WALL EQUIVALENT
CLIMATE ZONE	U-FACTOR	U-FACTOR	U-FACTOR
2	0.082	0.165	0.091-0.094
3	0.082	0.141	0.103-0.116
5 and Marine 4	0.057	0.082	0.064-0.068

Table 5.6 Climate zones, IECC U-factor of no-mass wall and "mass wall," and the U-factor for the "mass wall" to transmit the same amount of heat as IECC no-mass wall

5.9 PCM on Exterior as "Mass Wall"

In the IECC, the "mass wall" in Dayton, Ohio, can have a U-factor reduction of $0.082 \text{ Btu/hr} \cdot \text{ft}^2 \cdot ^\circ\text{F}$. The no-mass wall with a U-factor of $0.082 \text{ Btu/hr} \cdot \text{ft}^2 \cdot ^\circ\text{F}$ has an annual cooling load of $1,313 \text{ Btu/ft}^2 - \text{yr}$ and an annual heating load of $14,405 \text{ Btu/ft}^2 - \text{yr}$. 6-inch thick concrete on the interior reduces this to an annual cooling load of $352 \text{ Btu/ft}^2 - \text{yr}$ and an annual heating load of $13,534 \text{ Btu/ft}^2 - \text{yr}$. 1/2-inch thick PCM on the exterior with 1/8 of the insulation on the exterior and a melting temperature 73°F reduces the annual cooling load to $85 \text{ Btu/ft}^2 - \text{yr}$ and the annual heating load to $13,178 \text{ Btu/ft}^2 - \text{yr}$. Thus, the 1/2-inch thick PCM on the exterior is more effective than 6-inches of concrete on the interior. The PCM became more effective as the melt temperature approached interior temperature.

CHAPTER 6

EFFECT OF THERMAL MASS ON THERMAL TRANSMISSION USING TMY2 WEATHER FILE FOR DAYTON, OHIO

Portions of the TMY2 weather file for Dayton, Ohio, are used to compare the effects of a 6-inch thick "mass wall" to a no-mass wall. A portion of the weather file, with the cyclic sol-air temperature below the interior set point temperature, is examined and a comparison is made between the "mass wall" and the no-mass wall. Another portion of the weather file, with the cyclic sol-air temperature cycling above and below the interior set point temperature, is examined and a comparison is made between the "mass wall" and the no-mass wall.

6.1: TMY2 Weather File for Dayton, Ohio

Figure 6.1 plots the average sol-air temperature against the hour of the year from the TMY2 weather file for Dayton, Ohio. The finite-difference model reads time, air temperature and solar radiation data from a TMY2 file and calculates the solar radiation on the north, east, south, and west vertical surfaces. It then calculates the sol-air temperature at each surface. It then averages the four sol-air temperatures and uses the averaged sol-air temperature as the exterior temperature. The interior air set point of 72 °F is also shown.

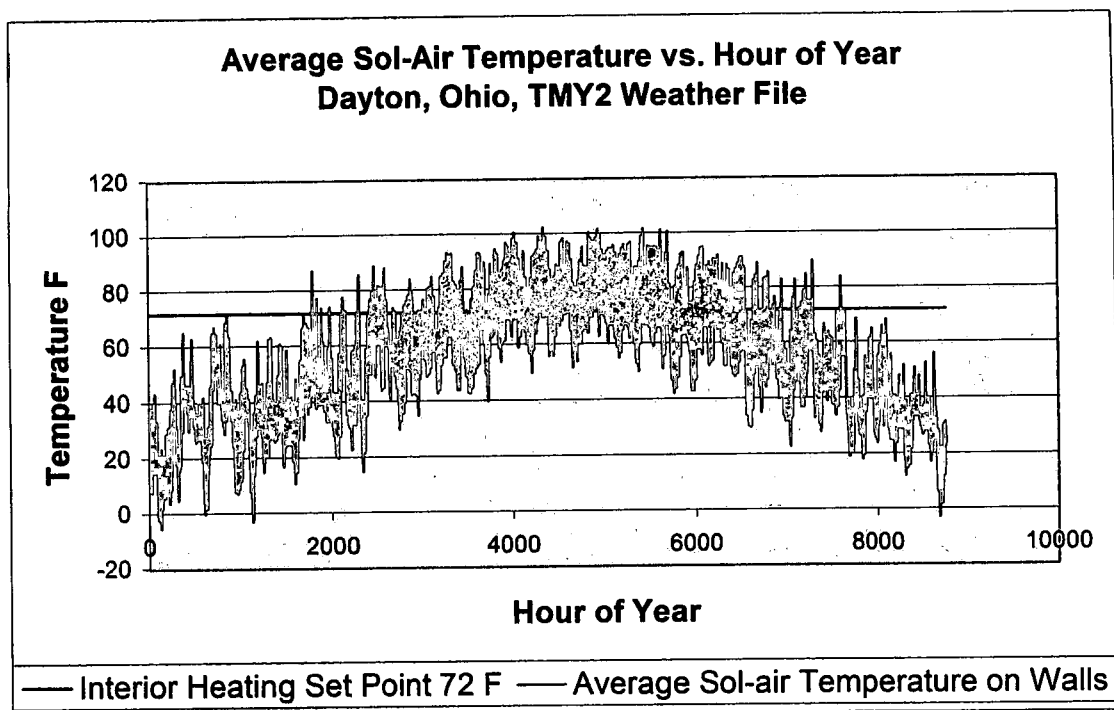


Figure 6.1 Average sol-air temperatures vs. hour of year for Dayton, Ohio, TMY2 weather file

Thermal mass will have little or no effects on heat transfer through a wall between the hours of 0 and 1500 and between 7000 and 8760 because the sol-air temperature does not pass through the interior set point temperature. Thermal mass will reduce heat transfer through the wall between the hours of 2500 and 4000 and between 5000 and 7000 hours because the sol-air temperature passes above and below the interior set point temperature.

6.2: Comparison of Heat Transfer of "Mass Wall" to No-Mass Wall for Hours 0 to 1500 and Hours 2500 to 4000

Figure 6.2 compares the heat transfer of a no-mass wall with a U-factor of 0.082 to a "mass wall" with 6-inches of concrete on the interior of the

insulation with the same U-factor of 0.082. The no-mass wall has a total heat transfer between hours 0 and 1,500 of $5,001 \text{ Btu/hr} \cdot \text{ft}^2$ for heating and the mass wall has a total heat transfer of $5,026 \text{ Btu/hr} \cdot \text{ft}^2$ for heating. Thus, as expected thermal mass has little effect in the middle of the winter.

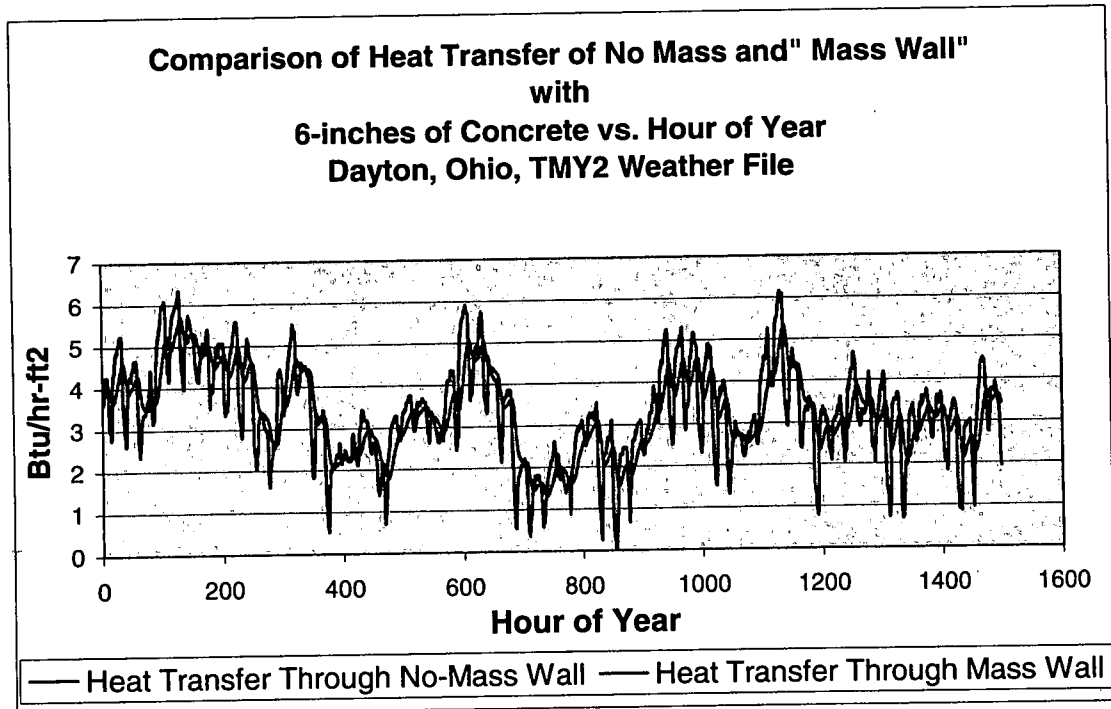


Figure 6.2 Comparison of heat transfer of no mass wall and "mass wall" with 6-inches of concrete hours 0 to 1500.

Figure 6.3 compares the heat transfer of a no-mass wall with a U-factor of 0.082 to a "mass wall" with 6-inches of concrete on the interior of the insulation with the same U-factor of 0.082. The no-mass wall has a total heat transfer between hours 2500 and 4000 of $1,196 \text{ Btu/hr} \cdot \text{ft}^2$ for heating and the "mass wall" has a total heat transfer of $972 \text{ Btu/hr} \cdot \text{ft}^2$ for heating. This is a reduction in heating of approximately 19% over this time period.

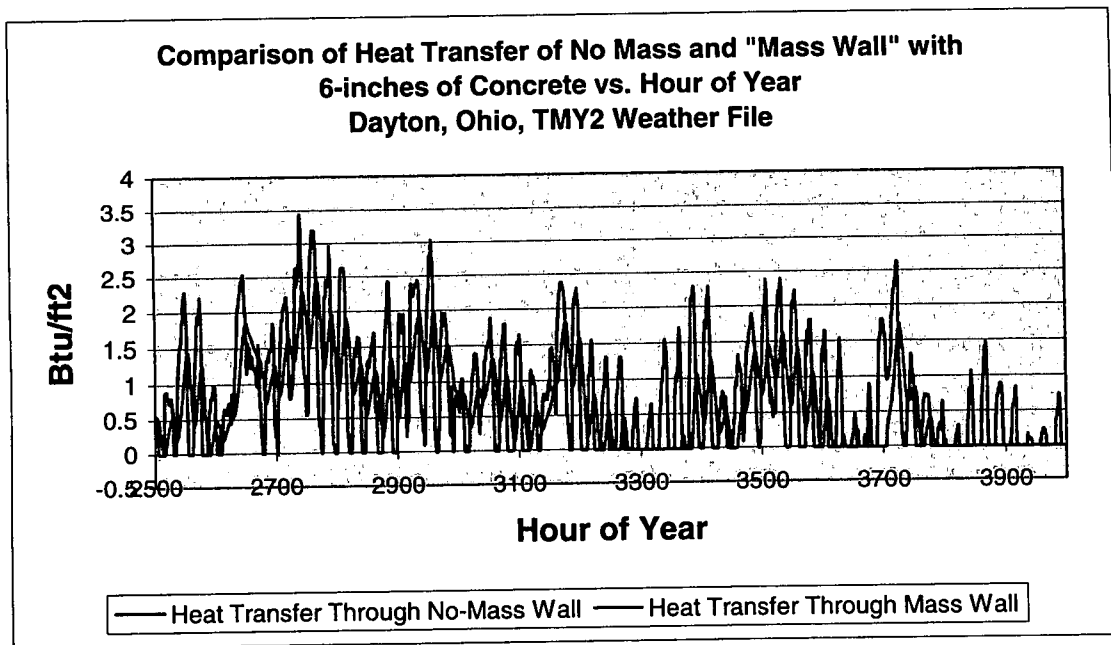


Figure 6.3 Comparison of heat transfer of no-mass wall and "mass wall" with 6-inches of concrete hours 2500 to 4000.

Figure 6.4 plots the required heating, heat transfer, with the average sol-air temperature. The slope of the straight line is the U-factor of the wall, $0.082 \text{ Btu} / \text{ft}^2 \cdot \text{hr} \cdot ^\circ \text{F}$. This linearity makes it possible to plot the heat transfer through a no-mass wall if the U-factor is determined [26, 27].

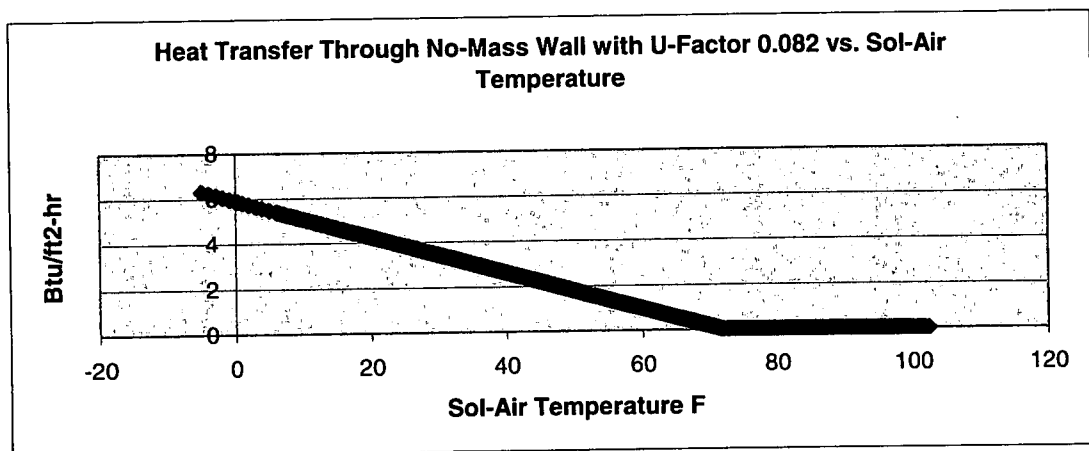


Figure 6.4 Heat transfer through a no-mass wall with a U-factor of 0.082 vs. sol-air temperature $^\circ \text{F}$

Figure 6.5 plots the heat transfer, required heating, through the “mass wall” vs. the sol-air temperature. The single straight line relationship between the heating and the sol-air temperature of the no-mass wall becomes a broad scattering of points. The slope of the curve fit straight line remains approximately the same and the no-mass case, $0.082 \text{ Btu} / \text{ft}^2 \cdot \text{hr} \cdot ^\circ \text{F}$.

The narrow straight line as in figure 6.4 is lost due the inside wall temperature, and heat transfer, lagging behind the outside sol-air temperature. As the sol-air temperature is increasing, the lagging heat transfer is plotted against the higher temperature. As the sol-air temperature is decreasing, the lagging heat transfer is plotted against a lower temperature. Therefore there are a range of temperatures plotted to a heat transfer value.

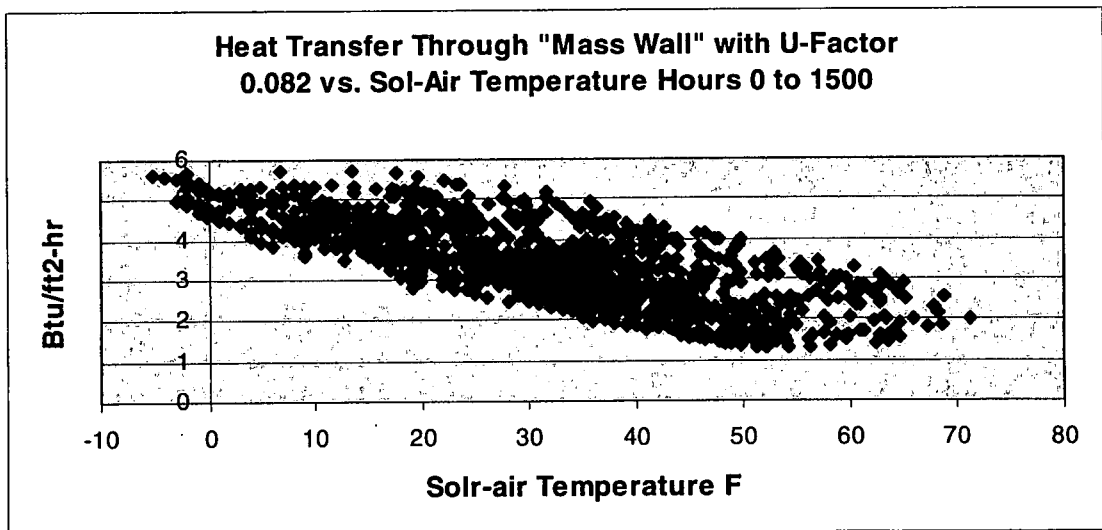


Figure 6.5 Heat transfer through a “mass wall” with a U-factor of 0.082 vs. sol-air temperatures $^\circ \text{F}$, hours 0 to 1500.

Figure 6.6 plots the heat transfer out of a “mass wall” versus the sol-air temperature for the hours 2500 to 4000. This is the time period in which the “mass wall” has the greatest effect on heat transfer. The scatter

demonstrates that heat transfer cannot be calculated using a steady-state U-factor alone. The thermal mass must be included.

In figure 6.6, the same lagging occurs as in figure 6.5 resulting in a range of temperatures plotted to a value of the heat transfer. The slope of the plotted points change as the thermal mass reduces the heat transfer.

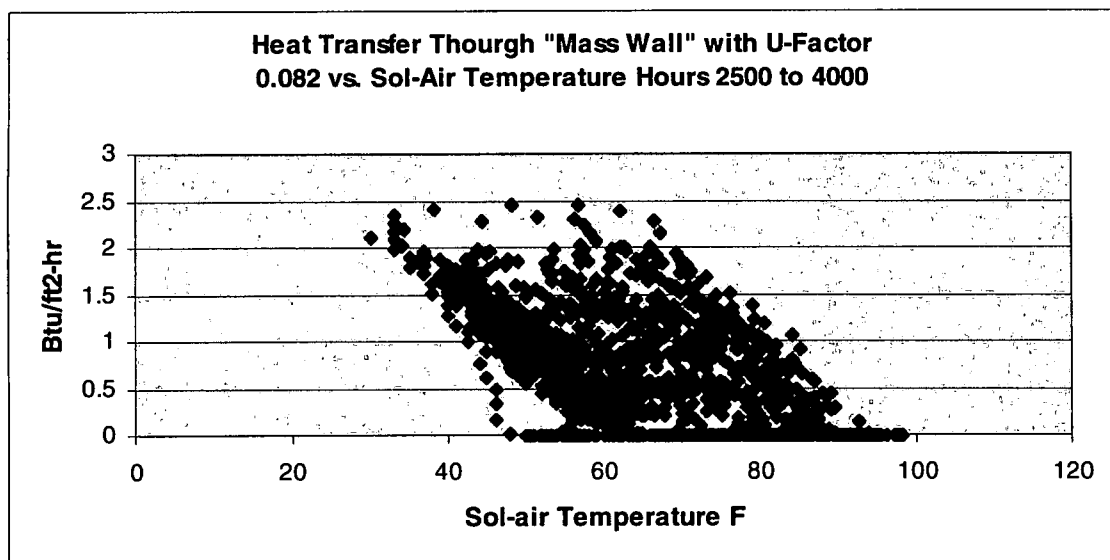


Figure 6.6 Heat transfer through a "mass wall" with a U-factor of 0.082 vs. sol-air temperature $^{\circ}F$, hours 2500 to 4000.

The finite-difference model with the BESTEST specifications was used to compare the lightweight case against the heavyweight case for both the 0 to 1500 hour time period and the 2500 to 4000 hour time period. No windows, infiltration or internal gains were considered. The interior air set points were $72^{\circ}F$ and $75^{\circ}F$ respectively for the heating and the cooling. The required heating for the 0 to 1500 hour time period was 5.74 MBtu for the lightweight case and 5.72 for the heavyweight case. As the outside sol-air temperature, average and peak, was almost always below the interior air

temperature set point, the mass of the heavyweight had no effect on the required heating load. The required heating for the time period of 2500 to 400 hours was 0.98 MBtu for the lightweight case and 0.79 MBtu for the heavyweight case. The peak outside sol-air temperature was above the interior air temperature set point many times and therefore, the mass of the heavyweight case reduced the required heating by 19%.

BESTEST has 14 qualification cases. All have windows. The diagnostic cases, 195, 395, 430, and 800 have no windows or a high conductance wall. The high conductance wall has 12 square meter of window on the south side with zero short wave transmittance. This research software compared to BESTEST:

Case 195, low mass no window, set point 20, 20, 0 internal gain, 0 infiltration
BESTEST heating; 4.167 to 5.871, mean 4.99 MWH
Research software; 5.32 MWH
BESTEST cooling; 0.413 to 0.510, mean 0.436 MWH
Research software; 0.43 MWH

Case 395, low mass, no window, set point 20,27, 0 internal gain, 0 infiltration
BESTEST heating: 4.799 to 5.202, mean 5.085 MWH
Research Software; 5.19 MWH
BESTEST cooling; 0.0 to 0.016 MWH
Research software; 0.01 MWH

Case 430, low mass, set point 20, 27, 200 W internal, 0.5 infiltration, high conductance wall
BESTEST heating; 5.429 to 7.827, mean 6.723 MWH
Research software; 7.58 MWH
BESTEST cooling; 0.422 to 0.875, mean 0.628 MWH
Research software; 0.66 MWH

Case 800, high mass, same as 430
BESTEST heating; 4.868 to 7.228, mean 6.153 MWH
Research software; 7.01 MWH
BESTEST cooling; 0.055 to 0.325, mean 0.202 MWH
Research software; 0.21 MWH

CHAPTER 7

EXPERIMENT OF EFFECT OF THERMAL MASS ON THERMAL TRANSMISSION

A test cell was constructed with one 5-1/2-inch thick concrete wall. The test cell has a heater to control the interior temperature. The test cell was placed in the ambient weather in Beavercreek, Ohio. The interior set point temperature was set above the highest peak ambient temperature. Data was recorded of the ambient temperature, interior cell temperature and the energy required to maintain the interior temperature at set point. Then, the interior set point temperature was set at the average ambient temperature and data was recorded. A comparison was made between the required energy and the calculated no-mass energy at the two set points.

7.1: Experimental Apparatus

A one foot interior cubical cell was constructed. One wall of the cube was constructed of a 5-1/2-inch thick, 1 foot square slab and covered with 1-3/8-inch thick bead board. Figure 7.1 is a photo of the concrete being cast.

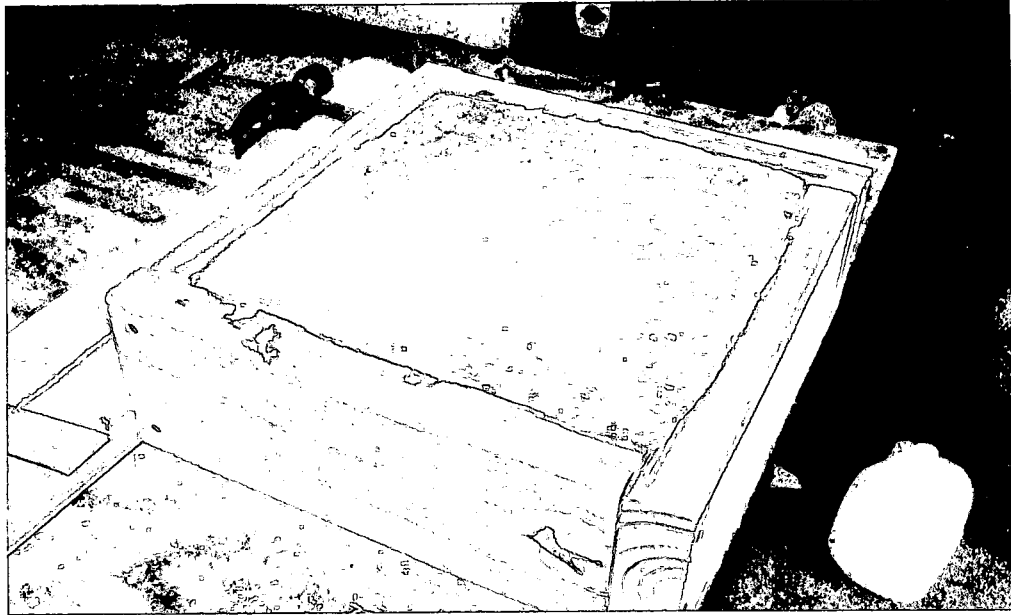


Figure 7.1 1-foot square 5-1/2-inch thick wall section being cast.

Figure 7.2 is a photo of the concrete wall section in place on the test apparatus platform.

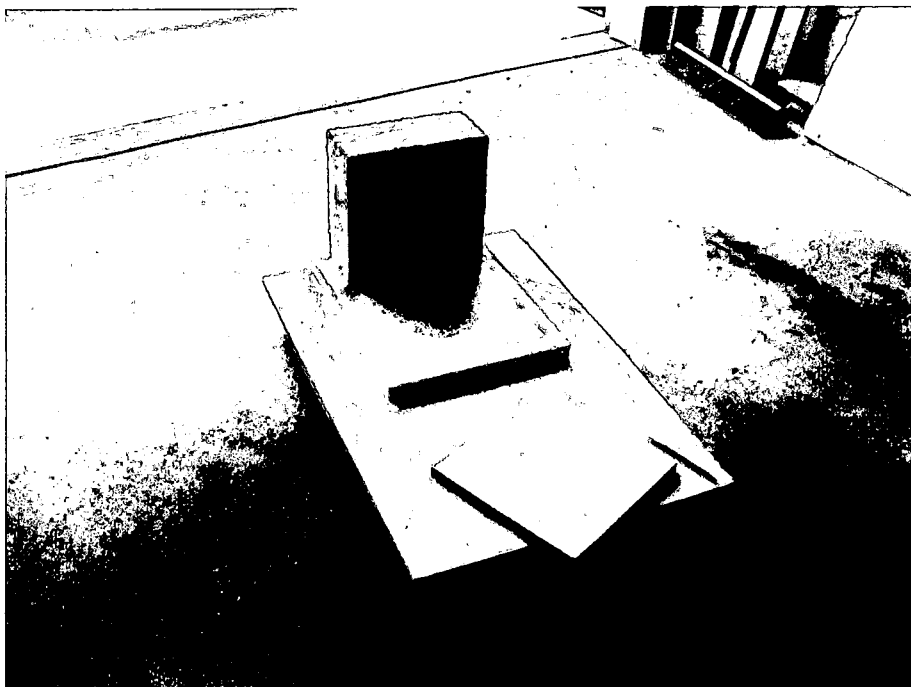


Figure 7.2 1-foot square, 5-1/2-inch thick wall section on test platform.

A residential heating thermostat was wired in series with a 24-volt transformer and a 24-volt coil, 115-volt contactor. When energized by the thermostat, the contactor turned on a 13 watt CFL which was used as a heating source for the test cell. Figure 7.3 is a photo of the test platform with the concrete wall section in place and the thermostat-CFL circuits. The thermostat was mounted on a piece of 2x6 facing away from the light and facing the concrete wall section. A metal shield reflector was mounted on the top of the 2x6 to shield the thermostat and temperature probes from any direct light from the CFL.

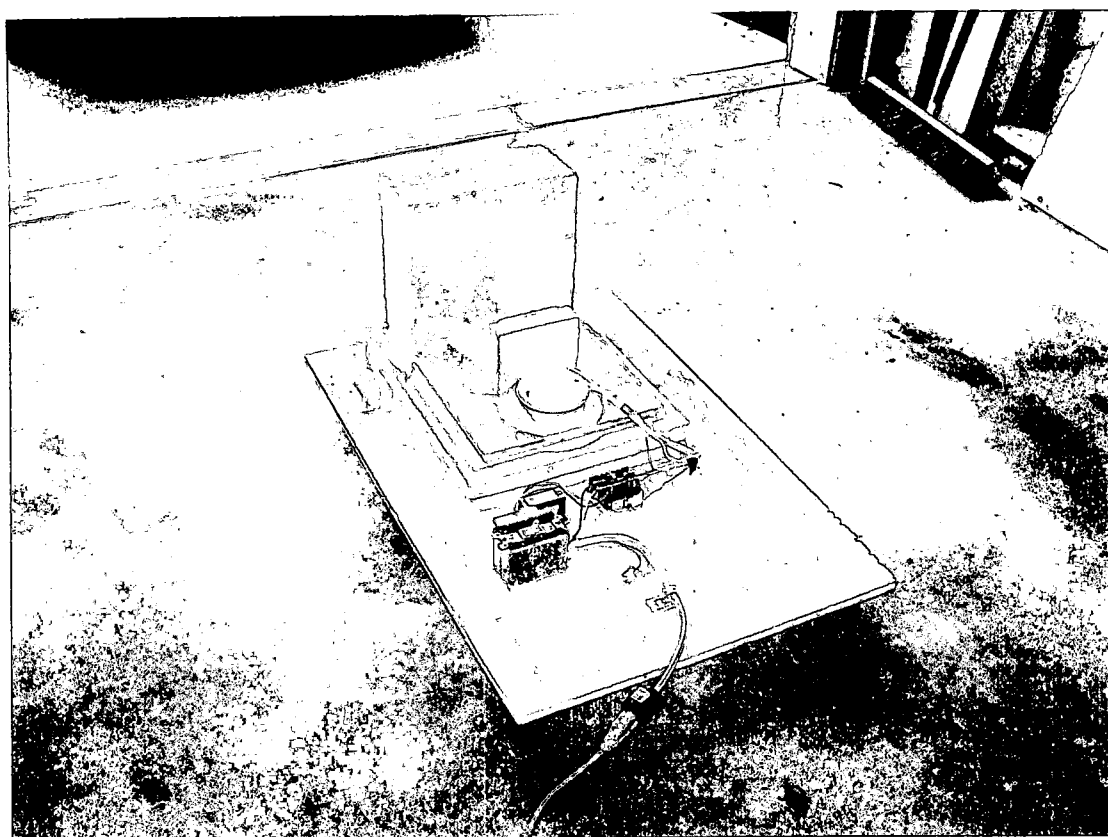


Figure 7.3 Test platform with the concrete wall section in place and the thermostat-CFL circuits.

Figure 7.4 is a photo of the test platform with the temperature probes, the photo cell, and the data logger. Originally, one temperature probe was mounted above the thermostat, one probe was mounted on the inner surface of the concrete wall, and one probe, shown in Fig. 7.5, on the outer surface of the concrete wall. The probe on the outer surface of the concrete was later moved to the exterior of the test cell to measure the outside air temperature. The shield over the CFL is shown in the photo.

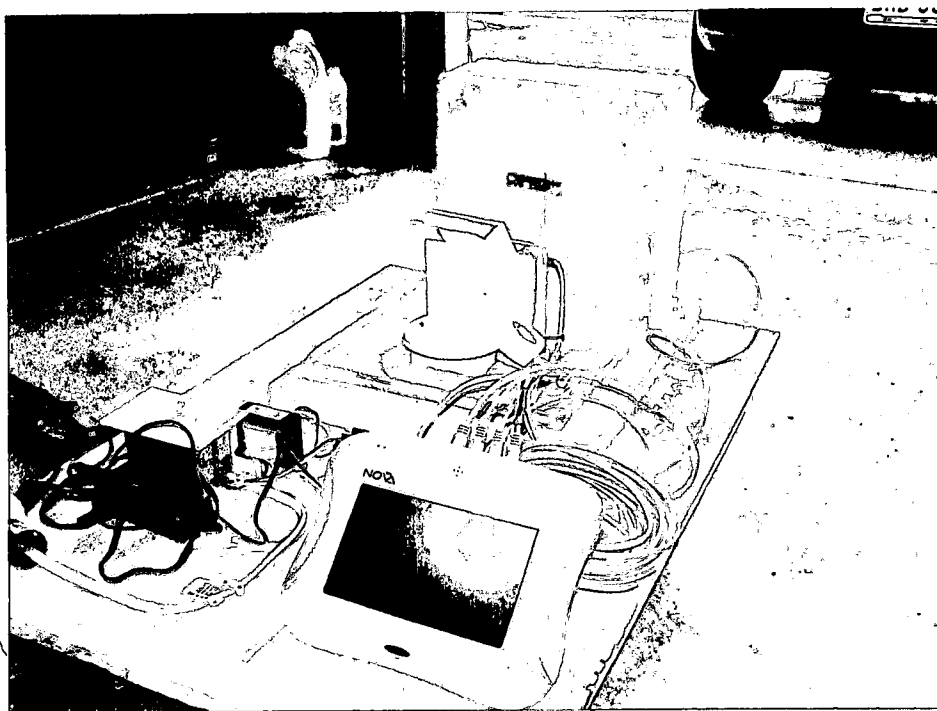


Figure 7.4 Photo of the test platform with the temperature probes mounted, the photo cell in location and the data logger.

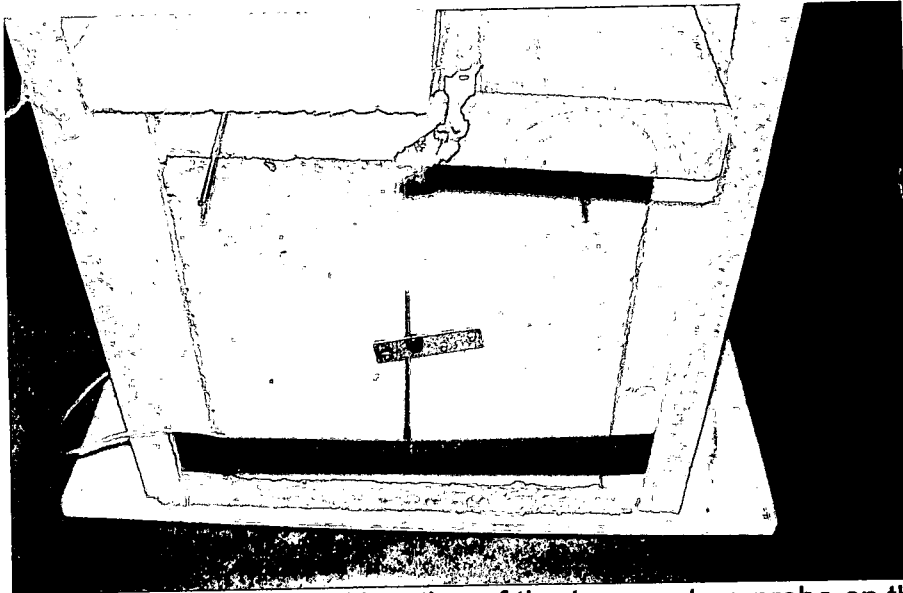


Figure 7.5 Photo of the original location of the temperature probe on the outer surface of the concrete wall.

Two layers of 1-3/8-inch thick bead board were used to construct the two sides, top, and rear walls of the test cell. One layer of bead board was used to cover the outside of the concrete wall. The floor, bottom, of the cell is one layer of bead board sandwiched between two layers of 3/4-inch thick plywood. Figure 7.6 is a photo of beginning of the construction of the bead board walls.

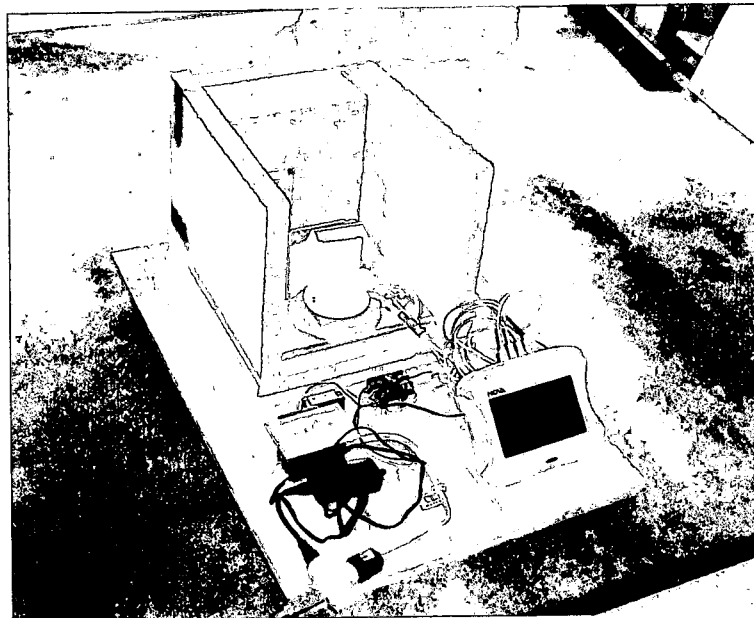


Figure 7.6 Photo of beginning of the construction of the bead board walls.

Figure 7.7 and 7.8 are photos of the completed test cell. Bead board has a listed R-value of $3.57 \text{ ft}^2 \cdot \text{hr} \cdot ^\circ\text{F} / \text{Btu} \cdot \text{in.}$ This gives the cell a preliminary estimated UA of approximately $0.58 \text{ Btu/hr} \cdot ^\circ\text{F}.$

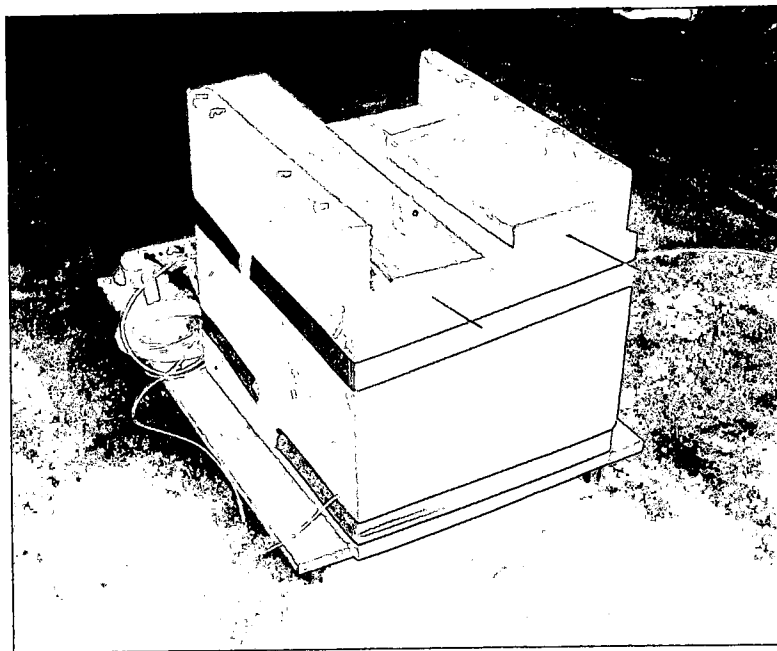


Figure 7.7 Photo of front of completed test cell.

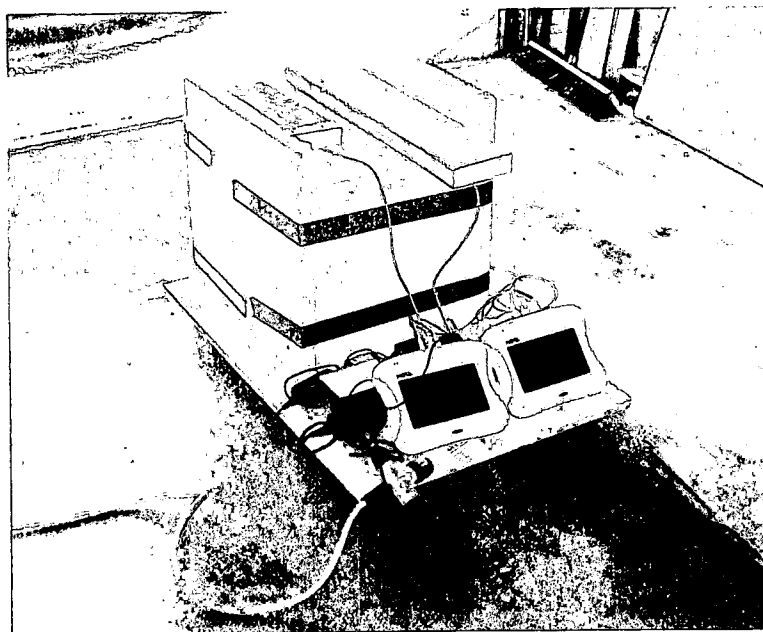


Figure 7.8 Photo of rear of completed test cell.

7.2: Test Procedure

The test procedure consisted of three parts:

1. Determine the UA of the test cell.
 - a. Place the test cell in a controlled environment held at a constant temperature.
 - b. Set the interior thermostat of the test cell at the highest temperature so heater will be on full time.
 - c. Turn on the power to the cell heater.
 - d. Determine when the cell and concrete wall are in steady state.
 - e. Record cell and outside of cell temperature.
 - f. Collect data on the required power input to the cell to maintain the interior temperature set point.
 - i. Monitor the voltage and amperage to the CFL heater.
2. Collect temperature and power input data when the exterior temperature, average and peak, are below the interior set point.
 - a. Observe weather temperature projection for a week in the future.
 - b. Set the interior cell thermostat to a temperature estimated to be below the average and peak of the forthcoming weather temperature.

- c. Collect data on the required power input to the cell to maintain the interior temperature set point.
 - i. Monitor the voltage and amperage to the CFL heater.
- 3. Collect temperature and power input data when the exterior temperature, average and peak, are oscillating evenly above and below the interior set point.
 - a. Observe weather temperature projection for a week in the future.
 - b. Set the interior cell thermostat to a temperature estimated to be at the average of the forthcoming weather temperature.
 - c. Collect data on the required power input to the cell to maintain the interior temperature set point.
 - i. Monitor the voltage and amperage to the CFL heater.

7.3: Results

7.3.1: Determination of Test Cell UA

The test cell was placed on the interior of a home in which the temperature is maintained at a constant temperature of approximately $70^{\circ}F$. The interior cell thermostat was set at the highest temperature, approximately $100^{\circ}F$. Originally a temperature probe was attached to the exterior surface

of the concrete. Two data loggers were used. One data logger logged three exterior air temperatures at locations around the test cell. The second data logger logged the interior air temperature of the cell at a location above the thermostat, the inner surface of the concrete, the outer surface of the concrete, and the energizing of the CFL. The time interval for data logging was one minute. The data logger collecting the exterior air temperature had a smaller storage capacity and occasionally would stop collecting data before the logger collecting the test cell data. This made it necessary to synchronize the data from each of loggers. To insure the exterior air temperature was in synchronous with the cell data, the temperature probe on the exterior of the concrete was repositioned on the exterior of the test cell to log the exterior temperature.

The original time period of one minute was determined to be satisfactory for determining steady state with the heater, CFL, on full time. Figure 7.9 plots the interior cell temperature, the temperature of the inner surface of the concrete, the exterior to the cell air temperature, and the energizing of the CFL heater. The input power to the CFL was determined to be an average of 0.06 amps at 119-volts for 7.14 watts or 24.36 Btu/hr . The cell temperature was recorded at 95°F and the outside of the cell temperature was recorded at 66°F . The UA was determined to be:

$$UA = \frac{24.36 \text{ Btu}}{\text{hour}} \frac{1}{(95^{\circ}\text{F} - 66^{\circ}\text{F})} \quad (7.1)$$

$$UA = 0.84 \frac{\text{Btu}}{\text{hr}^{\circ}\text{F}}$$

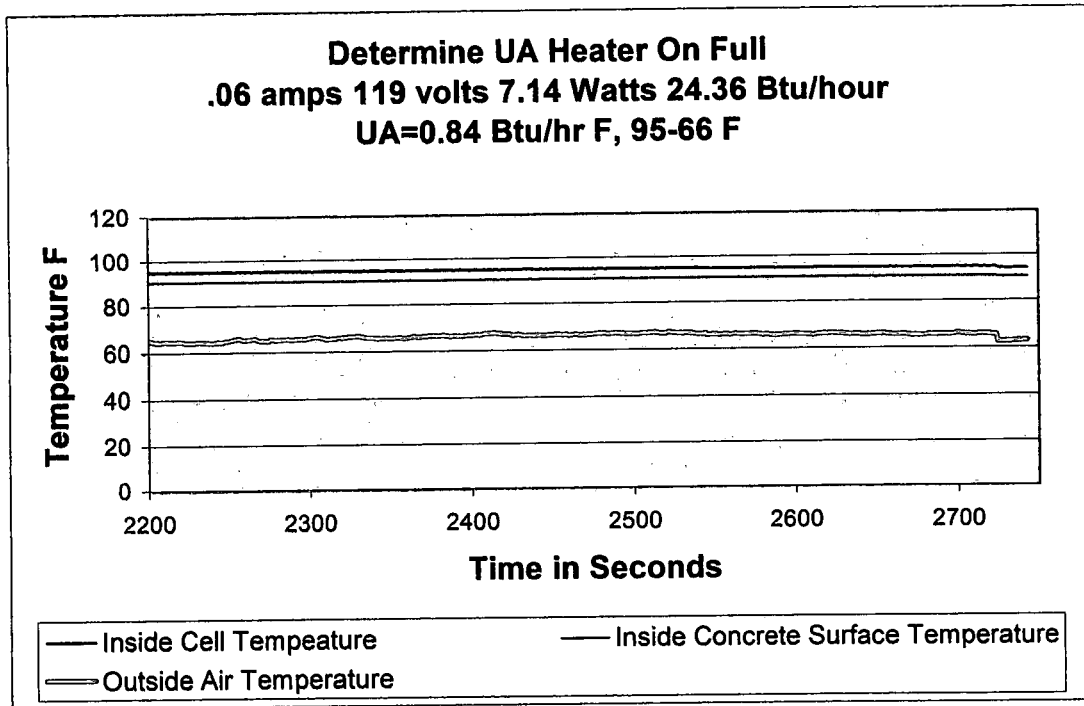


Figure 7.9 Interior cell, interior concrete surface, and outside air temperature

7.3.2: Data Analysis of Average and Peak Exterior Air Temperature Below Interior Set Point

Figure 6.16 plots the interior cell temperature vs. the outside air temperature. The required heating of the cell without thermal mass is:

$$Btu_{Heat} = UA \sum_1^n \left[\left(T_{cell} - T_{outside\ air} \right) \frac{\%}{hr} \right] \quad (7.2)$$

After solving Eq. (7.2) with this data, the heating without thermal mass is:

$$Btu_{Heat} = 0.84 \frac{Btu}{hr^{\circ}F} (15.34 average \Delta T) 4.73 hr$$

$$Btu_{Heat} = 60.9 Btu$$

The actual required heating of the cell with the 5-1/2-inch thick concrete thermal mass wall is:

$$Btu_{Actual\ Heat} = \frac{0.406 Btu}{min} 83.5 min \quad (7.3)$$

$$Btu_{Actual\ Heat} = 33.9 Btu$$

The temperature decrease in the concrete was $1.81^{\circ}F$.

$$\Delta E_{system} = \sum E_{in} - \sum E_{out} \quad (7.4)$$

$$\Delta E_{test\ cell} = 33.9 Btu - 60.9 Btu$$

$$\Delta E_{test\ cell} = -27 Btu$$

$$\Delta E_{test\ cell} = \rho C_p V \Delta T$$

$$\Delta E_{test\ cell} = 150 \frac{lb}{ft^3} 0.2 \frac{Btu}{lb^{\circ}F} \frac{5.5}{12} ft^3 (-1.81^{\circ}F) \quad (7.5)$$

$$\Delta E_{test\ cell} = -24.9 Btu$$

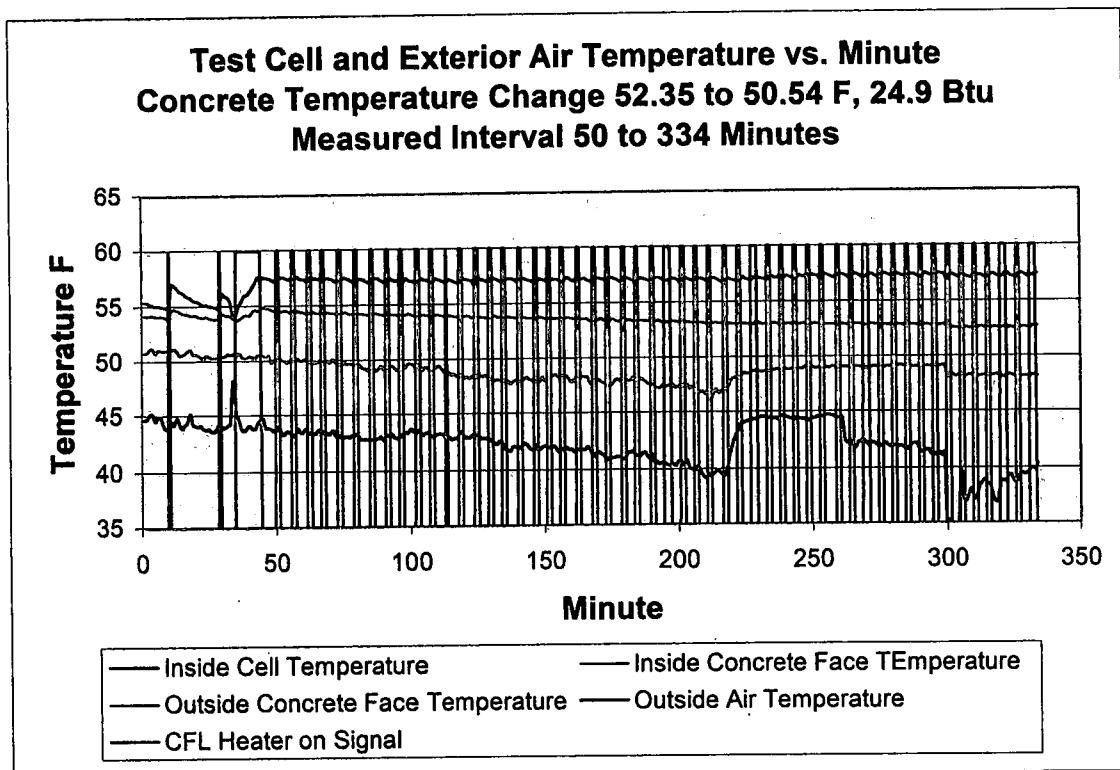


Figure 7.10 Plots of interior cell temperature vs. outside air temperature.

A complete cycle was not captured. It is necessary for the mass to return to the beginning temperature to complete the cycle. However, when the outside

temperature increases, the temperature of the concrete will also increase and there will more heat into the system. As the outside temperature never goes above the interior set point, the heat flow is always from the interior to the concrete. The fact that the total heat flows are essentially the same supports the theory that if the peak cyclic temperature is not above the interior air temperature, thermal mass will not affect the net heating load requirements.

7.3.3: Data Analysis of Average Exterior Air Temperature At the Interior Set Point Temperature

Figure 7.11 plots interior cell temperature, inside concrete surface temperature, outside air temperature, and CFL heat on indicator. The average outside temperature is approximately equal to the interior cell set point temperature.

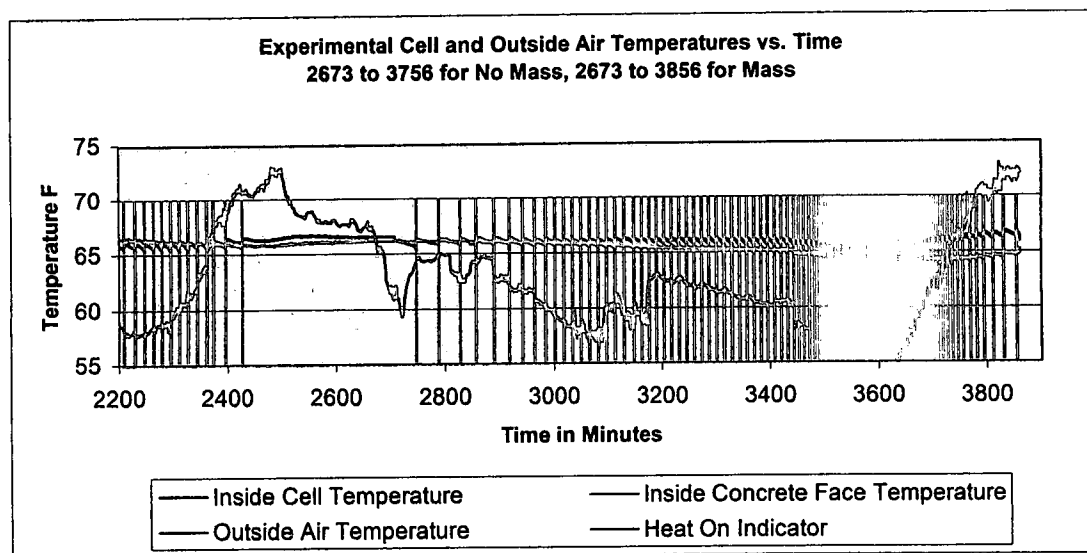


Figure 7.11 Interior cell, inside concrete surface, outside air temperature, and CFL heat on indicator vs. time. Average outside temperature approximately equal to the interior cell set point temperature.

Applying Equation (7.2) for the time period between 2,700 and 3,452 minutes, the time period in which the outside air temperature was below the interior cell set point temperature yields a no-mass heating requirement of:

$$Btu = 0.84 \frac{Btu}{hr^{\circ}F} (7.116 \text{ average } \Delta T) 18.05 \text{ hr}$$

$$Btu = 104 \text{ Btu}$$

The actual required heating was determined with Equation (7.3) to be:

$$Btu = \frac{0.406 Btu}{\text{min}} 118.7 \text{ min}$$

$$Btu = 48.2 \text{ Btu}$$

The mass temperature at the beginning of the measured cycle was $66.01^{\circ}F$ and $65.27^{\circ}F$ at the end of the measured cycle. If the temperature difference is accounted for in Equation (7.5), another 10.2 Btu are added to the actual heating for a total of 58.4 Btu. Taking this addition into account, the reduction is 45.6 Btu or 44%. The decrease in required heating with the thermal mass wall supports the theory that if the peak cyclic outside air temperature is above the interior air set point temperature, thermal mass can reduce the net heating load requirement.

Figure 7.11 is an expanded plot of a longer time period. It is observed that the interior cell temperature is above the inside concrete surface temperature when the outside air temperature is above the inside cell temperature. This indicates large heat transfer through the bead board wall of the test cell. It is also observed that the inside concrete surface temperature is reducing linearly and is not proportional to the outside air

temperature. Although the inner surface temperature of the bead board was not data logged, it is assumed that due to the small thermal mass of the bead board, the inner surface temperature would be proportional to the outside air temperature. The retained inner concrete surface temperature is reducing heat transfer through the concrete wall. The concrete wall has only one layer of bead board insulation on its exterior and therefore has a smaller R-value.

7.4: Conclusion

The data generated when the average and the peak cyclic temperatures were below the interior cell set point temperature, gave a no-mass calculated heating requirement of 60.9 Btu, compared to a logged heating requirement of 58.8 Btu for the "mass wall" case. These data support the theory that when the average and peak cyclic exterior air temperature are below the interior air, thermal mass does not reduce thermal transmission through the mass wall.

The data logged with the peak cyclic outside air temperature above the interior air set point gave a no-mass heating requirement of 104 Btu and an adjusted logged heating requirement for the mass wall of 58.4 Btu. The reduction of 44% of the heating requirements supports the theory that when the peak cyclic outside air temperature is above the interior air set point, the net thermal transmission and heating load can be reduced with the addition of thermal mass.

7.5: Recommendations

Difficulty was experienced because the data loggers unable to collect data for more than several hours. It is recommended that data loggers be used with a logging capability of at least one week. It is also recommended that a data logger be used that can collect data from at least eight sensors simultaneously. This will make synchronizing more than one data logger unnecessary. It is also recommended that temperature data be collected at interior cell wall surfaces other than just the concrete. It is also recommended that a watt sensor be used to monitor the required heating load.

The data indicated that the interior cell temperature would rise above the interior surface temperature of the concrete wall. This indicated that there was significant heat transfer through the non-thermal mass walls. It is therefore recommended that the entire cell be constructed of concrete with insulation on the exterior or the non-concrete wall be constructed with a higher R-value.

CHAPTER 8

SUMMARY AND CONCLUSIONS AND FUTURE WORK

Chapter 2 is a research of the cyclic environmental conditions under which thermal mass has an effect on thermal transmission. It makes explicit that the effect of thermal mass is climate specific. The following conclusions are drawn:

- a. When the mean cyclic exterior sol-air temperature is equal to or greater than the interior set point temperature, the heating thermal load can be completely eliminated with thermal mass.
- b. When the mean cyclic exterior sol-air temperature is below the interior set point temperature and the peak exterior sol-air temperature is above the interior set point temperature, the heating thermal load can be reduced to a minimum of a variation of Equation (2.4).

$$Q_{heating} \left[\frac{WH}{m^2 day} \right] = U_{total} \frac{W}{m^2 C} (T_{set} - T_{mean \text{ exterior air}}) C \frac{24hr}{day}$$

- c. When the mean cyclic exterior sol-air temperature and the peak exterior sol-air temperature are below the interior set point

temperature, thermal mass does not reduce the net thermal transmission and the net heating thermal load.

Similarly, the results presented so far support the following observations about the relationship between thermal mass and cooling load:

d. When the mean cyclic exterior sol-air temperature is equal to or less than the interior set point temperature, thermal transmission and the cooling thermal load can be completely eliminated with thermal mass.

e. When the mean cyclic exterior air temperature is above the interior set point temperature, and the minimum exterior air temperature is below the interior set point temperature, the cooling thermal load can be reduced to a minimum of variation of Equation (2.4):

$$Q_{cooling} \left[\frac{WH}{m^2 day} \right] = U_{total} \frac{W}{m^2 C} (T_{mean \text{ exterior air}} - T_{set}) C \frac{24hr}{day}$$

f. When the mean cyclic exterior sol-air temperature and the peak exterior air temperature are above the interior set point temperature, thermal mass does not reduce the net thermal transmission and the net cooling thermal load.

The net effect of thermal mass is to reduce the amplitude of the sol-air temperature to the average temperature and result in a time delay of the temperature variation through the thermal mass. It is demonstrated the minimum thermal load resulting from the addition of thermal mass can be estimated by averaging the sol-air temperature over a 24 hour cycle in Equations (2.6) and (2.7).

$$ThermalLoad = U \sum_{i=1}^{8760} (T_{set} - \bar{T}_{24,i})_i \quad (2.6)$$

Where,

$$\bar{T}_{24,i} = \frac{\sum_{j=-12}^{12} T_{i+j}}{24} \quad (2.7)$$

Chapter 3 is a research of the effect of phase change material on thermal transmission. It is concluded that the sensible thermal mass of the phase change material has the same effect as the thermal mass in Chapter 2 under the same required conditions. However, for the latent mass of the phase change material to affect thermal transmission, the phase change material must be placed in the wall so that it will pass through its melting point.

Chapter 4 address the "mass wall" as defined the International Energy Conservation Code, IECC. The IECC allows a reduction in required R-value and/or increase in U-factor with the incorporation of a "mass wall" within the exterior envelope of a building. The IECC defines a "mass wall" as a wall with

a heat capacity of $6 \text{ Btu} / \text{ft}^2 {}^\circ\text{F}$. This equates to 2-1/2-inch thick stand and weight concrete. The research confirmed that 2-1/2 inch thick concrete was the thickness at which the effectiveness leveled and therefore, is the optimum concrete thickness. The IECC also requires no more than one half of the thermal resistance of the insulation to be installed on the interior of the mass. The IECC requires a reduction in allowances if more than one half of the thermal resistance of the insulation is on the interior. This research concluded the optimum location for the mass is in the center of the thermal resistance of the insulation and the mass remains effective with as much as three quarters on the interior. The IECC allowed reduction in R-value and increase in U-factor is climate specific. This research confirmed that the climate zones as defined by the IECC properly grouped the climate specific effectiveness of thermal mass. However, this research concluded the allowances given for a "mass wall" by the IECC are larger than the required allowances that ensure the "mass wall" will perform equal to the no-mass wall.

Four climate zones were investigated in this research. The IECC 2009 specifies a U-factor, in climate zone 4 and marine 5, of 0.057 for a no-mass wall and allows an increase to 0.082 for a "mass wall." This research supports a "mass wall" increase to 0.064 to 0.068. The IECC 2009 specifies a U-factor, in climate zone 3, of 0.082 for a no-mass wall and allows an increase to only 0.141 for a "mass wall." This research supports a "mass wall" increase to only 0.091 to 0.094. The IECC 2009 specifies a U-factor, in

climate zone 2, of 0.082 for a no-mass wall and allows an increase to 0.165 for a "mass wall." This research supports a "mass wall" increase of only 0.103 to 0.116.

This research investigated the use of a phase change material on the exterior of a building envelope wall with seven eighths of the insulation on the interior. The phase change material was given a melt temperature of 73 °F . This is in the middle of the 72 °F heating and 75 °F cooling set points specified in the IECC. The exterior location of the phase change material exposed it to temperature swings through its melt temperature and the temperature cycle which meets the requirements for thermal mass and phase change material to be effective at reducing thermal transmission. ½-inch of this simulated material was determined to be more effective at reducing thermal transmission than the 2-1/2-inch thick concrete on the interior. It is suggested that further research be conducted with respect to the use of phase change material on the exterior of the building envelope to reduce thermal transmission.

This research investigated concrete as the thermal mass material. It is suggested that further research be conducted on other standard building components including composite wall structures consisting of brick, block, and air spaces to determine their required effective sizes.

This research treated the required energy for cooling equally with the required energy for heating and gave no quantification to the different environmental impacts of the energy production for each. It is suggested that

research be conducted to quantify the environmental impacts and suggest a weighting factor to be used when quantifying the different energy production methods for cooling and heating.

BIBLIOGRAPHY

- [1] International Energy Conservation Code. (2009). International Code Council, Inc.
- [2] REScheck. (2009). U.S.Department of Energy. *Building Technologies Program*.
- [3] Khalifa, A.J.N. and Abbas, E.F.(2009). "A Comparative Study of Some Thermal Storage Materials Used for Solar Space Heating." *Energy and Buildings*, 41, pp. 407-415.
- [4] Gajda, J., Marceau, M., and Vangeem, M. (2004) "HVAC Sizing Methodology for Insulated Concrete Homes." U.S. Department of Housing and Urban Development Office of Policy Development and Research.
- [5] Kosny, J. Christian, J. Desjarlais, A. (1998). "The Performance Check between Whole Building Thermal Performance Criteria and Exterior Wall; Measured Clear Wall R-value, Thermal Bridging, Thermal Mass and Air-tightness." *ASHRAE Summer Transactions..*
- [6] Gajda, J., Marceau, M. and VanGeem, M. (2004). "HVAC Sizing Methodology for Insulated Concrete Homes." U.S. Department

of Housing and Urban Development, Office of Policy Development and Research.

- [7] Kalogirou, S.A., Florides, G., and Tassou, S. (2002). "Energy Analysis of Buildings Employing Thermal Mass in Cyprus." *Renewable Energy*, Vol. 7, (3), pp. 353-368.
- [8] Al-Homoud, M.S. (2000). "Computer-aided Building Energy Analysis Techniques." *Building and Environment*, Vol. 36 (4), 421-433.
- [9] Balaras, C.A. (1996). "The Role of Thermal Mass on the Cooling Load of Buildings: An Overview of Computational Methods." *Energy and Buildings*, Vol. 24 (1), pp. 1-10.
- [10] Abbott, A.B. and Ellis, M.W. (2007). "Analysis of Thermal Energy Collection From Precast Concrete Roof Assemblies." *Proc. ES2007 Energy Sustainability Conference*.
- [11] Kissock, K. and Limas, S. (2006). "Diurnal Load Reduction Through Phase-change Building Components." *ASHRAE Transactions*, 112, pp. 500-517.
- [12] Salyer, I.O. and Sircar, A.K. (1995). "Advanced Phase Change Materials Technology; Evaluation in Lightweight Solite Hollow-core Building Blocks." *Proc. 30th Intersociety Energy Conversion Engineering Conference*
- [13] Salyer, I.O. and Sircar, A.K. (1997). "A Review of Phase Change Materials Research for Thermal Energy Storage in Heating and

Cooling Applications at the University of Dayton from 1982-1996. *International Journal of Global Energy Issues*, Vol. 9, pp. 183-198.

- [14] Kissock, K. (2000). "Thermal Load Reduction From Phase-change Building Components in Temperature-Controlled Buildings." *Proc. Solar 2000: Solar Powers Life, Share the Energy*.
- [15] Pasupathy, A. and Velraj, R. (2008). "Effect of Double Layer Phase Change Material in Bulding Roof for Year Round Thermal Management." *Energy Buildings*, Vol. 40, pp. 193-203.
- [16] Mirza, K. and Kissock, K. (2007). "An Analytical Solution for Dynamic Thermal Transmission Loads." *Proc. of ES2007 Energy Sustainability Conference*. Paper No. ES2007-36094.
- [17] Gilbert, R.B. and Kissock, K. (2007). "The Effect of Thermal Mass on Thermal Transmission Loads." *Proc. of ES2007 Energy Sustainability Conference*. Paper No. ES2007-36101.
- [18] Kissock, K., Hannig, J.M., Whitney, T.I., and Drake, M.L. (1999). "Testing and Simulation of Phase Change Wallboard for Thermal Storage in Buildings." *ASME-JSEE*, May 11, 1999.
- [19] Castellon, C., Medrano, M. Roca, J., Fontanals, G., and Cabeza, L.F. (2007). "Improve Thermal Comfort in Concrete Buildings by Using Phase Change Material. *Proc. Of ES2007 Energy Sustainability Conference*. Paper No. ES2007-36073.

- [20] Alawadhi, E.M. (2008). "Thermal Analysis of a Building Brick Containing Phase Change Material." *Energy and Buildings*, Vol. 40, pp. 351-357.
- [21] Gilbert, R.B. (2009). "The Effects of Thermal Mass and Phase Change Material on a Buildings' Thermal Load." *Proc. of ES2009 Energy Sustainability Conference*. Paper No. ES2009-90367.
- [22] Gilbert, R.B. and Kissock, K. (2007). "The Effect of Thermal Mass on Thermal Transmission Loads." *Proc. of ES2007 Energy Sustainability Conference*. Paper No. ES2007-36101.
- [23] Incropera, F.P. and DeWitt, D. (2002) *Fundamentals of Heat Mass and Transfer*, John Wiley and Sons, Hoboken, N.J.
- [24] REScheck. (2009). U.S.Department of Energy. *Building Technologies Program*.
- [25] *2005 ASHRAE Handbook Fundamentals*, (2005) American Society of Heating, Refrigerating and Air-Conditioning Engineers, Inc., Atlanta, Ga.
- [26] Kissock, J.K. and Eger, C. (2007). "Measuring Industrial Energy Savings." *Applied Energy*, Vol. 85, pp. 347-361.
- [27] Raffio, G., Isambert, O., Mertz, G., Schreier, C., Kissock, K. (2007). "Targeting Residential Energy Assistance." *Proc. of ES2007 Energy Sustainability Conference*. Paper No. ES2007-36080.